

THE MINISTRY OF SCIENCE AND HIGHER EDUCATION OF THE RUSSIAN FEDERATION



ISSN 2687-0517

---

---

# **Computing, Telecommunications and Control**

---

---

**Vol. 16, No. 2  
2023**

Peter the Great St. Petersburg  
Polytechnic University  
2023

# COMPUTING, TELECOMMUNICATIONS AND CONTROL

## EDITORIAL COUNCIL

Prof. Dr. *Rafael M. Yusupov* corresponding member of RAS, St. Petersburg Institute for Informatics and Automation of the RAS, Russia,

Prof. Dr. *Sergey M. Abramov* corresponding member of RAS, full member of RAS, Ailamazyan Program Systems Institute of the RAS,

Prof. Dr. *Dmitry G. Arseniev* corresponding member of RAS, Peter the Great St. Petersburg Polytechnic University, Russia,

Prof. Dr. *Vladimir V. Voevodin* corresponding member of RAS, Lomonosov Moscow State University, Russia,

Prof. Dr. *Vladimir S. Zaborovsky*, Peter the Great St. Petersburg Polytechnic University, Russia,

Prof. Dr. *Vladimir N. Kozlov*, Peter the Great St. Petersburg Polytechnic University, Russia,

Prof. Dr. *Alexandr E. Fotiadi*, Peter the Great St. Petersburg Polytechnic University, Russia,

Prof. Dr. *Igor G. Chernorutsky*, Peter the Great St. Petersburg Polytechnic University, Russia.

## EDITORIAL BOARD

### Editor-in-chief

Prof. Dr. *Alexander S. Korotkov*, Peter the Great St. Petersburg Polytechnic University, Russia;

### Members:

Assoc. Prof. Dr. *Pavel D. Drobintsev*, Peter the Great St. Petersburg Polytechnic University, Russia;

Assoc. Prof. Dr. *Vladimir M. Itsyson*, Peter the Great St. Petersburg Polytechnic University, Russia;

Prof. Dr. *Philippe Ferrari*, Grenoble Alpes University, France;

Prof. Dr. *Yevgeni Koucheryavy*, Tampere University of Technology, Finland;

Prof. Dr. *Wolfgang Krauschneider*, Hamburg University of Technology, Germany;

Prof. Dr. *Fa-Long Luo*, University of Washington, USA;

Prof. Dr. *Sergey B. Makarov*, Peter the Great St. Petersburg Polytechnic University, Russia;

Prof. Dr. *Emil Novakov*, Grenoble Alpes University, France;

Prof. Dr. *Nikolay N. Prokopenko*, Don State Technical University, Russia;

Prof. Dr. *Mikhail G. Putrya*, National Research University of Electronic Technology, Russia;

Sen. Assoc. Prof. Dr. *Evgeny Pyshkin*, University of Aizu, Japan;

Prof. Dr. *Viacheslav P. Shkodyrev*, Peter the Great St. Petersburg Polytechnic University, Russia;

Prof. Dr. *Vladimir A. Sorotsky*, Peter the Great St. Petersburg Polytechnic University, Russia

Prof. Dr. *Peter V. Trifonov*, ITMO University, Russia;

Prof. Dr. *Igor A. Tsikin*, Peter the Great St. Petersburg Polytechnic University, Russia;

Prof. Dr. *Sergey M. Ustinov*, Peter the Great St. Petersburg Polytechnic University, Russia;

Prof. Dr. *Lev V. Utkin*, Peter the Great St. Petersburg Polytechnic University, Russia.

The journal is included in the List of Leading PeerReviewed Scientific Journals and other editions to publish major findings of PhD theses for the research degrees of Doctor of Sciences and Candidate of Sciences.

Open access journal is to publish articles of a high scientific level covering advanced experience, research results, theoretical and practical problems of informatics, electronics, telecommunications, and control.

The journal is indexed by Ulrich's Periodicals Directory, Google Scholar, EBSCO, ProQuest, Index Copernicus, VINITI RAS Abstract Journal (Referativnyi Zhurnal), VINITI RAS Scientific and Technical Literature Collection, Russian Science Citation Index (RSCI) database Scientific Electronic Library and Math-Net.ru databases.

The journal is registered with the Federal Service for Supervision in the Sphere of Telecom, Information Technologies and Mass Communications (ROSKOMNADZOR). Certificate ЭЛ No. ФС77-77378 issued 25.12.2019.

Editorial office

Dr. Sc., Professor A.S. Korotkov – Editor-in-Chief;

E.A. Kalinina – literary editor, proofreader; G.A. Pyshkina – editorial manager; A.A. Kononova – computer layout; D.Yu. Alekseeva – English translation.

Address: 195251 Polytekhnikeskaya Str. 29, St. Petersburg, Russia.

+7 (812) 552-6216, e-mail: infocom@spbstu.ru

Release date: 14.07.2023

© Peter the Great St. Petersburg Polytechnic University, 2023

МИНИСТЕРСТВО НАУКИ И ВЫСШЕГО ОБРАЗОВАНИЯ РОССИЙСКОЙ ФЕДЕРАЦИИ



ISSN 2687-0517

---

---

# **Информатика, телекоммуникации и управление**

---

---

**Том 16, № 2  
2023**

Санкт-Петербургский политехнический  
университет Петра Великого  
2023

# ИНФОРМАТИКА, ТЕЛЕКОММУНИКАЦИИ И УПРАВЛЕНИЕ

## РЕДАКЦИОННЫЙ СОВЕТ ЖУРНАЛА

*Юсупов Р.М.*, чл.-кор. РАН, Санкт-Петербургский институт информатики и автоматизации РАН, Санкт-Петербург, Россия; *Абрамов С.М.*, чл.-кор. РАН, Институт программных систем им. А.К. Айламазяна РАН, Москва, Россия; *Арсеньев Д.Г.*, чл.-кор. РАН, д-р техн. наук, профессор, Санкт-Петербургский политехнический университет Петра Великого, Санкт-Петербург, Россия; *Воеводин В.В.*, чл.-кор. РАН, Московский государственный университет им. М.В. Ломоносова, Москва, Россия; *Заборовский В.С.*, д-р техн. наук, профессор, Санкт-Петербургский политехнический университет Петра Великого, Санкт-Петербург, Россия; *Козлов В.Н.*, д-р техн. наук, профессор, Санкт-Петербургский политехнический университет Петра Великого, Санкт-Петербург, Россия; *Фотиади А.Э.*, д-р физ.-мат. наук, профессор, Санкт-Петербургский политехнический университет Петра Великого, Санкт-Петербург, Россия; *Черноруцкий И.Г.*, д-р техн. наук, профессор, Санкт-Петербургский политехнический университет Петра Великого, Санкт-Петербург, Россия.

## РЕДАКЦИОННАЯ КОЛЛЕГИЯ ЖУРНАЛА

### Главный редактор

*Коротков А.С.*, д-р техн. наук, профессор, Санкт-Петербургский политехнический университет Петра Великого, Санкт-Петербург, Россия;

### Редакционная коллегия:

*Дробинцев П.Д.*, канд. техн. наук, доцент, Санкт-Петербургский политехнический университет Петра Великого, Санкт-Петербург, Россия;

*Ицыксон В.М.*, канд. техн. наук, доцент, Санкт-Петербургский политехнический университет Петра Великого, Санкт-Петербург, Россия;

*Феррари Ф.*, профессор, Университет Гренобль-Альпы, Гренобль, Франция;

*Краутишнайдер В.*, профессор, Гамбургский технический университет, Гамбург, Германия;

*Кучерявый Е.А.*, канд. техн. наук, профессор, Университет Тампере, Финляндия.

*Люо Ф.-Л.*, University of Washington, Washington, USA;

*Макаров С.Б.*, д-р техн. наук, профессор, Санкт-Петербургский политехнический университет Петра Великого, Санкт-Петербург, Россия;

*Новаков Э.*, профессор, Университет Гренобль-Альпы, Гренобль, Франция;

*Прокопенко Н.Н.*, д-р техн. наук, профессор, Донской государственный технический университет, г. Ростов-на-Дону, Россия;

*Путря М.Г.*, д-р техн. наук, профессор, Национальный исследовательский университет «Московский институт электронной техники», Москва, Россия;

*Пышкин Е.В.*, профессор, Университет Айзу, Айзу-Вакаматсу, Япония;

*Сороцкий В.А.*, д-р техн. наук, профессор, Санкт-Петербургский политехнический университет Петра Великого, Санкт-Петербург, Россия;

*Трифонов П.В.*, д-р техн. наук, доцент, Национальный исследовательский университет ИТМО, Санкт-Петербург, Россия;

*Устинов С.М.*, д-р техн. наук, профессор, Санкт-Петербургский политехнический университет Петра Великого, Санкт-Петербург, Россия;

*Уткин Л.В.*, д-р техн. наук, профессор, Санкт-Петербургский политехнический университет Петра Великого, Санкт-Петербург, Россия;

*Цикин И.А.*, д-р техн. наук, профессор, Санкт-Петербургский политехнический университет Петра Великого, Санкт-Петербург, Россия;

*Шкодырев В.П.*, д-р техн. наук, профессор, Санкт-Петербургский политехнический университет Петра Великого, Санкт-Петербург, Россия.

Журнал с 2002 года входит в Перечень ведущих рецензируемых научных журналов и изданий, в которых должны быть опубликованы основные результаты диссертаций на соискание ученой степени доктора и кандидата наук.

Сетевое издание открытого доступа публикует статьи высокого научного уровня, освещающие передовой опыт, результаты НИР, теоретические и практические проблемы информатики, электроники, телекоммуникаций, управления.

Сведения о публикациях представлены в Реферативном журнале ВИНТИ РАН, в международной справочной системе «Ulrich`s Periodical Directory», в Российской государственной библиотеке. В базах данных: Российский индекс научного цитирования (РИНЦ), Google Scholar, EBSCO, Math-Net.Ru, ProQuest, Index Copernicus.

Журнал зарегистрирован Федеральной службой по надзору в сфере информационных технологий и массовых коммуникаций (Роскомнадзор). Свидетельство о регистрации Эл № ФС77-77378 от 25.12.2019.

Учредитель и издатель: Санкт-Петербургский политехнический университет Петра Великого, Санкт-Петербург, Российская Федерация.

Редакция журнала

д-р техн. наук, профессор А.С. Коротков – главный редактор;

Е.А. Калинина – литературный редактор, корректор; Г.А. Пышкина – ответственный секретарь, выпускающий редактор;

А.А. Кононова – компьютерная вёрстка; Д.Ю. Алексеева – перевод на английский язык.

Адрес редакции: Россия, 195251, Санкт-Петербург, ул. Политехническая, д. 29.

Тел. редакции +7(812) 552-62-16, e-mail: infocom@spbstu.ru

Дата выхода: 14.07.2023

© Санкт-Петербургский политехнический университет Петра Великого, 2023

# Contents

## Intellectual Systems and Technologies

**Konstantinov A.V., Utkin L.V., Kirpichenko S.R.** Flexible deep forest classifier with multi-head attention ..... 7

**Potekhin V.V., Alekseev A.P., Kuklin E.V., Khitrova Ya.D., Kozhubaev Yu.N.** Cloud distributed control system based on open process automation platform ..... 17

## Simulations of Computer, Telecommunications, Control and Social Systems

**Redrugina N.M.** A set of simulation models of workflow elements for transactional services of infocommunication systems ..... 29

**Kuptsov V.D., Ivanov S.I.** Multichannel multistatic combined TSoA and TDoA positioning system based on precise analytical solution of positioning equations ..... 40

## Telecommunication Systems and Computer Networks

**Safonov A.V.** Influence of technological processes on the uncertainty of systems measuring liquefied natural gas energy ..... 55

## Содержание

### **Интеллектуальные системы и технологии**

**Константинов А.В., Уткин Л.В., Кирпиченко С.Р.** Гибкий классификатор на основе глубокого леса с использованием многомерного внимания ..... 7

**Потехин В.В., Алексеев А.П., Куклин Е.В., Хитрова Я.Д., Кожубаев Ю.Н.** Облачная распределенная система управления на базе открытой промышленной платформы автоматизации ..... 17

### **Моделирование вычислительных, телекоммуникационных, управляющих и социально-экономических систем**

**Редругина Н.М.** Комплекс имитационных моделей элементов рабочих процессов для транзакционных услуг инфокоммуникационных систем ..... 29

**Купцов В.Д., Иванов С.И.** Многоканальная мультистатическая комбинированная система позиционирования TSoA и TDoA, основанная на точном аналитическом решении уравнений позиционирования ..... 40

### **Телекоммуникационные системы и компьютерные сети**

**Сафонов А.В.** Влияние технологических процессов на неопределенность измерительных систем количества энергии сжиженного природного газа ..... 55

# Intellectual Systems and Technologies

# Интеллектуальные системы и технологии

Research article

DOI: <https://doi.org/10.18721/JCSTCS.16201>

UDC 004.85



## FLEXIBLE DEEP FOREST CLASSIFIER WITH MULTI-HEAD ATTENTION

*A.V. Konstantinov*<sup>1</sup> , *L.V. Utkin*<sup>1</sup>  ,  
*S.R. Kirpichenko*<sup>1</sup> 

<sup>1</sup> Peter the Great St. Petersburg Polytechnic University,  
St. Petersburg, Russian Federation

 [lev.utkin@gmail.com](mailto:lev.utkin@gmail.com)

**Abstract.** A new modification of the deep forest (DF), called the attention-based deep forest (ABDF), for solving classification problems is proposed in the paper. The main idea behind the modification is to use the attention mechanism to aggregate predictions of the random forests at each level of the DF to enhance the classification performance of the DF. The attention mechanism is implemented by assigning the attention weights with trainable parameters to class probability vectors. The trainable parameters are determined by solving an optimization problem minimizing the loss function of predictions at each level of the DF. In order to reduce the number of random forests, the multi-head attention is incorporated into the DF. Numerical experiments with real data illustrate the ABDF and compare it with the original DF.

**Keywords:** machine learning, classification, random forest, decision tree, deep learning, attention mechanism

**Acknowledgement:** This work is supported by the Russian Science Foundation under grant 21-11-00116.

**Citation:** Konstantinov A.V., Utkin L.V., Kirpichenko S.R. Flexible deep forest classifier with multi-head attention. *Computing, Telecommunications and Control*, 2023, Vol. 16, No. 2, Pp. 7–16. DOI: [10.18721/JCSTCS.16201](https://doi.org/10.18721/JCSTCS.16201)





Научная статья

DOI: <https://doi.org/10.18721/JCSTCS.16201>

УДК 004.85



## ГИБКИЙ КЛАССИФИКАТОР НА ОСНОВЕ ГЛУБОКОГО ЛЕСА С ИСПОЛЬЗОВАНИЕМ МНОГОМЕРНОГО ВНИМАНИЯ

А.В. Константинов<sup>1</sup> , Л.В. Уткин<sup>1</sup>  ,  
С.Р. Кирпиченко<sup>1</sup> 

<sup>1</sup> Санкт-Петербургский политехнический университет Петра Великого,  
Санкт-Петербург, Российская Федерация

 [lev.utkin@gmail.com](mailto:lev.utkin@gmail.com)

**Аннотация.** В статье предлагается новая модификация глубокого леса, называемая глубоким лесом на основе механизма внимания, для решения задач классификации при ограниченной выборке. Основная идея модификации заключается в использовании механизма внимания для агрегирования предсказаний случайных лесов в виде векторов вероятностей классов на каждом уровне или слое глубокого леса для повышения эффективности классификации все модели. Механизм внимания реализуется путем присвоения веса внимания конкатенированным векторам примеров и векторов вероятностей классов так, что модель внимания имеет обучаемые параметры. Обучаемые параметры определяются путем решения задачи оптимизации, минимизирующей функцию потерь ошибки предсказаний на каждом уровне глубокого леса в процессе обучения глубокого леса на каждом уровне. Чтобы уменьшить количество случайных лесов, в глубокий лес включено так называемое многомерное внимание. Численные эксперименты на реальных данных иллюстрируют предлагаемую модификацию с точки зрения точности классификации и сравнивают ее с оригинальным глубоким лесом.

**Ключевые слова:** машинное обучение, классификация, случайный лес, дерево решений, глубокое обучение, механизм внимания

**Финансирование:** Работа выполнена при поддержке гранта РНФ № 21-11-00116.

**Для цитирования:** Konstantinov A.V., Utkin L.V., Kirpichenko S.R. Flexible deep forest classifier with multi-head attention // Computing, Telecommunications and Control. 2023. Т. 16, № 2. С. 7–16. DOI: 10.18721/JCSTCS.16201

### Introduction

A lot of ensemble-based machine learning methods have been proposed [1, 2] due to their efficiency. These methods use a combination of the so-called base models to obtain more accurate predictions. Three types of the ensemble-based methods can be pointed out: bagging [3], stacking [4], and boosting [5]. Each type of methods has cons and pros. One of the important bagging methods is the random forest (RF) [6], which combines predictions of many randomly built decision trees. RFs are popular because they are simply trained and provide outstanding results for many datasets.

RFs can be regarded as powerful machine learning models. However, they cannot compete with deep neural networks. In order to partially overcome this disadvantage Zhou and Feng [7] proposed the so-called Deep Forest (DF) or gcForest, which copies the structure of multi-layer neural networks and consists of several layers or forest cascades. Each layer of the DF consists of several RFs, which produced predictions combined to use them at the next layer. The DF does not require gradient-based algorithms for training. This peculiarity makes the DF simple. Moreover, they have less hyperparameters in comparison with neural networks. Due to efficiency of the DF, many modifications have been proposed [8–16]. The DFs were used in various applications [17–21].



In order to improve RFs, the attention-based RFs were proposed in [22], where the trainable attention weights are assigned to each tree and each example. The weights depend on how far an instance, which falls into a leaf of a decision tree, is from the instances, which fall into the same leaf. The attention weights in the RF are used to compute the weighted average of the decision tree predictions.

It is important to note that the attention mechanism is successfully applied to neural networks to enhance their prediction abilities. It is based on the human perception property to concentrate on an important part of information and to ignore other information [23]. Therefore, the attention mechanism opened a door for implementing many neural network architectures, including transformers, the natural language processing models, etc., which are considered in detail in [23–26].

The attention-based RFs (ABRF) opened another door to the attention models different from the neural networks or their components. Therefore, we proposed a new attention-based model incorporated into the DF to enhance the DF prediction accuracy. The main idea behind the attention in the DF is to assign the attention weights to every RF at each layer to optimally combine the RF predictions and to produce new attended training feature vectors at each layer of the DF for training trees and RFs at the next layer. The attention-based DF is abbreviated as the ABDF.

The paper is organized as follows. A short description of the DF proposed by Zhou and Feng [7] and the attention mechanism are given in Section 2 and 3, respectively. Section 4 shows a general architecture of the attention-based DF. Numerical experiments with real data illustrate the attention-based DF and compare it with the original DF in Section 4. Concluding remarks are provided in Section 5.

### A short introduction to the DF

Before considering the weighted DF, we briefly introduce gcForest proposed by Zhou and Feng [7]. The DF can be divided into two parts. The main part of gcForest is a cascade forest structure where each level of a cascade receives feature information processed by its preceding level, and outputs its processing result to the next level [7].

The main part of the DF proposed in [7] is a cascade forest structure shown in Fig. 1. One can see from Fig. 1 that each layer (level) of the cascade consists of several RFs whose number is a tuning parameter. Every RF produces a class probability distribution vector. The probability distributions of classes are determined in the standard way by counting the percentage of different classes of instances at the leaf node where the considered instance falls into. The RF class probability vectors are computed by averaging the class distribution vectors across all trees in the RF. The vectors produced by all RFs at each level are concatenated to each other. Moreover, the obtained concatenated class probability distribution vectors are concatenated with the input feature vector producing the training or testing vector for the next level. The feature vectors of the last level are combined into a single class probability vector by means of averaging. The final prediction corresponds to the largest probability from the class probability vector. The greedy algorithm is used to train the DF so that the next level of the forest cascade is trained on the feature vectors obtained from the previous level.

We suppose that there are  $Q$  levels (layers) of the DF, every level contains  $F$  forests, every RF consists of  $T$  decision trees. It is assumed for simplicity that  $F$  and  $T$  are identical at all levels.

Suppose that there are  $n$  training instances  $S = \{(\mathbf{x}_1, y_1), (\mathbf{x}_2, y_2), \dots, (\mathbf{x}_n, y_n)\}$ ,  $\mathbf{x}_i = (x_{i1}, \dots, x_{im}) \in \mathbb{R}^m$ , is a feature vector from  $m$  features,  $y_i \in \{1, \dots, C\}$  is the target output. The class probability vector  $\mathbf{p}_l = (p_{l,1}, \dots, p_{l,C})$  as the prediction of the  $l^{\text{th}}$  tree is defined as follows. Let the vector  $\mathbf{x}$  fall into a leaf of the  $l^{\text{th}}$  tree. Then there holds

$$p_{l,c} = \Pr\{c|\mathbf{x}\} = \frac{n_{l,c}}{\sum_{i=1}^C n_{l,i}} = \frac{n_{l,c}}{n_l},$$

where  $c$  is the class index  $c \in \{1, \dots, C\}$ ,  $n_{l,c}$  is the number of instances from the class  $c$  which fall into the same leaf as the vector  $\mathbf{x}$  in the  $l^{\text{th}}$  tree.

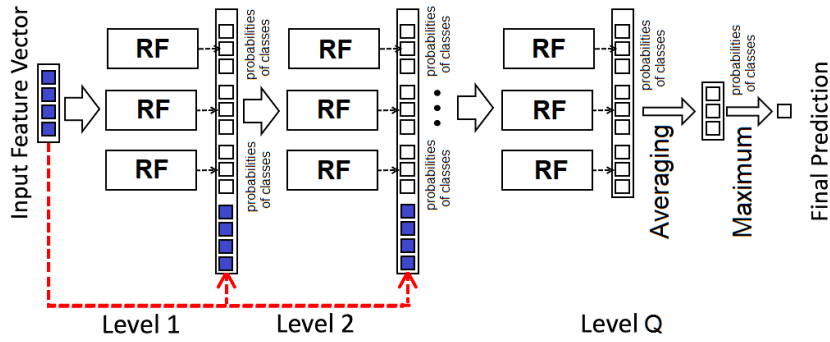


Fig. 1. Architecture of cascade forest

In other words,  $p_{l,c}$  is the percentage of instances from class  $c$ , which fall into the leaf where the instance  $\mathbf{x}$  falls into. The following condition is fulfilled for all trees:

$$\sum_{c=1}^C p_{l,c} = 1.$$

The class probability vector  $\mathbf{v}_j(i) = (v_{j,1}(i), \dots, v_{j,C}(i))$  as the prediction produced by the  $i^{\text{th}}$  RF for  $\mathbf{x}_j$  is defined as

$$v_{j,c}(i) = \frac{1}{T} \sum_{t=1}^T p_{j,c}^{(t)}, \quad c = 1, \dots, C.$$

According to [7], the concatenated vector  $\mathbf{x}_j^{(q)}$  after the  $q^{\text{th}}$  level of the DF cascade is

$$\mathbf{x}_j^{(q)} = (\mathbf{x}_j, \mathbf{v}_j(1), \dots, \mathbf{v}_j(F)).$$

It consists of the original vector  $\mathbf{x}_j$  and  $F$  class probability vectors obtained from  $F$  RFs.

#### The attention mechanism and the attention-based RF

According to [24], the attention mechanism can be considered in terms of the Nadaraya–Watson kernel regression model [27, 28]. Given the training set  $S$ , the machine learning task is to find a function  $f: \mathbb{R}^m \rightarrow \mathbb{R}$  predicting the target value  $\tilde{y}$  of a new instance  $\mathbf{x}$  based on the dataset  $S$ . Then the Nadaraya–Watson regression model can be written as follows:

$$\tilde{y} = \sum_{i=1}^n \alpha(\mathbf{x}, \mathbf{x}_i) y_i,$$

where  $\alpha(\mathbf{x}, \mathbf{x}_i)$  are the attention weights depending on how the vector  $\mathbf{x}_i$  from the training set is close to the input vector  $\mathbf{x}$ , i.e. the closer  $\mathbf{x}_i$  to  $\mathbf{x}$ , the greater  $\alpha(\mathbf{x}, \mathbf{x}_i)$ .

The weights are expressed through the kernel  $K$  as:

$$\alpha(\mathbf{x}, \mathbf{x}_i) = \frac{K(\mathbf{x}, \mathbf{x}_i)}{\sum_{j=1}^n K(\mathbf{x}, \mathbf{x}_j)}.$$

Vector  $\mathbf{x}$ , vectors  $\mathbf{x}_i$  and outputs  $y_i$  are called *query*, *keys* and *values*, respectively, [29]. Generally, weight  $\alpha(\mathbf{x}, \mathbf{x}_i)$  depends on the trainable parameters  $\mathbf{w}$ . If the Gaussian kernel is used to represent the attention weight, then we can write the following:

$$\alpha(\mathbf{x}, \mathbf{x}_i) = \text{softmax}(\mathbf{x}, \mathbf{x}_i, \mathbf{w}) = \frac{\exp\left(-\|\mathbf{w}(\mathbf{x} - \mathbf{x}_i)\|^2\right)}{\sum_{j=1}^n \exp\left(-\|\mathbf{w}(\mathbf{x} - \mathbf{x}_j)\|^2\right)}.$$

Here  $\mathbf{w}$  is the vector of trainable attention parameters,  $\alpha(\mathbf{x}, \mathbf{x}_i, \mathbf{w})$  is an attention scoring function that maps two vectors to a scalar. It should be noted that there are various forms of incorporating trainable parameters. As a result, different expressions for the attention weights or for the scoring function have been studied and proposed. One of the popular scoring functions is defined as

$$s(\mathbf{x}, \mathbf{x}_i) = \mathbf{w}_v^T \tanh(\mathbf{W}_q \mathbf{x} + \mathbf{W}_k \mathbf{x}_i),$$

where  $\mathbf{w}_v$  or  $\mathbf{W}_v$ ,  $\mathbf{W}_q$ , and  $\mathbf{W}_k$  are the vector and matrices of trainable parameters.

The corresponding attention is the well-known additive attention [29]. Another popular attention is the dot-product attention [30, 31]. The attention-based RF proposed in [22] is based on the Huber's  $\epsilon$ -contamination model [32] with a specific trainable parameter, which is the contamination probability distribution.

Generally, the attention function (pooling) can be represented as an attention function  $f$ :

$$\mathbf{e} = f(\mathbf{W}_q \mathbf{x}, \mathbf{W}_k \mathbf{x}_i, \mathbf{W}_v y_i),$$

where  $\mathbf{e}$  is the output of the attention module (embedding).

Another approach for improving and extending the attention mechanism is to use the multi-head attention which is based on joint use of the different representation of queries, keys, and values in order to take into account multiple different aspects of data. The multi-head attention is implemented by means of different trainable parameters (heads)  $\mathbf{w}_v^{(h)}$ ,  $\mathbf{W}_v^{(h)}$ , and  $\mathbf{W}_k^{(h)}$ . In this case, each attention head  $\mathbf{e}^{(h)}$  is written as

$$\mathbf{e}^{(h)} = f(\mathbf{W}_q^{(h)} \mathbf{x}, \mathbf{W}_k^{(h)} \mathbf{x}_i, \mathbf{W}_v^{(h)} y_i).$$

When the attention is implemented by neural networks, the heads are determined by different initialization of the neural network parameters. After computing vectors  $\mathbf{e}^{(h)}$ ,  $h = 1, \dots, H$ , the heads are concatenated.

### The attention-based DF

Let us return to the DF. Suppose that we have the trained RFs consisting of  $T$  decision trees at the first level of the forest cascade and the instance  $\mathbf{x}$  is fed to the  $i^{\text{th}}$  RF. Let us compute the reconstruction of input feature vector  $\hat{\mathbf{x}}(i)$  produced by the  $i^{\text{th}}$  RF as follows:

$$\hat{\mathbf{x}}(i) = \sum_{k=1}^T \alpha(\mathbf{x}, \hat{\mathbf{x}}^{(k)}(i)) \hat{\mathbf{x}}^{(k)}(i),$$

where the reconstruction produced by  $k^{\text{th}}$  tree is:

$$\hat{\mathbf{x}}^{(k)}(i) = \frac{1}{\#\mathfrak{S}_i^{(k)}(\mathbf{x})} \sum_{j \in \mathfrak{S}_i^{(k)}(\mathbf{x})} \mathbf{x}_j.$$

Here  $\mathfrak{S}_i^{(k)}(\mathbf{x})$  is the set of instances from the training set  $S$  which fall into the same leaf from the  $k^{\text{th}}$  trees in the  $i^{\text{th}}$  RF as the vector  $\mathbf{x}$  falls;  $\#\mathfrak{S}_i^{(k)}(\mathbf{x})$  is the number of elements in the set  $\mathfrak{S}_i^{(k)}(\mathbf{x})$ . It can be seen from

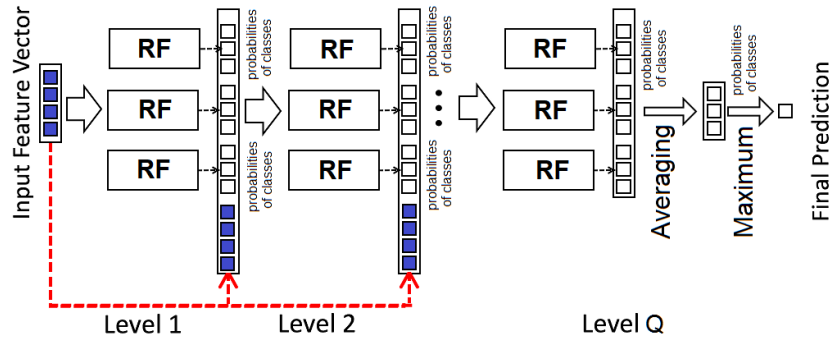


Fig. 2. The modified architecture of a level incorporating the multi-head attention

the above expression that  $\hat{\mathbf{x}}(i)$  can be viewed as the weighted average over the vectors from  $S$  which are close to  $\mathbf{x}$ . It is important to point out that attention mechanism parameters for obtaining  $\hat{\mathbf{x}}(i)$  can be optimized. However, these approaches complicate the training procedure, and we use the simplest averaging based on Gaussian kernel.

In order to indicate that the multi-head attention with  $H$  heads is used, we will denote the mean vectors  $\hat{\mathbf{x}}(i)$  and the vector  $\mathbf{v}(i)$  of the class probabilities as  $\hat{\mathbf{x}}(i, h)$  and  $\mathbf{v}(i, h)$ , where  $i$  is the number of the RF,  $i = 1, \dots, F$ ,  $h$  is the number of the head in the multi-head attention,  $h = 1, \dots, H$ . So, the prediction of the  $i^{\text{th}}$  RF at the first cascade, which is used in the  $h^{\text{th}}$  head of the attention, is the vector of probabilities  $\mathbf{v}(i, h)$ . We propose to concatenate the vectors  $\hat{\mathbf{x}}(i, h)$  and  $\mathbf{v}(i, h)$  in order to use the extended RF output  $(\hat{\mathbf{x}}(i, h) \parallel \mathbf{v}(i, h))$ . If there are  $F$  RFs at the level, then their outputs  $(\hat{\mathbf{x}}(i, h) \parallel \mathbf{v}(i, h))$ ,  $i = 1, \dots, F$ , can be combined by applying the multi-head attention with  $H$  heads. In this case, we obtain  $H$  embedding vectors  $\mathbf{e}^{(h)}(i)$ , which can be concatenated for training the next level of the DF. The concatenated vector denoted as  $\mathbf{E}$  is transformed to a vector  $\mathbf{x}_{new}$  of the smaller size to use it at the next level of the DF cascade. This scheme is repeated for each level.

The proposed attention-based architecture of the DF level is shown in Fig. 2. One can see from Fig. 2 that the input vector  $\mathbf{x}$  is fed  $F$  to RFs (RF- $i$ ), which provide mean vectors  $\hat{\mathbf{x}}(i, h)$  and the probabilities of classes  $\mathbf{v}(i, h)$ . Then concatenated vectors  $\hat{\mathbf{x}}(i, h) \parallel \mathbf{v}(i, h)$  are attended with the vector  $\mathbf{x}$  (Attent  $h$ ), and we obtain  $H$  vectors  $\mathbf{e}^{(h)}(i)$ , which are concatenated to each other into the vector  $\mathbf{E}$ . After that, the vector  $\mathbf{x}_{new}$  is calculated as  $\mathbf{x}_{new} = \mathbf{W}_c \mathbf{E}$ , where the matrix  $\mathbf{W}_c$  is trained jointly with the attention modules. Predictions of each head in the multi-head attention depend on subset of samples that correspond to the head: only samples from the subset are used to reconstruct the input vector and to estimate the class probabilities. The subsets for heads are generated using  $H$ -fold division of the training set  $S$ . The attention parameters are trained by using the same folds.

The proposed architecture has several advantages. First of all, it is flexible. We can change the number of RFs, the number of heads in the multi-head attention. We can change sizes of embeddings  $\mathbf{e}^{(h)}(i)$ , the size of the vector  $\mathbf{x}_{new}$ . All attention modules as well as the procedure of reducing the concatenated vector  $(\mathbf{e}^{(h)}(1) \parallel \dots \parallel \mathbf{e}^{(h)}(H))$  to the vector  $\mathbf{x}_{new}$  have trainable parameters which allow us to obtain the best results. Secondly, we can reduce the number of RFs, which are hardly trained, by increasing the number of heads in the multi-head attention. This is a very important feature of the attention-based architecture. Thirdly, changing parameters of each level, we can obtain the heterogeneous structure of the DF, which leads to improved predictions of the whole model.

The simplest implementation of the attention-based DF is when the non-parametric attention mechanisms are used and the output feature vector  $\mathbf{x}_{new}$  is obtained by averaging the vectors  $\mathbf{e}^{(h)}(1), \dots, \mathbf{e}^{(h)}(H)$ . In this case, we train only the RFs. Other components are performed by computing their outputs under condition of certain inputs.

## Numerical Experiments

In order to illustrate the attention-based DF, we investigate the model for datasets from UCI Machine Learning Repository [33]. Table 1 is a brief introduction about these datasets, while more detailed information can be found from the data resources. Table 1 contains the number of features  $m$  for the corresponding data set, the number of instances  $n$  and the number of classes  $C$ .

The ABDF implementation is based on the Bosk framework which is available at <https://github.com/NTAILab/bosk>.

Each level of the cascade structure consists of two RFs, each RF consists of 100 decision trees for almost all datasets except for the datasets WDBC, TTTE and Biodeg where numbers of trees in the corresponding RFs are 1000, 500, 500. The number of cascade levels is taken 3. The number of heads in the multi-head attention is 4.

Accuracy measure  $A$  used in numerical experiments is the proportion of correctly classified cases on a sample of data. To evaluate the average accuracy, we perform a cross-validation with 100 repetitions, where in each run, we randomly select  $n_{tr} = 3n/4$  training data and  $n_{test} = n/4$  testing data. Different values for the hyperparameters were tested, choosing those leading to the best results.

Numerical results of comparison of the original DF and the ABDF are shown in Table 2, where the first column contains abbreviations of the tested data sets, the second column contains the accuracy (the mean and standard deviation) of the ABDF, the third column contains accuracy values of the original DF. It can be seen from Table 2 that the proposed attention-based DF outperforms the original DF for most considered datasets.

Another interesting question is how the number of heads in the multi-head attention impacts the prediction accuracy. To study this question, datasets WDBC and TTTE are used, and the accuracy measures are obtained for numbers of heads 2, 4, and 6. The corresponding values of the accuracy for the dataset WDBC are 95.34, 96.64, and 97.20. Values of the accuracy for the dataset TTTE are 96.87, 97.08, and 97.36. It can be seen from the results that the number of heads increases the classification accuracy. On the other hand, the large number of heads in the multi-head attention significantly increase the computation time for training the ABDF. An optimal number of heads can be selected only in the testing phase.

Table 1

### Brief introduction to datasets

Data set	Abbreviation	$m$	$n$	$C$
Haberman's Breast Cancer Survival	Haberman	3	306	2
Ionosphere	Ion	34	351	2
Seeds	Seeds	7	210	3
Teaching Assistant Evaluation	TAE	5	151	3
Tic-Tac-Toe Endgame	TTTE	9	958	2
QSAR Biodegradation	Biodeg	41	1055	2
Parkinsons	Parkinsons	22	195	2
Connectionist Bench	Sonar	60	208	2
SPECT Heart	SPECT	22	267	2
SPECTF Heart	SPECTF	44	267	2
Breast Cancer Wisconsin	WDBC	30	569	2

Table 2

Accuracy values (the mean and standard deviation) for comparison of the ABDF with the original DF

Dataset	ABDF	DF
Haberman	71.69±3.38	67.4±4.25
Ion	93.98±1.76	91.7±2.74
Parkinsons	92.65±2.08	91.84±3.65
Seed	95.28±3.50	93.21±2.56
SPECTF	80.15±4.63	81.04±4.43
SPECT	82.94±4.33	82.18±6.46
WDBC	96.41±2.14	95.31±1.90
Sonar	85.77±5.52	83.08±4.11
TAE	61.05±8.47	59.74±7.81
TTTE	97.92±1.05	97.63±0.93
Biodeg	86.63±1.38	87.27±1.65

### Conclusion

The paper presented a new efficient modification of the DF. The main idea behind the proposed model is to incorporate the multi-head attention into each level of the DF. Numerical experiments showed that this idea leads to the model that outperforms the original DF.

The proposed model has several advantages. First, it allows us to reduce the number of RFs by increasing the number of heads in the multi-head attention mechanism at each level of the DF cascade. We can even use a single RF because the multi-head attention plays role of the base models like RFs. Secondly, it provides outperforming results due to usage of the attention-mechanism. Thirdly, it is flexible due to the data representation at the levels of the DF. Indeed, the output vector  $\mathbf{x}_{new}$  can have a structure different from the input vector produced by the previous level. As a results, RFs at the next level do not depend on RFs from the previous level, and we can expect better results due to some kind of the diversity of the base models. Fourthly, the ABDF opens the door for developing new modifications of the DF based on various forms of the attention mechanism. One of the direct modifications is to change the procedure for computing the average feature vector  $\hat{\mathbf{x}}(i)$  producing by the  $i^{\text{th}}$  RF. We used the simplest procedure of weighted averaging of all vectors that fall into leaves jointly with the vector  $\mathbf{x}(i)$ . However, the self-attention can be applied to take into account the context of data as it is performed in Transformers. The self-attention can be incorporated into the multi-head attention. The above modifications as well as many other ones can be regarded as directions for further research.

### REFERENCES

1. Rokach L. Ensemble-based classifiers. *Artificial Intelligence Review*, 2010, Vol. 33 (1-2), pp. 1–39.
2. Zhou Z.-FI. Ensemble Methods: Foundations and Algorithms. CRC Press, Boca Raton, 2012.
3. Breiman L. Bagging predictors. *Machine Learning*, 1996, Vol. 24 (2), pp. 123–140.
4. FI D. Stacked generalization. *Neural networks*, 1992, Vol. 5 (2), pp. 241–259.
5. Freund F.I., Schapire R.E. A decision theoretic generalization of on-line learning and an application to boosting. *Journal of Computer and System Sciences*, 1997, Vol. 55 (1), pp. 119–139.
6. Breiman L. Random forests. *Machine learning*, 2001, Vol. 45 (1), pp. 5–32.

7. **Zhou Z.-FI., Feng J.** Deep forest: Towards an alternative to deep neural networks. Proceedings of the 26<sup>th</sup> International Joint Conference on Artificial Intelligence (IJ-CAI17), strony 3553–3559, Melbourne, Australia, AAAI Press, 2017.
8. **Shen-Huan Lyu, Yi-Xiao He, Zhi-Hua Zhou.** Depth is more powerful than width with prediction concatenation in deep forest. *Advances in Neural Information Processing Systems*, 2022, no. 35, pp. 29719–29732.
9. **Miller K., Hettinger C., Humpherys J., Jarvis T., Kartchner D.** Forward thinking: Building deep random forests. arXiv:1705.07366, 20 May 2017.
10. **Pang M., Ting K.M., Zhao P., Zhou Z.-FI.** Improving deep forest by confidence screening. Proceedings of the 18<sup>th</sup> IEEE International Conference on Data Mining (ICDM18), strony 1–6, Singapore, 2018.
11. **Utkin L.V.** An imprecise deep forest for classification. *Expert Systems with Applications*, 2020, Vol. 141 (112978), pp. 1–11.
12. **Utkin L.V., Konstantinov A.V., Chukanov V.S., Meldo A.A.** A new adaptive weighted deep forest and its modifications. *International Journal of Information Technology & Decision Making*, 2020, Vol. 19 (4), pp. 963–986.
13. **Utkin L.V., Ryabinin M.A.** A Siamese deep forest. *Knowledge-Based Systems*, 2018, no. 139, pp. 13–22.
14. **Wen FI., Zhang J., Lin Q., Yang K., Jin T., Lv F., Pan X., Huang P., Zha Z.-J.** Multi-level deep cascade trees for conversion rate prediction. arXiv:1805.09484, May 2018.
15. **Heng Xia, Jian Tang, Junfei Qiao, Jian Zhang, Wen Yu.** DF classification algorithm for constructing a small sample size of data-oriented DF regression model. *Neural Computing and Applications*, 2022, Vol. 34 (4), pp. 2785–2810.
16. **Zhang X., Wang M.** Weighted random forest algorithm based on bayesian algorithm. *Journal of Physics: Conference Series*, wolumen 1924, strona 012006. IOP Publishing, 2021.
17. **Soheila Molaeei, Amirhossein Havvaei, Hadi Zare, Mahdi Jalili.** Collaborative deep forest learning for recommender systems. *IEEE Access*, 2021, no. 9, pp. 22053–22061.
18. **Bishnupriya Panda, Shrabanee Swagatika, Sipra Sahoo, Debabrata Singh.** A novel approach for breast cancer data classification using deep forest network. *Intelligent and Cloud Computing: Proceedings of ICICC 2019*, Springer, 2021, no. 2, pp. 309–316.
19. **Liang Sun, Zhanhao Mo, Fuhua Yan, Liming Xia, Fei Shan, Zhongxiang Ding, Bin Song, Wanchun Gao, Wei Shao, Feng Shi, i in.** Adaptive feature selection guided deep forest for covid-19 classification with chest ct. *IEEE Journal of Biomedical and Health Informatics*, 2020, Vol. 24 (10), pp. 2798–2805.
20. **Ran Su, Xinyi Liu, Leyi Wei, Quan Zou.** Deep-resp-forest: a deep forest model to predict anti-cancer drug response. *Methods*, 2019, no. 166, pp. 91–102.
21. **Tianchi Zhou, Xiaobing Sun, Xin Xia, Bin Li, Xiang Chen.** Improving defect prediction with deep forest. *Information and Software Technology*, 2019, no. 114, pp. 204–216.
22. **Utkin L.V., Konstantinov A.V.** Attention-based random forest and contamination model. *Neural Networks*, 2022, no. 154, pp. 346–359.
23. **Niu Z., Zhong G., Yu FI.** A review on the attention mechanism of deep learning. *Neurocomputing*, 2021, no. 452, pp. 48–62.
24. **Chaudhari S., Mithal V., Polatkan G., Ramanath R.** An attentive survey of attention models. *ACM Transactions on Intelligent Systems and Technology*, 2021, Vol. 12 (5), pp. 1–32. Article 53.
25. **Correia A.S., Colombini E.L.** Attention, please! A survey of neural attention models in deep learning. *Artificial Intelligence Review*, 2022, Vol. 55 (8), pp. 6037–6124.
26. **Lin T., Wang FI., Liu X., Qiu X.** A survey of transformers. arXiv:2106.04554, Jul 2021.
27. **Nadaraya E.A.** On estimating regression. *Theory of Probability & Its Applications*, 1964, Vol. 9(1), pp. 141–142.
28. **Watson G.S.** Smooth regression analysis. *Sankhya: The Indian Journal of Statistics, Series A*, 1964, pp. 359–372.
29. **Bahdanau D., Cho K., Bengio FI.** Neural machine translation by jointly learning to align and translate. arXiv: 1409.0473, Sep 2014.

30. **Luong T., Pham FI., Manning C.D.** Effective approaches to attention-based neural machine translation. Proceedings of the 2015 Conference on Empirical Methods in Natural Language Processing, The Association for Computational Linguistics, 2015, pp. 1412–1421.

31. **Vaswani A., Shazeer N., Parmar N., Uszkoreit J., Jones L., Gomez A.N., Kaiser L., Polosukhin I.** Attention is all you need. Advances in Neural Information Processing Systems, 2017, pp. 5998–6008.

32. **Huber P.J.** Robust Statistics. Wiley, New York, 1981.

33. **Lichman M.** UCI machine learning repository, 2013. <https://archive.ics.uci.edu/ml/index.php>

#### **INFORMATION ABOUT AUTHORS / СВЕДЕНИЯ ОБ АВТОРАХ**

**Andrei V. Konstantinov**

**Константинов Андрей Владимирович**

E-mail: [andrue.konst@gmail.com](mailto:andrue.konst@gmail.com)

<https://orcid.org/0000-0003-2275-1473>

**Lev V. Utkin**

**Уткин Лев Владимирович**

E-mail: [lev.utkin@gmail.com](mailto:lev.utkin@gmail.com)

<https://orcid.org/0000-0002-5637-1420>

**Stanislav R. Kirpichenko**

**Кирпиченко Станислав Романович**

E-mail: [kirpichenko.sr@gmail.com](mailto:kirpichenko.sr@gmail.com)

<https://orcid.org/0000-0003-2275-1473>

*Submitted: 28.05.2023; Approved: 25.06.2023; Accepted: 06.07.2023.*

*Поступила: 28.05.2023; Одобрена: 25.06.2023; Принята: 06.07.2023.*



Research article

DOI: <https://doi.org/10.18721/JCSTCS.16202>

UDC 62-503.55



## CLOUD DISTRIBUTED CONTROL SYSTEM BASED ON OPEN PROCESS AUTOMATION PLATFORM

*V.V. Potekhin*<sup>1</sup>  , *A.P. Alekseev*<sup>2</sup>,  
*E.V. Kuklin*<sup>3</sup>, *Ya.D. Khitrova*<sup>4</sup>, *Yu.N. Kozhubaev*<sup>5</sup>

<sup>1,2,3,4,5</sup> Peter the Great St. Petersburg Polytechnic University,  
St. Petersburg, Russian Federation

 [Slava.Potekhin@spbstu.ru](mailto:Slava.Potekhin@spbstu.ru)

**Abstract.** The article shows the relevance of using cloud technologies in the field of industrial automation of technological processes. Typical architectures of modern automated control systems, as well as new standards and approaches to the design of industrial control systems developed by international communities are analyzed. A prototype of an open cloud distributed control system based on IEC 61131 has been demonstrated. The dependences of the computing power of virtual controllers on the number of processed objects are given. The Open Process Automation initiative aims to enhance the full lifecycle benefits of industrial control systems through the use of a standards-based, open, secure, interoperable architecture and open business model. The OPAS standard based on this initiative uses a “standard of standards” approach.

**Keywords:** Industry 4.0, OPAS, Cloud DCS, Cloud computing, Internet of Things

**Citation:** Potekhin V.V., Alekseev A.P., Kuklin E.V., et al. Cloud distributed control system based on open process automation platform. Computing, Telecommunications and Control, 2023, Vol. 16, No. 2, Pp. 17–28. DOI: 10.18721/JCSTCS.16202

Научная статья

DOI: <https://doi.org/10.18721/JCSTCS.16202>

УДК 62-503.55



## ОБЛАЧНАЯ РАСПРЕДЕЛЕННАЯ СИСТЕМА УПРАВЛЕНИЯ НА БАЗЕ ОТКРЫТОЙ ПРОМЫШЛЕННОЙ ПЛАТФОРМЫ АВТОМАТИЗАЦИИ

*В.В. Потехин<sup>1</sup> , А.П. Алексеев<sup>2</sup>,  
Е.В. Куклин<sup>3</sup>, Я.Д. Хитрова<sup>4</sup>, Ю.Н. Кожубаев<sup>5</sup>*

<sup>1,2,3,4,5</sup> Санкт-Петербургский политехнический университет Петра Великого,  
Санкт-Петербург, Российская Федерация

✉ [Slava.Potekhin@spbstu.ru](mailto:Slava.Potekhin@spbstu.ru)

**Аннотация.** Сегодня массовое сотрудничество в сфере разработки программного обеспечения и открытых архитектур меняет фундаментальную структуру бизнеса и перестраивает методы работы организаций в условиях жесткой конкуренции. В статье показана актуальность использования облачных технологий в сфере промышленной автоматизации технологических процессов. Разобраны типовые архитектуры современных АСУ ТП, а также разрабатываемые международными сообществами новые стандарты и подходы к проектированию промышленных систем управления. Продемонстрирован прототип открытой облачной распределенной системы управления на базе МЭК 61131. Приведены зависимости вычислительной мощности виртуальных контроллеров от количество обрабатываемых объектов. Инициатива Open Process Automation направлена на улучшение всех преимуществ жизненного цикла промышленных систем управления благодаря использованию основанной на стандартах, открытой, безопасной, совместимой архитектуры и открытой бизнес-модели. Стандарт OPAS на базе этой инициативы использует подход «стандарт стандартов». В рамках тестирования архитектуры в соответствии с OPAS был сделан ряд выводов об использовании технологии.

**Ключевые слова:** Индустрия 4.0, OPAS, облачная PCSU, облачные вычисления, АСУ ТП, интернет вещей, архитектура автоматизации

**Для цитирования:** Potekhin V.V., Alekseev A.P., Kuklin E.V., et al. Cloud distributed control system based on open process automation platform // Computing, Telecommunications and Control. 2023. Т. 16, № 2. С. 17–28. DOI: 10.18721/JCSTCS.16202

### Introduction

Today, massive collaboration in software development and open architectures is changing the fundamental structure of business and reshaping the way organizations operate in a highly competitive environment. Collaboration fueled by open methodologies and peer-to-peer production, is forcing management to rethink their strategies. Organizations that previously built proprietary systems are beginning to develop open-source products and creating public foundations where everyone can develop and contribute to push the boundaries of their business as well as the boundaries of the industries in which they operate.

It is important to note that at the moment, the development under the Open Source concept is far advanced in the field of information technology (IT), but in the field of industrial automation is still dominated by the proprietary segment. Companies are reluctant to disclose their code base, mainly the flagships of programmable logic controllers (PLC, PLC) and SCADA have closed interfaces, which do not easily create a synergy of equipment from different manufacturers, forcing companies to use the products of one company [1].

The lag of operation technologies (OT) from IT is caused by the fact that the development of open solutions is not fully supported by large companies and spheres. Open Source developers are not only small

startups looking for new revolutionary solutions. These are companies with billions of dollars: Google, Apple, Facebook, Amazon, releasing their products with open source code, available for modification to each individual developer.

To develop OT at the same speed as IT, it is necessary to move to the concept of an open industrial platform, where development is carried out jointly with developers interested in improving products, free competition, and rapid implementation of new technologies in existing facilities. Previously, the IT sphere borrowed the concept of lean manufacturing and developed the DevOps methodology for continuous product improvement. In the OT-sphere it is necessary to borrow the Open Source concept as one of the options for the effective implementation of new tools and technologies in the field of industrial automation. The Open Process Automation Forum (OPAF) is addressing this challenge.

The article discusses new methods for solving process control problems, as well as the results of their application on assembled laboratory benches.

### **Open industrial automation platform standards**

Open Process Automation is an industry initiative aimed at improving the full lifecycle benefits of industrial control systems through the use of a standards-based, open, secure, interoperable architecture and open business model. The Open Process Automation Forum of The Open Group is the primary beneficiary. As of July 2022, OPAF consists of 800 member organizations, most major distributed control system (DCS) vendors, many hardware and software vendors, and system integrators [2].

The OPAF standards and architecture implement the new Industry 4.0 concepts of Cloud, Edge, and Field computing, while allowing legacy management systems to be connected. The standards are generic guidelines for the design of process control systems in the new paradigm.

Quality attributes have been defined as goals for the Open Process Automation Standard (OPAS):

- Interoperability,
- Modularity,
- Scalability,
- Securability,
- Reliability,
- Portability,
- Affordability,
- Availability,
- Discoverability,
- Evolvability,
- Manageability,
- Compatibility,
- Configurability,
- Discoverability,
- Usability,
- Flexibility,
- Testability,
- Reusability,
- Traceability.

The attributes of interoperability and portability are basic compared to currently available commercial RSCs and PLCs.

A “standard of standards” approach is used to define the standard. OPAF has interoperability agreements that allow information to be exchanged before publication with many organizations, including NAMUR, ZVEI, and PL Copen.

#### 1. Architecture



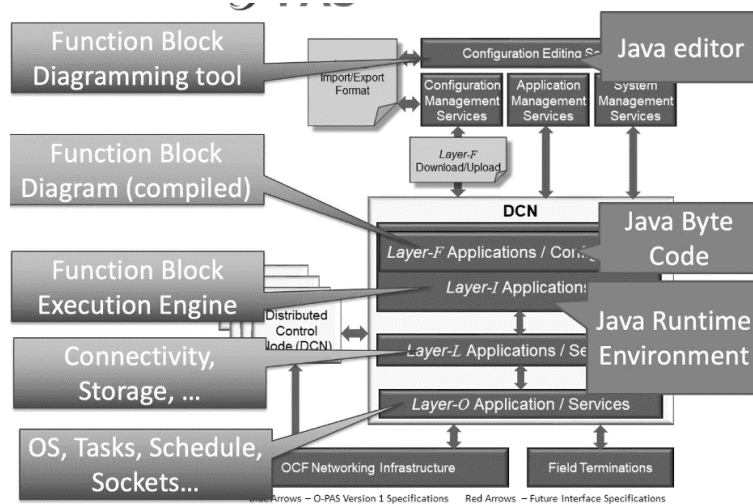


Fig. 2. Application structure of DCN

Enterprise IT Data Centers has the largest computing power and is responsible for the primary accounting of equipment, collecting heterogeneous technological information, aggregation, forecasting and reporting. [5] From this component, information about the composition of the installed equipment, the assignment of IP-addresses to network devices, the locations of devices is taken. This is also where the log collector is located.

## 2. Prototype of Cloud-based DCS

### 2.1 Prototype of ExxonMobil

ExxonMobil has developed a prototype that meets the quality attributes described earlier in this article. The essence of the experiments they performed on the prototype are described in the figure below.

Interoperability is the ability of two or more systems/components to exchange and use information. This was demonstrated by combining components from 10 different vendors into a single system. For example, three components were used to perform a simple PID control cycle: one component provided input, another component performed PID calculation, and the third component sent output to the field.

Interchangeability is the ability to replace one component with another while the system continues to operate. Basic I/O and regulatory control were originally performed in an IEC 61499 environment on a Raspberry Pi device. This device was replaced with a DCN provided by Intel.

Configuration portability is the ease with which configuration information can be exported from one application, imported, and then deployed to another application. The control function was originally run in an IEC 61499 runtime environment provided by 4DIAC, which is an open source implementation of the IEC 61499 standard. The configuration of this application was exported and imported into another IEC 61499 environment. Finally, the information was deployed and successfully implemented in another execution engine provided by NXTControl, which is a commercial implementation of IEC 61499.

Application portability is the ease with which an application running in one environment can be re-assigned and deployed to another environment. A simple PID control algorithm was run on an edge in a DCN provided by Intel. The controller was reassigned and deployed in an NXTControl environment running in ACP.

### 2.2 Structured description of prototype

We managed not only to repeat the experiments described above, but also to carry out high-load tests of a physical DCN and a virtual DCN.

A schematic of the prototype and scenarios are shown in Figure 4.

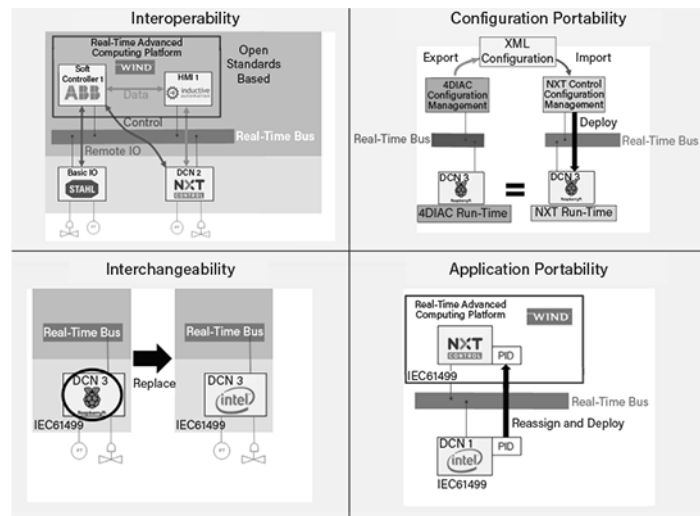


Fig. 3. Checking quality attributes

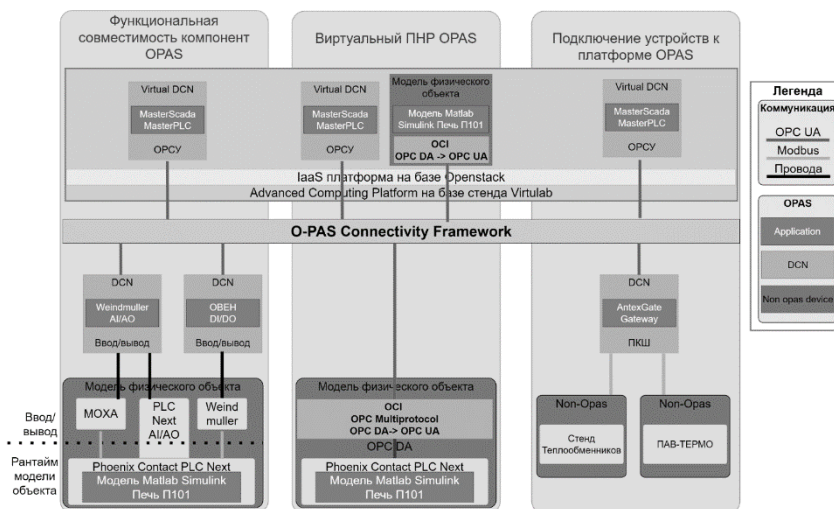


Fig. 4. Architecture of platform prototype

The stand was based on an open IaaS platform used as an ACP. Soft-PLC, virtual controllers running on Linux OS, were used as DCNs.

In our case the evaluation of quality attributes was as follows:

– Interoperability was demonstrated by combining components from several different vendors into a single system. For example, a virtual DCN took over the function of PID control, while the other two physical DCNs from different vendors were responsible for analog and discrete signals.

– Interchangeability: a physical DCN was replaced by a virtual DCN with the same program. It also shows the attribute of application portability.

We were able to apply a gateway to connect non-OPAS devices to the shared bus. It was also possible to test the possibility of virtual NDP-code debugging on the virtual controller and model with further loading into the physical DCN.

### 2.3 Test results

The results of the prototype testing are presented in this paragraph. Testing involved determining and comparing groups of characteristics by performing the checks listed below:

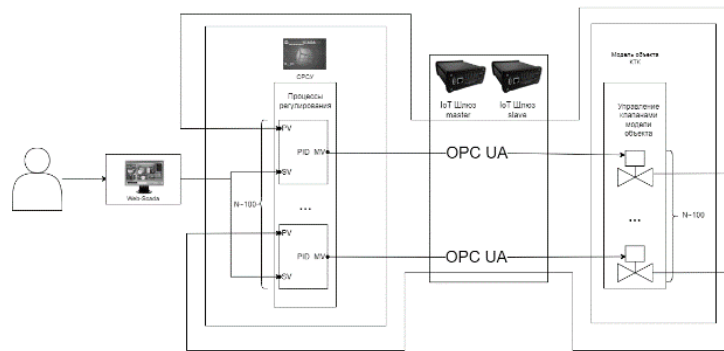


Fig. 5. Common diagram of test

- High-load testing.
- Testing of cloud NMC for signal throughput rate.
- Cloud NMC backup in the cloud.

#### Test 1 – High-load testing

This test verifies compliance with virtual DCN target function requirements by establishing and comparing functionality and characteristics.

The user sets setpoints/process variables (SV) of PID controllers from the web SCADA (web-SCADA). The cloud distributed control system (CDCS) controller implements PID control loops, which supply control actions – control of valve opening percentage. The calculated percentage of valve opening in the controller is transmitted to the objects in the model via IIoT-gateway over the OPC UA protocol. The number of PID controllers is about 100. In addition, the current values of analog sensors and the forecast value are displayed.

User can also change the mode of PID-controllers (AUT-MAN-CASCAD), set values to the valve output in the manual PID-controller mode, and change PID-controller coefficients from web SCADA (web-SCADA).

This test allows you to set the maximum loads on the cloud-based DCS.

Tests were conducted on a virtual machine with the following computing characteristics:

- CPU: Intel Xeon Processor (Cascadelake) 2.7 GHz 1 Core;
- RAM: 2 GB;
- ROM: 20 GB;
- Network adapter: 10GbE Intel C622, 1000 Mb/s.

#### Test Order:

1. The telemetry values are read without load.
2. Next, the projects were loaded into the cloud-based DCS controller for 50, 100, 150, and 200 sensors in turn, and then telemetry readings were taken for each option.

3. We added node power to 2 CPUs and up to 4 GB of RAM, and then performed steps 1–2 again.

Examples of test results are shown in Figures 6–8.

CPU load was unloaded as a percentage.

RAM load was loaded in absolute ratio.

Average cycle time was calculated in absolute value:

$$\text{Cycle time} = K * x,$$

where  $K$  is adjustment factor,  $x$  is the number of sensors/objects

As a result of the test, the readings of telemetry without load, as well as with load at 50, 100, 150 and 200 sensors were measured. As the number of sensors increases, the telemetry readings increase linearly.

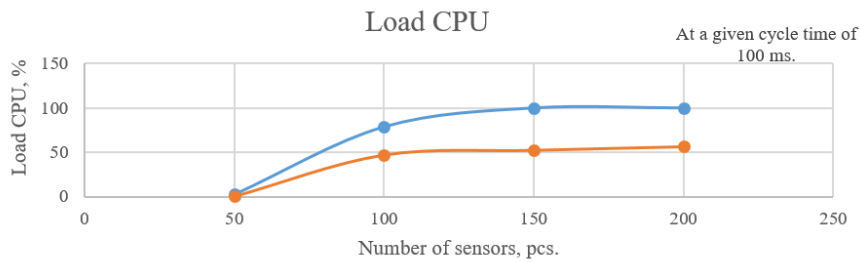


Fig. 6. Load CPU

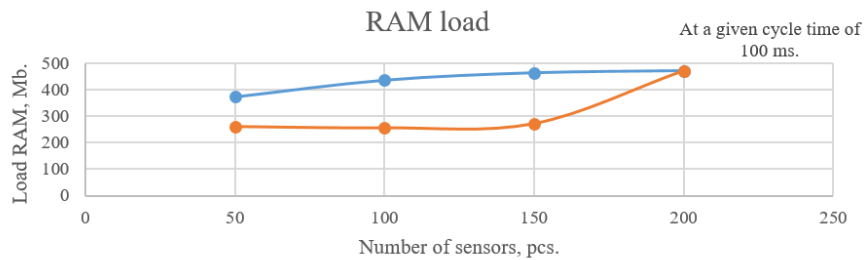


Fig. 7. Load RAM

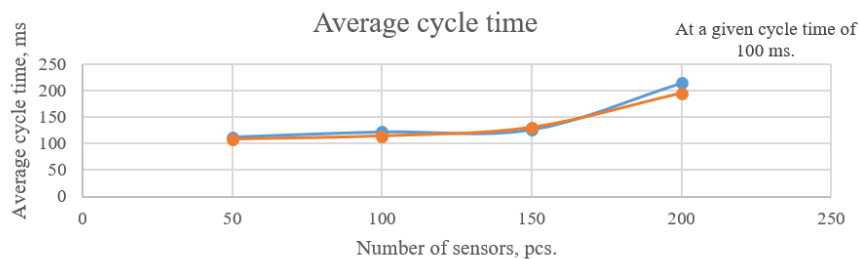


Fig. 8. Average cycle time

When processing 200 sensors with predictive analytics, there is a 120 ms deviation in controller cycle time, which is 120%. With this virtual machine configuration, no more than 150 sensors can be effectively controlled. After increasing the computing power of the virtual machine on which the runtime environment is deployed, the behavior of the node did not change: when the number of sensors is increased, the telemetry readings grow linearly.

**Test 2. OPC-testing for signal throughput rate**

In this test we check the speed of signals passing through the full route (SCADA – DCN – IIoT-gateway – Output Device – Input Device – IIoT-gateway – DCN – SCADA).

This test verifies compliance with the virtual DCN's target function requirements by establishing and comparing functionality and features: Signal Delay Times. Signal Delay Times are fixed as follows:

- During the test, the input and output signals are recorded in the database and plotted in Web-SCADA.
- After the test passes, the csv file with the time stamps and the corresponding values on the input and output signal plots should be uploaded.
- The signal delay is calculated by the difference of the input and output signal timestamps.



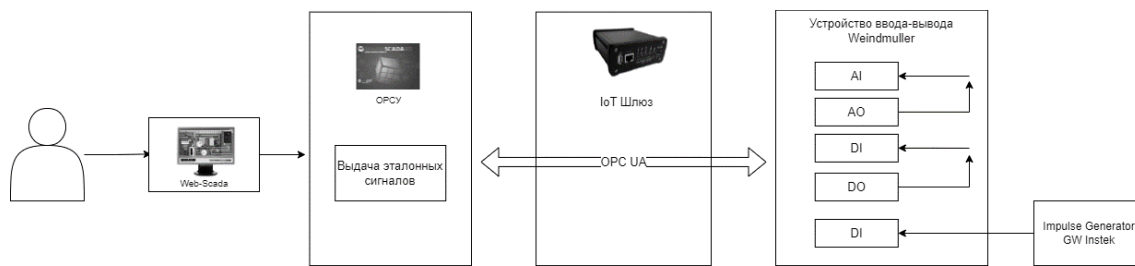


Fig. 9. Common diagram of test 2

Testing of SCADA system for performance and quality of processing of input analog and discrete signals received via physical communication channels:

1. Open SCADA system in the browser, “Speed” tab.
2. Start generation of signals in the form of a sine wave with a period of 10, 60 and 100 seconds.

As a result of the test, the performance and processing quality of the input analog and discrete signals received via physical communication channels were tested. The average delay for all signals was 108 ms. Generation of signals from the signal setter is displayed in Web-SCADA without data loss. The delay was calculated using the following formula:

$$\text{Delay} = T_{in} - T_{out},$$

where  $T_{in}$  is input signal time,  $T_{out}$  is output signal time.

### Test 3. OPC redundancy in the cloud

Web-SCADA and soft-PLC were created in the MasterSCADA development environment. MasterSCADA allows you to organize the redundancy of the runtime system. The program is loaded to the controller copy, executed in parallel without I/O access, while the main (master) controller is running. As soon as the failure occurs in the main controller, the system switches to the second (standby) controller without significant delays and suspension of the programs execution with duplication of the current states in the previous controller. After control transition, the standby controller is not initialized with initial values; it contains the same values as the primary controller.

This test demonstrates the results of redundancy, both the hardware part (disconnecting the compute node from power) and the software part (disconnecting the virtual machine). As the virtual machine is deployed on one of the compute nodes, its shutdown will be the same as that of the compute node.

Testing of the system for redundancy is done as follows: on the redundancy tab, there is a counter, which is incremented every half a second. After starting the counter you need to shut down virtual machine/computing node, where virtual controller is deployed.

When incrementing the counter, all values are written to the database on the local controller (each to its own).

After the main controller shutdown, control went to the backup controller's virtual machine. The standby controller started writing values from 66, which suggests that about 6 values were lost during the switchover. This amounts to about 1.5 seconds (2 values once per second).

Results of the test:

- MasterSCADA allows implementing software redundancy. Computing nodes implement hardware redundancy (redundant virtual machines are located on different computing nodes).
- Switching delay was about 1.5 seconds.
- MasterSCADA does not record the data in the backup archive, until the moment of switching controllers.

Software, developed on the basis of the IEC 61131 standard [6], as MasterSCADA in the prototype of OCSADA, in recent years is criticized because of non-compliance with modern methods of software de-

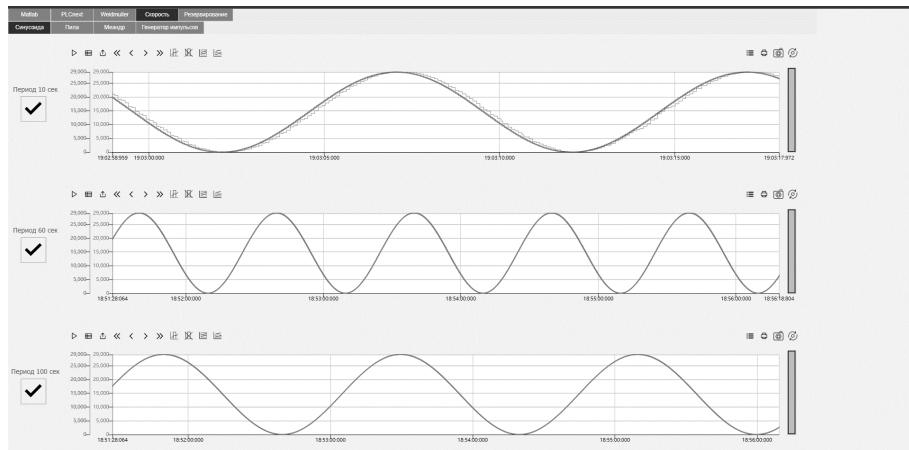


Fig. 10. Signal generation

velopment. Current IEC 61131-3 [7] compliant software architectures for industrial process measurement and control systems do not conceptually support reconfiguration and distribution. On the other hand, according to the articles “Design and Execution Issues in IEC 61499 Distributed Automation and Control Systems” [8] and “Is IEC 61499 in Harmony with IEC 61131-3” [9] identified as requirements for future automation systems:

*Portability.* Software tools can open and correctly interpret program components and system configuration that were developed in other software tools.

*Configurability.* Any device and its software components can be configured by software tools from multiple vendors.

*Interoperability.* Distributed devices can communicate with each other to perform the functions of a distributed control system.

*Reconfigurability.* Software tools can change software and hardware configuration while the device is running.

*Distributability.* Software components can be distributed to different devices in the system.

To address the limitations as well as new challenges in the development of industrial automation systems, the technical committee of the International Electrotechnical Commission (IEC) was tasked with developing a new standard. The standard was named IEC 61499.

### Conclusion

The Open Process Automation initiative aims to improve the full lifecycle benefits of industrial control systems through the use of a standards-based, open, secure, interoperable architecture and an open business model. The OPAS standard, based on this initiative, takes a “standards standard” approach. As part of the OPAS architecture testing, the following conclusions were drawn.

For test 1 on the high-load test, telemetry readings were measured without load as well as with load when 25, 50, 75, and 100 PID controllers were operating. As the number of PIDs increases, the telemetry readings increase linearly. At the same time, it was proven possible to dynamically change the maximum computing power on the virtual machine, thereby allowing the virtual controller to load more objects. The 25 controls increase the RAM fill by about 20 MB, the CPU load by 10%. CPU load increases quite quickly when you increase the number of PID controllers, it may be worth increasing the number of cores in the virtual machine with a multiple increase in objects. With this configuration the virtual controller will run 200 PID controllers.

For test 2 on the speed of signals, we tested the performance and processing quality of the input analog and discrete signals received through the physical communication channels. The average delay

for all signals was 108 ms. Signal generation from the signal setter was displayed in Web-SCADA without data loss.

For test 3 on redundancy of the OPC in the cloud, the processes occurring when one of the nodes is powered down were investigated. The switching of the control servers occurs seamlessly for the system components. When power fails on the control node, control shifts to the backup node; delays are observed only in the operation of the web interface of the IaaS platform. If the control server is restarted, the web-interface crashes with an error until the server reboots. MasterSCADA allows you to implement software redundancy. Compute nodes implement hardware redundancy (redundant virtual machines are on different compute nodes).

OPAS includes standards that result in portability and interoperability. One such standard is IEC 61499. The IEC 61499 standard is part of the OPAS architecture. The requirements of this standard for the control system are the same as those for OPAS. This standard mainly differs from the IEC 61131 standard in the way functional blocks are processed. In IEC 61499 the processing of functional blocks is event-driven: event inputs and outputs are added to the interface of the functional block.

As a result of the work, new methods and technologies for solving process control problems on the basis of the assembled laboratory bench were considered. Tests were conducted to show how the process can change with the application of new control approaches and what the benefits of their use are.

## REFERENCES

1. Church P., Mueller H., Ryan C., Gogouvis S.V., Goscinski A., Tari Z. Migration of a SCADA system to IaaS clouds – a case study. *Journal of Cloud Computing: Advances, Systems and Applications*, 2017, pp. 6–12.
2. Bartusiak R.D., Bitar S., L.DeBari D., Houk B.G., Heaton M., Strebel R., Stevens D., Fitzpatrick B., Sloan P. Open Process Automation: A standards-based, open, secure, interoperable process control architecture, 2020, pp. 2–3.
3. Lizhi Wang, Yanuyan Qin, Zefan Tang, Peng Zhang P. Software-Defined Microgrid Control: The Genesis of Decoupled Cyber-Physical Microgrids. *IEEE Open Access J. Power Energy*, 2020, pp. 173–182.
4. Wenbin D., Laurynas R., Peng W., Valeriy V., Xinping G. A Cloud-Based Decision Support System for Self-Healing in Distributed Automation Systems Using Fault Tree Analysis. *IEEE Transactions on Industrial Informatics*. 2018, pp. 989–1000.
5. Vrba P., Tichý P., Mařík V., Hall K.H., Staron R.J., Maturana F.P., Kadera P. Rockwell Automation's Holonic and Multiagent Control Systems Compendium. *IEEE Transactions on Systems, Man, and Cybernetics, Part C: Applications and Reviews*. 2011, Vol. 41, pp. 14–30.
6. International Electrotechnical Commission. IEC International Standard IEC 61131–3: Programmable Controllers, Part 3: Programming Languages, IEC. 2003.
7. Otto, Hellmans K. IEC 61131: A general overview and Emerging trends. *IEEE Ind. Electron. Mag.* 2009, Vol. 3, pp. 27–31.
8. Strasser T., Zoitl A., Christensen J.H., Sunder C. Design and Execution Issues in IEC 61499 Distributed Automation and Control Systems. *IEEE Transactions on Systems, Man, and Cybernetics, Part C: Applications and Reviews*. 2011, Vol. 41, no. 1, pp. 1–2.
9. Zoitl T., Strasser C., Sunder Baier T. Is IEC 61499 in harmony with IEC 61131-3? *IEEE Ind. Electron. Mag.* 2009, Vol. 3, pp. 49–55.
10. Khokhlovskiy V., Oleynikov V., Kostenko D., Onufriev V., Potekhin V. Modernisation of a Production Process Using Multicriteria Optimisation Logic and Augmented Reality. In: Proceedings of the 30<sup>th</sup> DAAAM International Symposium, DAAAM International, Vienna, Austria, 2019, pp. 0500–0507.
11. Woo E.H.C., White, P., Lai C.W.K. Ergonomics standards and guidelines for computer workstation design and the impact on users' health – a review. *Ergonomics*, 2015, Vol. 59 (3), pp. 464–475.

12. **Bucur P.A., Armbrust P., Hungerländer P.** On the propagation of quality requirements for mechanical assemblies in industrial manufacturing. *Expert Systems with Applications*. Klagenfurt, Austria, 2019.

13. **Ximing L.** Configuration, Programming, Implementation, and Evaluation of Distributed Control System for a Process Simulator. Electronic Thesis and Dissertation Repository of The University of Western Ontario. Ontario, Canada, 2015.

14. **Katalinic B., Eliseev A., Breido I., Bobryakov A., Kabanov A., Khomchenko V., Potekhin V., Stazhkov S., Filaretov V.** Experience of application of network technologies in engineering education. *EAI Endorsed Transactions on Energy Web*, 2018, Vol. 5(16).

15. **Fedorov A.V., Zobnin S.S., Potekhin V.V.** Prescriptive analytics in distributed automation systems, in Proceedings of Symposium on Automated Systems and Technologies, Hannover, PZH Verlag, 2014, pp. 43–49.

### INFORMATION ABOUT AUTHORS / СВЕДЕНИЯ ОБ АВТОРАХ

**Vyacheslav V. Potekhin**

**Потехин Вячеслав Витальевич**

E-mail: Slava.Potekhin@spbstu.ru

<https://orcid.org/0000-0001-9850-9558>

**Anton P. Alekseev**

**Алексеев Антон Павлович**

E-mail: alekseev.ap@edu.spbstu.ru

**Egor V. Kuklin**

**Куклин Егор Вадимович**

E-mail: kuklin.ev@edu.spbstu.ru

**Yana D. Khitrova**

**Хитрова Яна Дмитриевна**

E-mail: hitrova.yad@edu.spbstu.ru

**Yury N. Kozhubaev**

**Кожубаев Юрий Нурғалиевич**

E-mail: kozhubaev\_yun@spbstu.ru

*Submitted: 20.04.2023; Approved: 25.06.2023; Accepted: 06.07.2023.*

*Поступила: 20.04.2023; Одобрена: 25.06.2023; Принята: 06.07.2023.*

# Simulations of Computer, Telecommunications, Control and Social Systems

## Моделирование вычислительных, телекоммуникационных, управляющих и социально-экономических систем

Research article

DOI: <https://doi.org/10.18721/JCSTCS.16203>

UDC 519.876.5



### A SET OF SIMULATION MODELS OF WORKFLOW ELEMENTS FOR TRANSACTIONAL SERVICES OF INFOCOMMUNICATION SYSTEMS

*N.M. Redrugina*<sup>1</sup> ✉

<sup>1</sup> Bonch-Bruевич Saint Petersburg State University  
of Telecommunications, St. Petersburg, Russian Federation

✉ [redrugina.nm@sut.ru](mailto:redrugina.nm@sut.ru)

**Abstract.** This article describes the development of a set of simulation models for workflow elements related to transactional services in infocommunication systems. The article presents modeling methods used to calculate, analyze and predict various indicators of the quality of infocommunication services, such as delays, service delivery time and productivity. The necessity of using this method is due to the reduction of labor costs for modeling complex systems and the evaluation of the rationality of the developed mathematical models. The article presents the results of the study in the form of a library of components for simulation modeling, which can be used to improve the quality of transactional services in the development of modern high-load infocommunication systems. The approach described in the article is an effective tool for research and optimization of the quality of transactional services. It can be applied in various areas where analysis and improvement of the performance of data processing systems are required, including for the development of integrated solutions for big data processing, cloud computing or the development of digital counterparts of infocommunication infrastructure.

**Keywords:** simulation modeling, transactions, work-flow, infocommunication systems, fork-join, parallel processing

**Citation:** Redrugina N.M. A set of simulation models of workflow elements for transactional services of infocommunication systems. *Computing, Telecommunications and Control*, 2023, Vol. 16, No. 2, Pp. 29–39. DOI: 10.18721/JCSTCS.16203

Научная статья

DOI: <https://doi.org/10.18721/JCSTCS.16203>

УДК 519.876.5



## КОМПЛЕКС ИМИТАЦИОННЫХ МОДЕЛЕЙ ЭЛЕМЕНТОВ РАБОЧИХ ПРОЦЕССОВ ДЛЯ ТРАНЗАКЦИОННЫХ УСЛУГ ИНФОКОММУНИКАЦИОННЫХ СИСТЕМ

Н.М. Редругина<sup>1</sup> ✉

<sup>1</sup> Санкт-Петербургский государственный университет телекоммуникаций  
им. проф. М.А. Бонч-Бруевича, Санкт-Петербург, Российская Федерация

✉ [redrugina.nm@sut.ru](mailto:redrugina.nm@sut.ru)

**Аннотация.** Данная статья описывает разработку комплекса имитационных моделей элементов рабочих процессов, связанных с транзакционными услугами в инфокоммуникационных системах. В статье представлены методы моделирования, используемые для расчета, анализа и прогнозирования различных показателей качества инфокоммуникационных услуг, таких как задержки, время предоставления услуги и производительность. Необходимость применения данного метода обусловлена снижением трудозатрат на моделирование сложных систем и оценкой рациональности разработанных математических моделей. В статье представлены результаты исследования в виде библиотеки компонент для имитационного моделирования, которые могут быть использованы для повышения качества обслуживания транзакционных услуг при разработке современных высоконагруженных инфокоммуникационных систем. Описанный в статье подход является эффективным инструментом для исследования и оптимизации качества предоставления транзакционных услуг, и может быть применен в различных областях, где требуется анализ и улучшение производительности систем обработки данных, в том числе для разработки комплексных решений обработки больших данных, облачных вычислений или при разработке цифровых двойников инфокоммуникационной инфраструктуры.

**Ключевые слова:** имитационное моделирование, транзакции, work-flow, инфокоммуникационные системы, fork-join, параллельная обработка

**Для цитирования:** Redrugina N.M. A set of simulation models of workflow elements for transactional services of infocommunication systems // Computing, Telecommunications and Control. 2023. Т. 16, № 2. С. 29–39. DOI: 10.18721/JCSTCS.16203

### Introduction

The purpose of the study is to develop models for calculating and determining the qualitative characteristics of infocommunication services in general and their elements. The works [1–2] describe the reasons why it is irrational to collect statistics and analyze the behavior of the system under the influence of various external and internal factors on the functioning system, which led to the need for their modeling. In [3–6], a comparative analysis of modeling methods and their differentiation, as well as the synthesis of results, is carried out.

In the case of high labor costs for mathematical modeling of systems with complex architecture, when introducing complex distributions into the model (for example, long-tailed distributions: Weibull or Pareto), or if it is necessary to calculate error correlation, it is advisable to use simulation models, a comparative analysis of software tools for the development of which is presented in [7–8].

The goal set within the framework of this work is to develop a family of simulation models for calculating the qualitative characteristics of infocommunication loosely coupled transaction services, including the development of a library of components of the *workflow* for servicing tasks within transactional services.

To achieve this goal, the following tasks are proposed:

1. Study of the main technologies and methods of implementing transaction servicing in loosely coupled services. Including using the queuing theory apparatus.
2. Development of a workflow component Library: Creating a library that contains ready-made components used in task maintenance workflows within transactional services.
3. Implementation of simulation models: Development of software code for the implementation of simulation models based on a specific architecture and components from the library.
4. Evaluation of simulation results with a combination of components in the workflow.

The research carried out within the framework of this work will allow develop simulation models of architectures of varying complexity for infocommunication networks and systems, to assess and predict the characteristics of the service being developed. This will shorten the development and implementation time, verify and verify the results obtained by using a mathematical apparatus, as well as obtain qualitative characteristics of systems that are complex enough for mathematical modeling. Thus, the approach to software development based on Model-Driven Architecture models allows you to use models as a set of recommendations for structuring specifications used in software design.

The authors of works on simulation modeling of infocommunication services [9-10], simulate specific services in order to obtain their characteristics, which does not allow using the proposed models for the analysis of other systems. Separately, it should be noted the work of the author [11] in the framework of which an analysis of a particular service was presented with a detailed description of the approach to its modeling, however, the lack of a description of the implementation of structural elements does not allow to accurately reproduce the study.

1. Approach to the development of simulation models of systems.

The research methods used in this work include empirical studies using mathematical and simulation models to analyze qualitative characteristics. As well as analytical methods for formalizing processes, applying statistical methods to extract information from data. Designing a library of workflow components, which includes defining the functionality of each component, their interaction and interfaces for information exchange.

To create a simulation model of an infocommunication service, the following steps must be performed [12–13]:

- 1) Definition of the purpose of modeling. This will help determine the required level of detail, quantitative characteristics and other parameters of the model.
- 2) Collecting data that will be used as input characteristics of the system. This can be data on the flow of applications processed in the system, the characteristics of the network infrastructure, the number of users, and others.
- 3) Definition of the model structure – based on the data and modeling goals, the structure of the model, the processes occurring in the system, and the parameters of each block are determined.
- 4) Creating a program for the implementation of the model, using special software tools, such as AnyLogic.
- 5) Run the simulation and analyze the results. As a result of the analysis, it is possible to determine the efficiency of the system, optimize processes and suggest possible improvements.

There are many different types of simulation models, each of which has its own characteristics and applications. Within the framework of this work, it is advisable to use discrete event modeling methods. These models are quite flexible in the implementation of the necessary functionality and can be used to model a large number of different processes. Examples of the implementation of a transactional service [14–15] and a session service [16–18]. In this paper, simulation modeling of infocommunication services and their elements is carried out in the Anylogic development environment [19].

The main element of the model is a queuing system (QS), which can be part of a network of queuing systems implementing a complex service of applications, data blocks, users depending on the purpose of the system being modelled.

The quality of the system functioning is determined by many factors such as:

- Response time: This is the mathematical expectation and variance of the time it takes the system to process a request and send a response. For most transactional systems, the response time should be minimal.
- Lead time: this is the time it takes the system to perform the operation. For transactional systems, the execution time should also be minimal.
- Downtime: this is the time when the system does not work and does not process requests. The less downtime, the better for users.
- System reliability: this is the probability that the system will be able to process the request.
- Throughput: This is the number of requests the system can handle per unit of time. For transactional systems, throughput should be high enough to meet the needs of users.
- The system's node utilisation factor is a measure of the extent to which a particular node's resources are utilised within a distributed system.

For the latter, the expression for the mathematical calculation of the load factor is as follows:

$$\rho_i = \frac{\lambda_i \times t_i}{v_i} = \frac{\lambda_i}{\mu_i \times v_i}. \quad (1)$$

To obtain this parameter in the system, the following algorithm is required at the "Queue" input:

```
count= count+delay.size(); // counts the total number of delays in the node
```

```
ro=count/(v*number); // determines the average node load
```

This paper considers modern information systems that include transactional systems designed to automate business processes by entering, storing and processing information. They are an important component of infocommunication systems that support workflows [20] and e-commerce applications. Transactional systems play an important role in the operation of such systems by enabling interaction between various components, including web services, servers, local databases and other business transactional participants.

In this paper, the definition of workflows is presented as rule-based software that coordinates and controls the execution of the activities (transactions) that constitute a business process. Workflow can include issues of concepts (Cloud-Fog-Edge), distributed systems, multi-phase maintenance, etc. [21–22].

### Simulation models of workflow scenarios

The study of transactional systems using simulation modelling provides accurate estimates of the probabilistic and temporal characteristics in various task processing scenarios in transactional services.

Since transactional services are an implementation of a workflow for servicing a user task, there are an infinite number of implementation options. It can be argued that there is no universal model of workflow definitions. In the following, the developed approaches to the simulation of the main elements of the workflow are presented.

A sequential chain of local transactions is a series of connected mass service systems, where the output from one QS is the input to the other. An example implementation of a workflow simulation model of this type will be shown in Figure 3.

The branching model of system workflow scenarios, allows to consider the processes of a task along the route of local nodes (e.g. Node1 → Node 2, Node 1 → Node 3, Node 1 → Node 4). An example of a service with this approach could be a payment system with different payment methods, the choice of which implements several scenarios. The user information notification system works in the same way with the following scenarios (through SMS, push notifications and mail).

This model includes the ability to choose the path of a request to nodes. The probabilities of user transitions between nodes in the system are given by an indecomposable stochastic matrix  $R = \|p_{ij}\|$ , in the case of a system of three nodes:



$$R = \begin{pmatrix} p_{11} & p_{12} & p_{13} \\ p_{21} & p_{22} & p_{23} \\ p_{31} & p_{32} & p_{33} \end{pmatrix}.$$

The route selection blocks "SelectOutputOut" → "Probability", or "Variable" → "Initial value" with reference to the database include the following condition

**SELECT** *probability of change* **FROM** "DB name"

**WHERE** *route = "pij"* // select the correct transition, from i to node j

In the scenarios of this model, the intensity of requests to the Semo nodes will be calculated as follows:

$$\lambda_i = \Lambda \times p_{0i} + \sum_{j=1}^Y \lambda_j \times p_{ji}. \quad (2)$$

A script for aggregating requests from different sources to merge, process and generate either a merged request by work result or split up and redistribute between the next units in the workflow chain.

When modelling such a structure, it is essential to identify the requests within the workflow, to set the route and conditions for the distribution between nodes in the system.

The result of modelling systems with scenario partitioning and reallocation of requests to nodes in a mass service network is presented in [17].

3) Parallel service (Fork-Join [23]) involves replicating a request to  $M$  nodes, with two possible objectives, the first of which involves simulating the process of simultaneously polling two loosely coupled services in order to get a response from all nodes.

The approximate distribution function for the whole network with replication factor equal to  $m$ , is calculated by the expression:

$$F_{FJ}(t) \approx 1 - \sum_{i=1}^M c_i [1 - F_{Si}(t)] \prod_{j=1}^{i-1} F_{Sj}(t) \approx \sum_{i=1}^M (c_i - c_{i+1}) \prod_{j=1}^i F_{Sj}(t), \quad (3)$$

where  $c_i$  – is the replication factor, equal to  $c_{M+1} = 0$ ,  $c_1 = 1$ ,  $c_2 = 1 - p_1/4$  and

$$c_i \approx \left(1 - \frac{p_{i-1}}{8}\right) \left(1 - \frac{p_{i-2}}{8}\right), \quad 3 \leq i \leq M. \quad (4)$$

The second option involves the need to divide the task into smaller equal parts (data block) and service them simultaneously by parallel nodes [24]. It should be noted that then the maintenance time of the transaction needs to be changed:

$$t_{\text{serv.}}^* = \frac{t_{\text{serv.}}}{M}. \quad (5)$$

A simulation model of this type of system has been implemented as follows:

It is worth noting that this simulation model automates the process of changing the number of replicas by introducing the functions described below:

This model has resulted in a software module for characterising parallel transaction processing systems [25].

### Modelling results

The result of the simulation of a transaction service as a sequential chain of local transactions branching into parallel service Fork-Join  $M = 2$ , is the simulation model shown in Fig. 3.

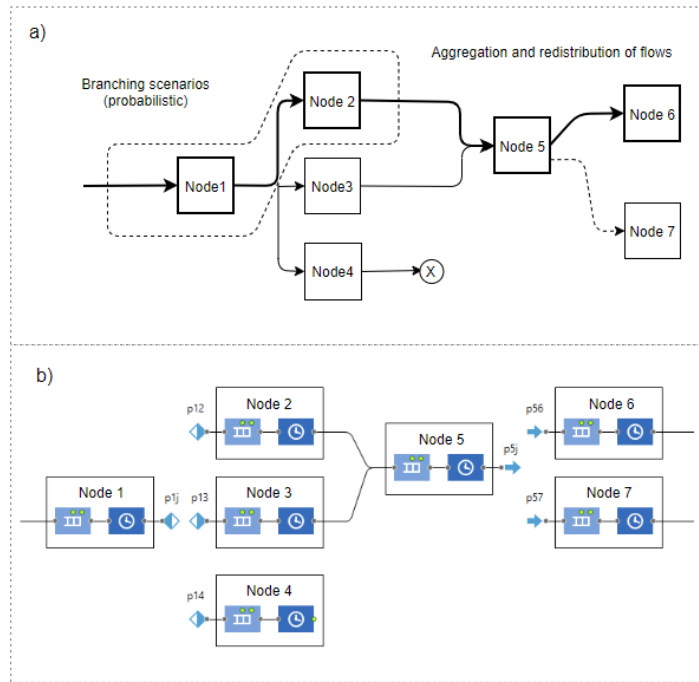


Fig. 1. Branching, aggregation and redistribution of flows a) scheme b) model

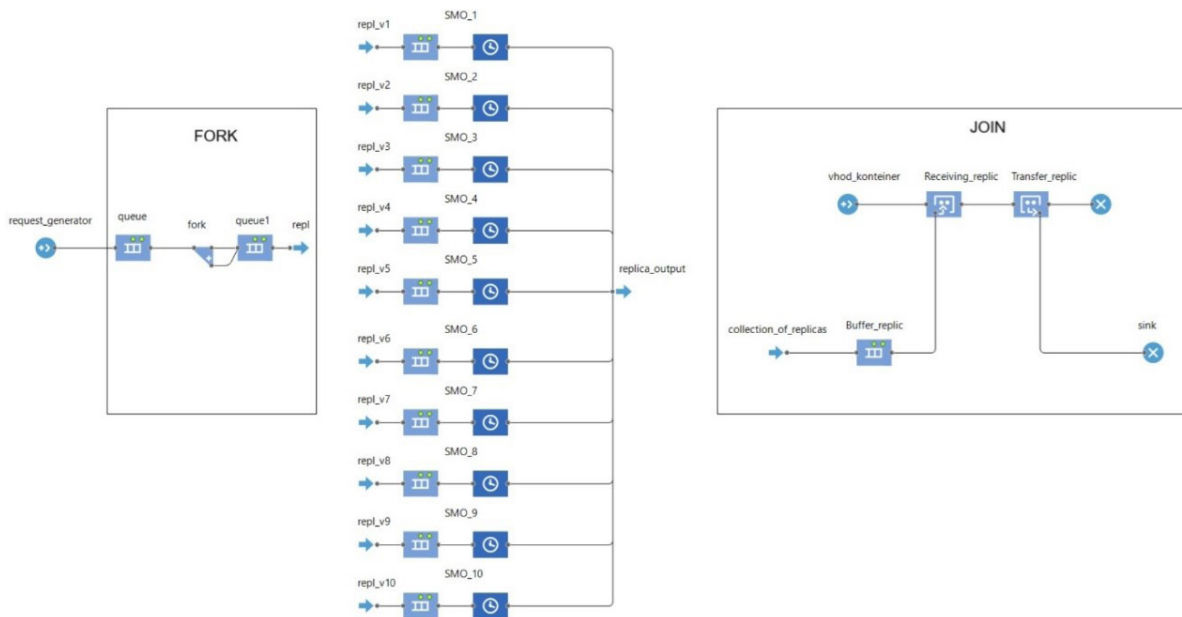


Fig. 2. Fork-Join M node simulation model

As a result of the simulation, the time characteristics were obtained as a function of the input load intensity of the workflow and the performance of its fragments (service intensity  $\mu_j$ ). Also using the convolution equation, the results of analytical modelling were obtained. The M/M/1 systems are independent systems, so the relative error of analytical modelling is insignificant. However, modeling systems with other distribution laws that are not included in the results of Burke's theorem is time consuming and may have a high percentage of inaccuracy. It is for such systems that it is rational to use simulation methods.

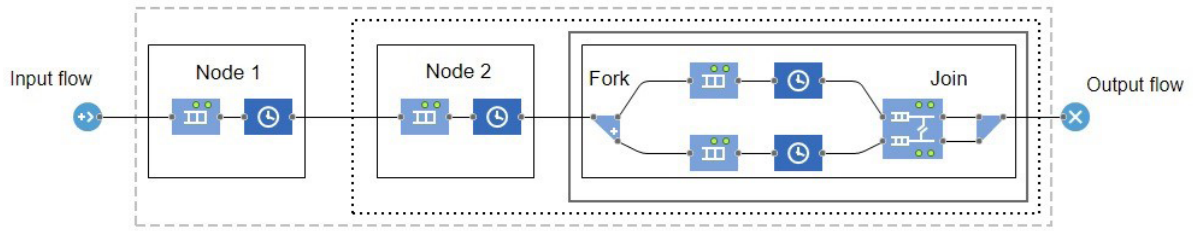


Fig. 3. Transaction chain simulation model with FJ

Table 1

## Description of the functional units in the FJ model

Block	Destination	Prerequisite
Function "number_of_nodes"	Changes the number of active nodes by the value defined in the "M_nodes" parameter	if (M_nodes == 1) {Nodes_1();} else if (M_nodes == 2) {Nodes_2();} etc.
Function "Nodes_i" where i=1...M	Determines the probabilities of replica processing by specific nodes	For replica factor M=2 M_1=1/M_nodes; M_2=1/M_nodes; M_3=0; etc.
Queue "Buffer_replic"	Waits for all M replicas to arrive before combining them into an application and ending service	ID=agent.number; replica_counter=0; for (i=0; i < Buffer_replic.size(); i++) { if ((Buffer_replic.get(i)).number==ID) {replica_counter++;} if (replica_counter==M_nodes){ vhod_konteiner.inject(); i=0; break;}}
Pickup "Receiving_replic"	Collects incoming replicas in the "Buffer_replic" block into a single application	Requirement: agent.number==ID;
Dropoff "Transfer_replic"	Transmits application from "Receiving_replic" to system output	Requirement: agent.v_replication==1

$$F_x(t) = F_1(t) * F_2(t) * F_{FJ}(t). \quad (6)$$

As can be seen from Fig. 4, when the input intensity is increased for the whole system, the task service time, or more precisely, the waiting time for service by an application in each element, increases. The increase occurs uniformly until the first node is overloaded at  $\Lambda_{crit.} = 1$  request/sec, at this point node 1 is identified as the bottleneck of the system, thereby slowing down the rate of requests to subsequent nodes.

Further modelling suggests that for a given critical input load  $\Lambda_{kpum.}$ , to gradually increase the service intensity at all nodes of the systems, which, as can be seen in Fig. 5, significantly reduces the time to implement the problem.

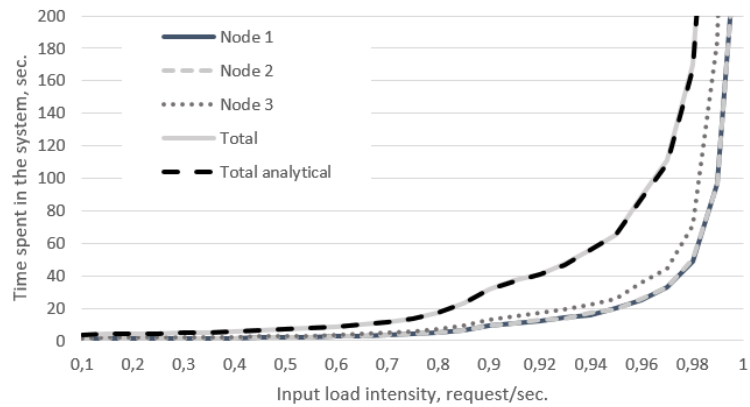


Fig. 4. Dependence of residence time on  $\Lambda$

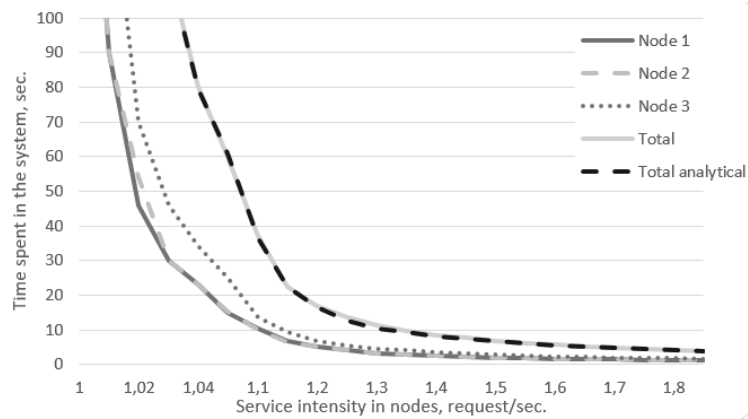


Fig. 5. Dependence of residence time on  $\mu_i$

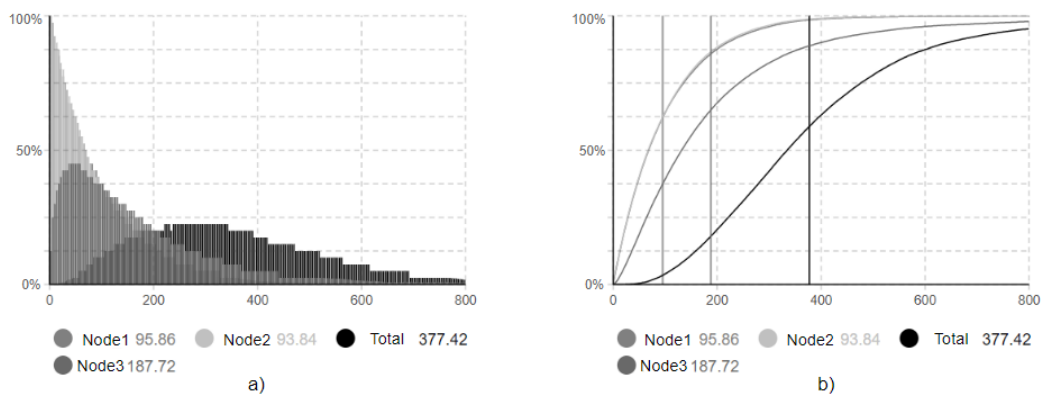


Fig. 6. Density (a) and distribution function (b) of time spent in systems

The moment when the load factor of all nodes  $\rho_i \rightarrow 1$  at the input intensity  $\Lambda = 0.99$  the system tends to overload and has an unacceptable service time. The density and probability of time in the system and in each element are shown in Fig. 6.

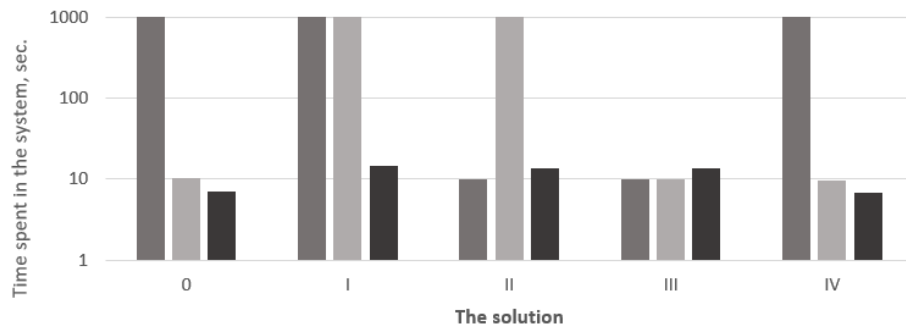


Fig. 7. Dependence of the time in the system on the chosen solution

The question of the rationality of improving the qualitative performance of all elements of the system at the same time has emerged. Simulation modelling allows the time characteristics of the system to be obtained with a minimum of effort by conducting a number of different experiments. This allows you to significantly reduce the cost of resources to provide the required quality of service. For example, Fig. 7 shows the results of a simulation of a transaction chain with the input characteristics given in Table 2.

Table 2

**Quantitative characteristics of node performance decisions**

	The solution				
	0	I	II	III	IV
$\lambda$ request /sec.	1,2	1,2	1,2	1,2	1,2
$\mu$ node 1 request /sec	1,1	1,2	1,3	1,3	1,2
$\mu$ node 2 request sec.	1,2	1,2	1,2	1,3	1,3
$\mu$ node 3 request /sec	1,3	1,3	1,3	1,3	1,4

The zero solution is the initially set system parameters, and as can be seen from the diagram, with an increase in the performance of a highly loaded node by 1–2 divisions, where division ( $\mu = 0.1$ ), the quality of service of the entire service will not increase, as it will overload the subsequent node. The most rational method in this experiment is to spend the same 3 divisions as in solution IV, but on the first and second node, thereby reducing the load on the nodes and not spending unnecessary resources on the stable node. This approach allows us to calculate the characteristics of the system when implementing an algorithm based on the equivalent microservices workflow focused on the quality-of-service delivery [26].

**Conclusion**

As part of this work, simulation models of the functional blocks required to create holistic infocommunication services were developed by assembling them into the request service workflow scenarios presented in the following elements:

- 1) a sequential chain of local transactions;
- 2) branching workflow scenarios;
- 3) scenarios for merging, splitting and redistributing query flows;
- 4) Fork-Join parallel service.

The model blocks presented are suitable for the layout of different variants of complex services. The use of simulation modelling was found to provide accurate estimates of the probabilistic and temporal charac-

teristics of task servicing in transactional service scenarios. More complex task processing scenarios can be considered in further studies, such as:

- 1) multiphase mass service networks;
- 2) distributed systems in workflow scenarios (Edge-Cloud computing concept);
- 3) systems for priority processing of requests;
- 4) transactional systems for handling requests initiated by session services.

This will extend the scope of simulation modelling and provide more accurate results for more complex task processing systems in transactional services.

## REFERENCES

1. **Khomonenko A.D., Basyrov A.G. i dr.** Modeli i metody issledovaniya informatsionnykh system [Models and methods of information systems research], 2019.
2. **Paramonov I.Yu. i dr.** Metody i modeli issledovaniya slozhnykh sistem i obrabotki bolshikh dannykh [Methods and models of complex systems research and big data processing], 2020.
3. **Shanthikumar J.G., Sargent R.G.** A unifying view of hybrid simulation/analytic models and modeling, *Operations research*, 1983. T. 31, no. 6. Pp. 1030–1052.
4. **Nyhuis P. et al.** Applying simulation and analytical models for logistic performance prediction, *CIRP annals*, 2005. T. 54, no. 1. Pp. 417–422.
5. **Litvinov V.L., Zhuravkova M.A.** Issledovaniye sredstv modelirovaniya slozhnykh sistem metodami sistemnoy dinamiki [Research of modeling tools of complex systems by methods of system dynamics], *Regional Informatics (RI-2022) Conference materials*. 2022, Pp. 561–562.
6. **Gaydamako V.V.** Comparative analysis of analytical modeling methods for evaluating the performance of cloud applications, *Vestnik Kyrgyzsko-Rossiyskogo Slavyanskogo universiteta*, 2020. T. 20, no. 12. Pp. 145–151.
7. **Kuznetsova T.A., Meshcheryakov V.A.** Comparison of software tools for simulation of queuing systems. *Materials of the international scientific and practical conference of students and postgraduates*. Omsk: National Development Strategy Fund, 2015, Pp. 187–192.
8. **Apanasenko A.V., Berg D.B.** Sravnitelnyy analiz metodov integratsii imitatsionnykh modeley s vneshnimi informatsionnymi sistemami [Comparative analysis of methods of integration of simulation models with external information systems], *Vesenniye dni nauki VShEM [Spring Days of HSE Science]*. 2019. Pp. 184–186.
9. **Dorosinskiy L.G., Aksenov K.A., Popov M.V.** Multiservices communications networks simulating dynamic modeling and their engineering design, *Nauchno-technicheskie vedomosti SPbGPU. Informatika, telekommunikatsii i upravleniye*. 2009, no. 1 (72). Pp. 153–159.
10. **Abdalov A.V., Grishako B.G., Loginov I.V.** An analysis of the efficiency of the process of servicing the flow of requests for creating IT-services used a simulation model, *Software & Systems*, 2022. T. 35, no. 1. Pp. 75–82. DOI: 10.15827/0236-235X.137.075-082
11. **Bykov A.Yu., Panfilov F.A., Sumarokova O.O.** Simulation with usage of the Java class library, developed for “cloud” services, *Inzhenernyy zhurnal: nauka i innovatsii*. 2013, no. 2 (14). P. 10.
12. **Kolesov Yu.B., Senichenkov Yu.B.** Modelirovaniye sistem. Obyektno-orientirovanny podkhod [Modeling of systems. Object-oriented approach], *BKhV-Peterburg*, 2012.
13. **Verzun N.A., Kolbanev M.O., Romanova A.A.** Imitatsionnoye modelirovaniye informatsionnogo vzaimodeystviya v kibertekhnicheskoy sisteme [Simulation modeling of information interaction in a cybertechnical system], *Conference Information Security of Russian regions (IBRD-2021)*, 2021. Pp. 211–212.
14. **Shatalova Yu.G.** Issledovaniye modeli obrabotki zaprosov k baze dannykh v srede AnyLogic [Investigation of the database query processing model in AnyLogic environment], *Vostochno-yevropeyskiy zhurnal peredovykh tekhnologiy [Eastern European Journal of Advanced Technologies]*, 2012. T. 4, no. 2 (58). Pp. 46–48.

15. **Nazarenko D.N., Sorokin A.A.** Diskretno-sobytiynaya model obrabotki zaprosov serverom sistemy distantsionnogo obucheniya v srede imitatsionnogo modelirovaniya AnyLogic [Discrete-event model of request processing by the server of the distance learning system in the AnyLogic simulation environment], *Aktualnyye problemy sovremennoy nauki – novomu pokoleniyu [Actual problems of modern science for a new generation]*. 2014. Pp. 171–175.
16. Svidetelstvo o gosudarstvennoy registratsii programmy dlya EVM 2015612377 Diskretno-sobytiynaya model Call-tsentra v srede imitatsionnogo modelirovaniya Anylogic [Certificate of state registration of a computer program 2015612377 Discrete event model of a Call center in the Anylogic simulation environment]. Sorokin A.A., Zhukov I.A., Melnikova K.V. 2015.
17. **Zarubin A.A., Redrugina N.M.** Modelirovaniye igrovyykh mnogopolzovatel'skikh servisov [Modeling of multi-user gaming services], *Vestnik svyazi [Bulletin of Communications]*, 2020. No. 8. Pp. 11–16.
18. **Redrugina N.M.** Models and methods for calculating delays in the provision of services by the user on the service platforms of session infocommunication services. *T-Comm*, 2023. Vol. 17, no. 4, pp. 32–38. (in Russian). DOI: 10.36724/2072-8735-2023-17-4-32-38
19. **Yefromeyeva Ye.V.** Simulation modeling: fundamentals of practical application in AnyLogic environment: tutorial / Ye.V. Yefromeyeva, N.M. Yefromeyev. Saratov: Vuzovskoye obrazovaniye, 2020.
20. Leff, Avraham & Rayfield, James. WSO: Developer-Oriented Transactional Orchestration of Web-Services. 2017. Pp. 714–720. DOI: 10.1109/ICWS.2017.86
21. **Vorobyev S.P., Gorobets V.V.** Issledovaniye modeli tranzaktsionnoy sistemy s replikatsiyey fragmentov bazy dannykh, postroyennoy po printsipam oblachnoy sredy [Investigation of a transactional system model with replication of database fragments built on the principles of a cloud environment], *Inzhenernyy vestnik Dona [Engineering Bulletin of the Don]*. 2012. T. 22, no. 4-1. P. 49.
22. **Wang S., Ding Z., Jiang C.** “Elastic Scheduling for Microservice Applications in Clouds”, in *IEEE Transactions on Parallel and Distributed Systems*, vol. 32, no. 1, pp. 98–115, 1 Jan. 2021, DOI: 10.1109/TPDS.2020.3011979
23. **Lokhvitskogo V.A., Khabarova R.S., Dudkina A.S.** Approximation of the residence time for a Fork-Join queuing system based on relationship invariants, *Intellektualnyye tekhnologii na transporte [Intelligent technologies in transport]*, 2020, no. 2, Pp. 46–50.
24. **Khalid M., Yousaf M.M.** A comparative analysis of big data frameworks: An adoption perspective. *Applied Sciences*, 2021, vol. 11, no. 22, article number: 11033. DOI: 10.3390/app112211033
25. Certificate of state registration of the computer program No. 2023618304 Russian Federation. A software module for calculating the characteristics of parallel transaction processing systems developed in the Anylogic environment / A.A. Zarubin, N.M. Redrugina; the applicant and the patent holder of SPbSUT. No. 2023616789; declared 07.04.24; publ. 21.04.23.
26. **Song Z., Tilevich E.** Equivalence-Enhanced Microservice Workflow Orchestration to Efficiently Increase Reliability. 2019, Pp. 426–433. DOI: 10.1109/ICWS.2019.00076

#### INFORMATION ABOUT AUTHOR / СВЕДЕНИЯ ОБ АВТОРЕ

**Nataliya M. Redrugina**  
**Редругина Наталия Михайловна**  
 E-mail: redrugina.nm@sut.ru

*Submitted: 16.04.2023; Approved: 25.06.2023; Accepted: 06.07.2023.*

*Поступила: 16.04.2023; Одобрена: 25.06.2023; Принята: 06.07.2023.*

Research article

DOI: <https://doi.org/10.18721/JCSTCS.16204>

UDC 621.396.96



## MULTICHANNEL MULTISTATIC COMBINED TSOA AND TDOA POSITIONING SYSTEM BASED ON PRECISE ANALYTICAL SOLUTION OF POSITIONING EQUATIONS

V.D. Kuptsov<sup>1</sup>  , S.I. Ivanov<sup>1</sup> 

<sup>1</sup> Peter the Great St. Petersburg Polytechnic University,  
St. Petersburg, Russian Federation

 [kuptsov@spbstu.ru](mailto:kuptsov@spbstu.ru)

**Abstract.** Exact analytical solutions of elliptic and hyperbolic equations in a multichannel multistatic positioning system are obtained. The results of modeling the Time Sum of Arrival (TSoA) and Time Difference of Arrival (TDoA) methods for estimating the object coordinates by arrival times with fluctuations are presented. Particular attention is paid to the causes of gross errors in case of problematic configurations of base stations (BS) and the position of the object. The study revealed that the advantages of the TSoA method over the TDoA method include a reduction in the area with anomalous errors and better accuracy outside the BS perimeter, and the advantage of TDoA over TSoA should include more accurate work inside the BS perimeter. Based on the identified advantages, optimization of a multichannel multistatic positioning system, which combines the advantages of TSoA and TDoA methods, is proposed. As a result of the simulation, it was found that the combined TSoA/TDoA method, based on the exact analytical solution of equations, has an order of magnitude higher accuracy in determining the object's coordinates than the frequently used method of linearization of hyperbolic equations. Due to these advantages, the proposed algorithm is promising for remote determination of the parameters of unmanned vehicles in “smart city” technologies.

**Keywords:** positioning; Time Difference of Arrival; Time Sum of Arrival; desynchronization in time of arrival; optimization of a positioning system; coordinate estimation; combined TSoA/TDoA

**Acknowledgements:** The reported study was funded by RFBR, project number 19-29-06034.

**Citation:** Kuptsov V.D., Ivanov S.I. Multichannel multistatic combined TSoA and TDoA positioning system based on precise analytical solution of positioning equations. *Computing, Telecommunications and Control*, 2023, Vol. 16, No. 2, Pp. 40–54. DOI: 10.18721/JCSTCS.16204



Научная статья

DOI: <https://doi.org/10.18721/JCSTCS.16204>

УДК 621.396.96



## МНОГОКАНАЛЬНАЯ МУЛЬТИСТАТИЧЕСКАЯ КОМБИНИРОВАННАЯ СИСТЕМА ПОЗИЦИОНИРОВАНИЯ TSOA И TDOA, ОСНОВАННАЯ НА ТОЧНОМ АНАЛИТИЧЕСКОМ РЕШЕНИИ УРАВНЕНИЙ ПОЗИЦИОНИРОВАНИЯ

В.Д. Купцов<sup>1</sup> , С.И. Иванов<sup>1</sup> <sup>1</sup> Санкт-Петербургский политехнический университет Петра Великого,  
Санкт-Петербург, Российская Федерация [kuptsov@spbstu.ru](mailto:kuptsov@spbstu.ru)

**Аннотация.** Получены точные аналитические решения эллиптических и гиперболических уравнений в многоканальной мультистатической системе позиционирования. Приведены результаты моделирования суммарно-дальномерного (TSoA) и разностно-дальномерного (TDoA) методов для оценки координат объекта по времени прихода с флуктуациями. Особое внимание уделено причинам возникновения грубых ошибок при проблемных конфигурациях базовых станций (БС) и положения объекта. В ходе исследования выявлено, что преимущества метода TSoA перед методом TDoA заключаются в уменьшении площади с аномальными ошибками и лучшей точности за пределами периметра БС, а преимущество TDoA перед методом TSoA заключается в более точной работе внутри периметра БС. На основе выявленных преимуществ предлагается оптимизация многоканальной мультистатической системы позиционирования, которая сочетает в себе преимущества методов TSoA и TDoA. В результате моделирования установлено, что комбинированный метод TSoA/TDoA, основанный на точном аналитическом решении уравнений, имеет на порядок более высокую точность определения координат объекта, чем часто используемый метод линеаризации гиперболических уравнений. Благодаря этим достоинствам предложенный алгоритм перспективен для дистанционного определения параметров беспилотных автомобилей в технологиях «умного города».

**Ключевые слова:** позиционирование; разностно-дальномерный метод; суммарно-дальномерный метод; рассинхронизация во времени прихода; оптимизация системы позиционирования; оценка координат; комбинированный TSoA/TDoA

**Благодарности:** Исследование выполнено при финансовой поддержке РФФИ, проект № 19-29-06034.

**Для цитирования:** Kuptsov V.D., Ivanov S.I. Multichannel multistatic combined TSoA and TDoA positioning system based on precise analytical solution of positioning equations // Computing, Telecommunications and Control. 2023. Т. 16, № 2. С. 40–54. DOI: 10.18721/JCSTCS.16204

### Introduction

Accurate remote determination of the object coordinates on the plane and in space is necessary in many technical applications, such as the control of unmanned vehicles in the “smart city”, in robotic production complexes, security systems in the city and at the workplace. The object coordinates are determined by several base stations (BS) receiving a signal from the object. In global positioning systems, for example GPS, the radio signal is received by navigation satellites; in local positioning systems, object signals are received by base stations. The main task of object positioning is to determine the object coordinates on the ground, which can be carried out using various algorithms. The main ones are: RSS (Received Strength Signal), AoA (Angle of Arrival), ToA (Time of Arrival), TDoA (Time Difference of Arrival) and TSoA (Time Sum of Arrival) [1].

Each of the methods has its own disadvantages and advantages. In the RSS method, the distance to an object is estimated by the power of the radio signal received at the base stations and emitted by the object. Hardware implementation of RSS measurements is relatively inexpensive due to the simplicity of the measurement data processing algorithm. However, the results of measurements of the power of the received radio signal for the RSSI algorithm are difficult to describe by theoretical models, and, as a result, are poorly predictable. The RSS method loses a lot in conditions of multipath signal propagation. In the AoA method, the location of an object is determined by the intersection of the axes of the antenna patterns of three base stations (modified triangulation method). The method has a great advantage – there is no need for precise time synchronization of transmitters and receivers. The disadvantage is that at base stations, receivers must have a very high angular resolution, which requires the use of multi-element phased antenna arrays. In the range of units of gigahertz, such receivers have significant dimensions, with an increase in radio frequency, the dimensions decrease, but the absorption of radio waves during propagation increases [2]. In the ToA method, the signal transit times from the object to the base stations are measured, the distance to the object is calculated based on the difference in the time of sending and receiving the signal. The disadvantage of the method is that it requires complete time synchronization of the transmitter at the object and the receivers at the base stations.

In the complex changing conditions of a “smart city” and a production facility, the TDoA method is preferred, since this method is highly accurate and requires time synchronization only at base stations [3]. In the TDoA method, the differences in the arrival times of radio signals between the reference BS and all other BSs are measured. The lines on which the difference in the times of arrival of radio signals to two BSs is constant are hyperbolas in the plane (hyperboloids in space), while both BSs are at the foci of the hyperbolas. The object's coordinates are the point of intersection of the entire set of hyperbolic curves in the plane, included in the system of equations. To obtain a position estimate at reasonable noise levels, the Taylor series method [4] is also used. In [5], it was proposed to use the expansion in a Taylor series and the linearization of hyperbolic equations. Certain advantages are provided by combined methods, for example, TDoA/RSS [6]. The use of TDoA/RSS reduces the number of required BSs to two. Good results in determining the position of an object are obtained by synthetic aperture radars using the time difference of arrival (TDoA) method [7].

The option of constructing a positioning system on a plane with 3 BS is the most cost-effective, but has the disadvantage that the intersection of two hyperbolas can occur at four points. In this case, it becomes problematic to identify the true position of the object. To eliminate the ambiguity in determining the position of an object, it is necessary to include a fourth BS in the positioning system. With the addition of the fourth BS, it becomes possible to solve three systems of equations that will have one common root corresponding to the true position of the target [13]. To solve the problem of positioning in space, the number of BS should be equal to five.

Of particular interest are studies in which the hyperbolic equations of the TDoA method are solved analytically, without the linearization approximation. This solution improves the accuracy and reliability of determining the coordinates of the object. A certain disadvantage of the analytical method for solving equations is the increased requirement for the processing power of the positioning system processor, since it becomes necessary to solve quadratic equations. However, with the development of microprocessor technology, this disadvantage is leveled. Analytical methods for solving hyperbolic equations in the TDoA method are presented in [9–11]. Transformation of the coordinates of a hyperbola during a shift and rotation on a plane can be found in [9]. According to this transformation in [10], the effectiveness of two methods of TDOA solution was compared based on the task of finding intersection points of hyperboloids (possible positions of a target). The first method analyzed was based on coordinate transformation from the initial system to a new system to simplify equations solving, and the second one was based on matrix. In [11], the results of an experimental verification of an analytical method based on coordinate transformation are presented. In [12] an analytical method for determining the position

of an object based on the analysis of the difference in time of arrival of microwave radar signals from a transmitter to base station receivers is proposed. The main feature of the method is that it allows you to eliminate the ambiguity in determining the 3D coordinates of the target and improve the accuracy of determining coordinates in the absence of synchronization of TDoA measurements between the object transmitter and BS receivers.

Algorithms based on TSoA are less frequently studied than TDoA algorithms, and the available articles note certain advantages of the TSoA method over the TDoA method [13]. Minor disadvantages of the TSoA method include the need for a larger number of ADC bits during analog-to-digital conversion since the sum signal has a larger value than the difference signal. In [13] investigates the time-sum-of-arrival (TSoA) based localization algorithm, where a two-step weighted least-squares algorithm is analytically derived according to the elliptical geometry. Simulations conducted in a wide range of scenarios show that in the presence of a large number of BSs, the TSoA-based algorithm performs better than the TDoA-based algorithm. In the scenario where the target is located near the cell boundary, the TSoA-based algorithm has better accuracy performance compared to the TDoA-based algorithm. In [14], the problem of two-dimensional elliptic localization with several spaced transmitters and receivers is considered. To determine the location, the signal reflected from the object (or relayed) is used under NLOS conditions of radio signal propagation. Two least squares methods are investigated: the use of the traditional linear LS estimate with an additional cost function; and parametrizing the ellipses defined by TSoA by the non-linear LS estimation criterion. The effectiveness of the proposed methods in reducing NLOS errors at acceptable computational costs is demonstrated. A novel computationally efficient solution for locating a single target from bistatic range measurements in distributed MIMO radar systems is proposed in [15]. The method is based on the method of least squares with restrictions. The positioning performance of the proposed method is shown to achieve the CRLB up to relatively high noise levels. A statistical model of the NLOS error in positioning systems based on the trilateration method was proposed in [16]. The maximum likelihood estimate (MLE) of the object location is calculated. With the help of Gaussian approximation, a unified (taking into account the measurements of ToA, TSoA and TDoA) closed form expression for the CRLB of the estimated object location variance is obtained. In [17] the problem of multistatic target localization using TSoA measurements in the presence of non-line-of-sight (NLOS) propagation errors and bursts in a MIMO radar system consisting of a single target,  $M$  transmitters, and  $N$  receivers is considered. The influence of NLOS errors or any other outliers in the measurements is eliminated by introducing an additional balancing parameter into the data model, after which the iterative algorithm for minimizing the NLWLS objective function is used. The TSoA-based Taylor series localization algorithm has been deeply investigated in [18], where the principle and motivation of this algorithm has been introduced. Simulations show that a large number of BSs will make the TSOA-based Taylor algorithm perform better than the TDOA based algorithm. Moreover, when object is far from reference BS, TSOA-based Taylor algorithm is also better than the TDOA based algorithm. In [19] derives a new algebraic positioning solution using a minimum number of measurements, and from which to develop an outlier detector and an object location estimator. It is claimed that two measurements are sufficient in 2-D and three in 3-D to yield a solution if they are consistent. The derived minimum measurement solution is exact and reduces the computation to the roots of a quadratic equation. The solution derivation leads to simple criteria to ascertain if the line of positions from two measurements intersect. The intersection condition enables us to establish an outlier detector based on graph processing.

The aim of this work is to develop the combined TSoA/TDoA algorithm to improve the accuracy of determining the coordinates of an object and reduce gross errors associated with zeroing the determinants of equations systems. To achieve that, elliptic and hyperbolic positioning equations were solved, the standard deviation of the object coordinates was simulated with fluctuations in arrival times by linearization methods and the exact analytical solution of hyperbolic and elliptic equations, were identified areas on the plane in which gross errors associated with the zeroing of the determinants of equations systems occur.

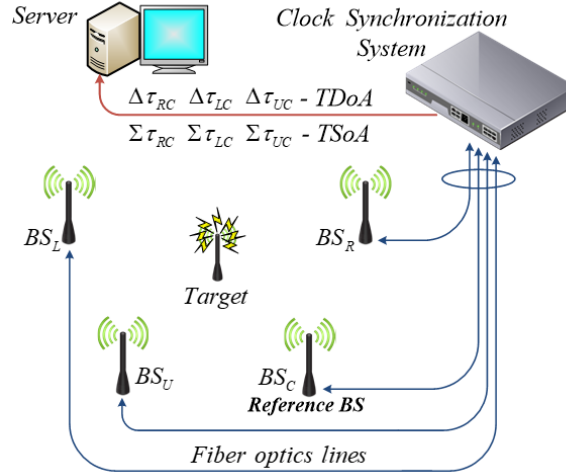


Fig. 1. Block diagram of a positioning system with 4 BS

### TSoA and TDoA positioning systems

Let consider a positioning system on a plane including four radio signal receivers:  $BS_C$ ,  $BS_L$ ,  $BS_R$  and  $BS_U$  (Fig. 1).

In the absence of TDoA measurement errors and receiving line-of-sight signals the real values of the sum and difference of the signal arrival times between the  $BS_i$  and the reference  $BS_C$  are determined by the expression:

$$\Delta\tau_{iC} = \frac{r_i \pm r_C}{c_i} = \frac{r_{iC}}{c_i}, \quad i = 2, \dots, 3, \quad (1)$$

where  $c_i$  – speed of light,  $r_i = \sqrt{(x_i - x)^2 + (y_i - y)^2}$  – distance between object and  $BS_i$ ,  $r_C$  – distance between the object and  $BS_C$ ,  $[x_i, y_i]$  –  $BS_i$  coordinates,  $[x, y]$  – object coordinates.

The transmitter position coordinates are solutions of the system of elliptic (TSoA method) and hyperbolic (TDoA method) equations:

$$\begin{cases} \sqrt{(x-x_L)^2 + (y-y_L)^2} \pm \sqrt{(x-x_C)^2 + (y-y_C)^2} = c \cdot \Delta\tau_{LC} \\ \sqrt{(x-x_R)^2 + (y-y_R)^2} \pm \sqrt{(x-x_C)^2 + (y-y_C)^2} = c \cdot \Delta\tau_{RC}, \\ \sqrt{(x-x_U)^2 + (y-y_U)^2} \pm \sqrt{(x-x_C)^2 + (y-y_C)^2} = c \cdot \Delta\tau_{UC} \end{cases} \quad (2)$$

where  $\Delta\tau_{LC}$ ,  $\Delta\tau_{RC}$ ,  $\Delta\tau_{UC}$  – the sum or difference in the times of arrival of the radio signal between  $BS_{L, R, U}$  and the  $BS_C$  reference station. The elliptic equations of the TSoA method correspond to the upper “+” sign in equations (2), the hyperbolic equations of the TDoA method correspond to the lower “-” sign in equations (2).

The method of linearization of hyperbolic equations is based on the expansion in a Taylor series in terms of the small parameter  $r_i/r_C \ll 1$  and taking into account only the linear terms of the expansion. Such an approximation is performed with a high degree of accuracy in global positioning satellite systems, since the object is on the Earth and the base stations on the satellites are in space. However, for local positioning systems the parameter  $r_i/r_C$  is not small.

In this regard, we obtained exact solutions of hyperbolic equations in [8] on the plane and in [12] in space, and developed an analytical algorithm that eliminates spatial ambiguity zones in determining the coordinates of the target on the plane and in space with high accuracy in determining the coordinates of the object. In this paper, we propose a combined TSoA/TDoA method for determining the coordinates of an object on a plane.

After substitution of  $X = x - x_c$ ,  $Y = y - y_c$ , the system of equations can be rewritten as:

$$\begin{cases} \sqrt{(X - X_L)^2 + (Y - Y_L)^2} \pm \sqrt{X^2 + Y^2} = L \\ \sqrt{(X - X_R)^2 + (Y - Y_R)^2} \pm \sqrt{X^2 + Y^2} = R \\ \sqrt{(X - X_U)^2 + (Y - Y_U)^2} \pm \sqrt{X^2 + Y^2} = U \end{cases}, \text{ where } \begin{cases} X_L = x_L - x_c, Y_L = y_L - y_c, L = c \cdot \Delta\tau_{LC} \\ X_R = x_R - x_c, Y_R = y_R - y_c, R = c \cdot \Delta\tau_{RC} \\ X_U = x_U - x_c, Y_U = y_U - y_c, U = c \cdot \Delta\tau_{UC} \end{cases} \quad (3)$$

Let us denote  $K = \sqrt{X^2 + Y^2}$ , where  $K > 0$ :

$$K^2 = X^2 + Y^2. \quad (4)$$

The system of Equations (5) can be rewritten as:

$$\begin{cases} \sqrt{(X - X_L)^2 + (Y - Y_L)^2} = \mp K + L \\ \sqrt{(X - X_R)^2 + (Y - Y_R)^2} = \mp K + R \\ \sqrt{(X - X_U)^2 + (Y - Y_U)^2} = \mp K + U \end{cases} \quad (5)$$

Squaring and reducing the general terms leads to the form:

$$\begin{cases} -2X_L X - 2Y_L Y = \mp 2LK + L^2 - X_L^2 - Y_L^2 \\ -2X_R X - 2Y_R Y = \mp 2RK + R^2 - X_R^2 - Y_R^2 \\ -2X_U X - 2Y_U Y = \mp 2UK + U^2 - X_U^2 - Y_U^2 \end{cases}, \text{ or } \begin{cases} -2X_L X - 2Y_L Y = E \mp 2LK \\ -2X_R X - 2Y_R Y = F \mp 2RK \\ -2X_U X - 2Y_U Y = G \mp 2UK \end{cases} \quad (6)$$

where  $E = L^2 - X_L^2 - Y_L^2$ ;  $F = R^2 - X_R^2 - Y_R^2$ ;  $G = U^2 - X_U^2 - Y_U^2$ .

In matrix form, the three systems of equations are:

$$\begin{aligned} \begin{bmatrix} -2X_L & -2Y_L \\ -2X_R & -2Y_R \end{bmatrix} \cdot \begin{bmatrix} X \\ Y \end{bmatrix} &= \begin{bmatrix} E \mp 2LK \\ F \mp 2RK \end{bmatrix}, & \begin{bmatrix} -2X_R & -2Y_R \\ -2X_U & -2Y_U \end{bmatrix} \cdot \begin{bmatrix} X \\ Y \end{bmatrix} &= \begin{bmatrix} F \mp 2RK \\ G \mp 2UK \end{bmatrix}, \\ \begin{bmatrix} -2X_U & -2Y_U \\ -2X_L & -2Y_L \end{bmatrix} \cdot \begin{bmatrix} X \\ Y \end{bmatrix} &= \begin{bmatrix} G \mp 2UK \\ E \mp 2LK \end{bmatrix}. \end{aligned} \quad (7)$$

Solution of the first system of equations ( $i = 1$ ) is:

$$X_1 = \frac{1}{\Delta_1} \cdot \begin{vmatrix} E \mp 2LK & -2Y_L \\ F \mp 2RK & -2Y_R \end{vmatrix} = M_{1X} \cdot K + N_{1X}, \quad (8)$$

where  $\Delta_1 = 4(X_L Y_R - Y_L X_R)$ ,  $M_{1X} = \frac{4}{\Delta_1} \cdot (\mp RY_L \pm LY_R)$ ,  $N_{1X} = \frac{2}{\Delta_1} \cdot (FY_L - EY_R)$ ;

$$Y_1 = \frac{1}{\Delta_1} \cdot \begin{vmatrix} -2X_L & E \mp 2LK \\ -2X_R & E \mp 2RK \end{vmatrix} = M_{1Y} \cdot K + N_{1Y}, \quad (9)$$

where  $M_{1Y} = \frac{4}{\Delta_1} \cdot (\mp LX_R \pm RX_L)$ ,  $N_{1Y} = \frac{2}{\Delta_1} \cdot (EX_R - FX_L) \cdot M_1$ ;

Solution of the second system of equations ( $i = 2$ ) is:

$$X_2 = \frac{1}{\Delta_2} \cdot \begin{vmatrix} F \mp 2RK & -2Y_R \\ G \mp 2UK & -2Y_U \end{vmatrix} = M_{2X} \cdot K + N_{2X}, \quad (10)$$

where  $\Delta_2 = 4(X_R Y_U - Y_R X_U)$ ,  $M_{2X} = \frac{4}{\Delta_2} \cdot (\mp UY_R \pm RY_U)$ ,  $N_{2X} = \frac{2}{\Delta_2} \cdot (GY_R - FY_U)$ ;

$$Y_2 = \frac{1}{\Delta_2} \cdot \begin{vmatrix} -2X_R & F \mp 2RK \\ -2X_U & G \mp 2UK \end{vmatrix} = M_{2Y} \cdot K + N_{2Y}, \quad (11)$$

where  $M_{2Y} = \frac{4}{\Delta_2} \cdot (\mp RX_U \pm UX_R)$ ,  $N_{2Y} = \frac{2}{\Delta_2} \cdot (FX_U - GX_R)$ .

Solution of the third system of equations ( $i = 3$ ) is:

$$X_3 = \frac{1}{\Delta_3} \cdot \begin{vmatrix} G \mp 2UK & -2Y_U \\ E \mp 2LK & -2Y_L \end{vmatrix} = M_{3X} \cdot K + N_{3X}, \quad (12)$$

where  $\Delta_3 = 4(X_U Y_L - Y_U X_L)$ ,  $M_{3X} = \frac{4}{\Delta_3} \cdot (\mp LY_U \pm UY_L)$ ,  $N_{3X} = \frac{2}{\Delta_3} \cdot (EY_U - GY_L)$ ;

$$Y_3 = \frac{1}{\Delta_3} \cdot \begin{vmatrix} -2X_U & G \mp 2UK \\ -2X_L & E \mp 2LK \end{vmatrix} = M_{3Y} \cdot K + N_{3Y}, \quad (13)$$

where  $M_{3Y} = \frac{4}{\Delta_3} \cdot (\mp UX_L \pm LX_U)$ ,  $N_{3Y} = \frac{2}{\Delta_3} \cdot (GX_L - EX_U)$ .

In expressions (2–13), at the summation sign “ $\pm$ ”, the superscript corresponds to the solution of the elliptic TSoA equations, the subscript corresponds to the solution of the hyperbolic TDoA equations. Thus, equations (2–13) are solutions to both elliptic and hyperbolic equations.

Substitution of Equation (8–13) into Equation (4) defines a quadratic equation with respect to the variable  $K$ :  $a_i K^2 + b_i K + c_i = 0$ , where  $i$  corresponds to the choice of a pair of ellipses or hyperboles,  $i = 1, 2, 3$ :

$$a_i = M_{iX}^2 + M_{iY}^2 - 1, \quad b_i = 2(M_{iX} N_{iX} + M_{iY} N_{iY}), \quad c_i = N_{iX}^2 + N_{iY}^2. \quad (14)$$

The roots of the quadratic equation are the following ( $b_i^2 - 4a_i c_i \geq 0$ ):

$$K_{i1} = \frac{-b_i + \sqrt{b_i^2 - 4a_i c_i}}{2a_i}, \quad K_{i2} = \frac{-b_i - \sqrt{b_i^2 - 4a_i c_i}}{2a_i}. \quad (15)$$

In the case that one of the two roots  $K_{i1}$  and  $K_{i2}$  is negative for the same value of  $i$ , it can be immediately excluded from the solution, and then another root of the equation remains in the algorithm. However, a situation is possible when both roots  $K_{i1}$  and  $K_{i2}$  are positive. In this case, it becomes impossible to determine the coordinates of the object. It is for such a fairly common case that it is necessary to use the fourth BS in the positioning system on the plane.

Substitution of roots  $K_{i1}$  and  $K_{i2}$  in Equation (8–13) defines six possible sets of  $[x; y]$  coordinates of an object, defining six points in plane:

$$[x_{i1} = X_{i1} + x_C, y_{i1} = Y_{i1} + y_C], [x_{i2} = X_{i2} + x_C, y_{i2} = Y_{i2} + y_C], \quad (16)$$

where  $X_{i1} = M_{iX} \cdot K_{i1} + N_{iX}$ ,  $Y_{i1} = M_{iY} \cdot K_{i1} + N_{iY}$ ,  $X_{i2} = M_{iX} \cdot K_{i2} + N_{iX}$ ,  $Y_{i2} = M_{iY} \cdot K_{i2} + N_{iY}$ .

In the absence of TDoA measurement errors from six calculated sets of  $[x; y]$  – coordinates, the coordinates of three points will be the same. It is this decision that is the true decision. To identify it, an algorithm was proposed in [8] and [12] based on finding the minimum distances between the intersection points of hyperboloids in space [12] and hyperbolas in the plane [8].

#### **Simulation of TSoA and TDoA algorithms for estimating object coordinates with fluctuations in the measurement of arrival time**

Arrival time measurement errors occur for three main reasons: 1) radio signal attenuation during propagation, 2) radio signal fading due to multipath propagation, 3) time desynchronization at base stations. In this work, the effect of base station time desynchronization on the accuracy of estimating object coordinates using a linearization algorithm and an exact analytical solution of elliptic and hyperbolic equations is studied. Using a computer experiment in the LabVIEW environment, the dependence of the root-mean square (RMS) deviation of the calculated object coordinates on the standard deviation of the difference in the times of arrival of radio signals at the BS was studied. To do this, Gaussian white noise with the same standard deviation for all BSs was added to the value of the arrival time at the input of each receiver of the positioning system. To determine the RMS deviation of the object position estimate,  $n = 100$  computational experiments were carried out for each value of the standard deviation of the Gaussian white noise. The standard deviation of the estimate of the object's coordinates was determined in accordance with the expression:

$$RMS = \sqrt{\frac{1}{n} \sum_{i=1}^n [(x_i - x)^2 + (y_i - y)^2]}, \quad (17)$$

where index  $i$  – experiment number,  $[x_i; y_i]$  – estimation of object coordinates in the  $i$ -th experiment,  $[x; y]$  – true object coordinates.

As noted in [12], the accuracy of determining the coordinates strongly depends on the choice of the BS position. If only one reference base station is used in the scenario of the positioning system, gross errors occur in determining the coordinates of the object at points, which the determinant of the system of equations becomes zero. An example of such a situation is shown in Fig. 2. The calculation of the RMS deviation was carried out for the number of computational experiments 100, time of arrival deviation (TSoA and TDoA) 0.4 ns, base station coordinates  $C: (-40; 40)$ ,  $L: (-40; -40)$ ,  $R: (40; -40)$ ,  $U: (40; 40)$  meters.

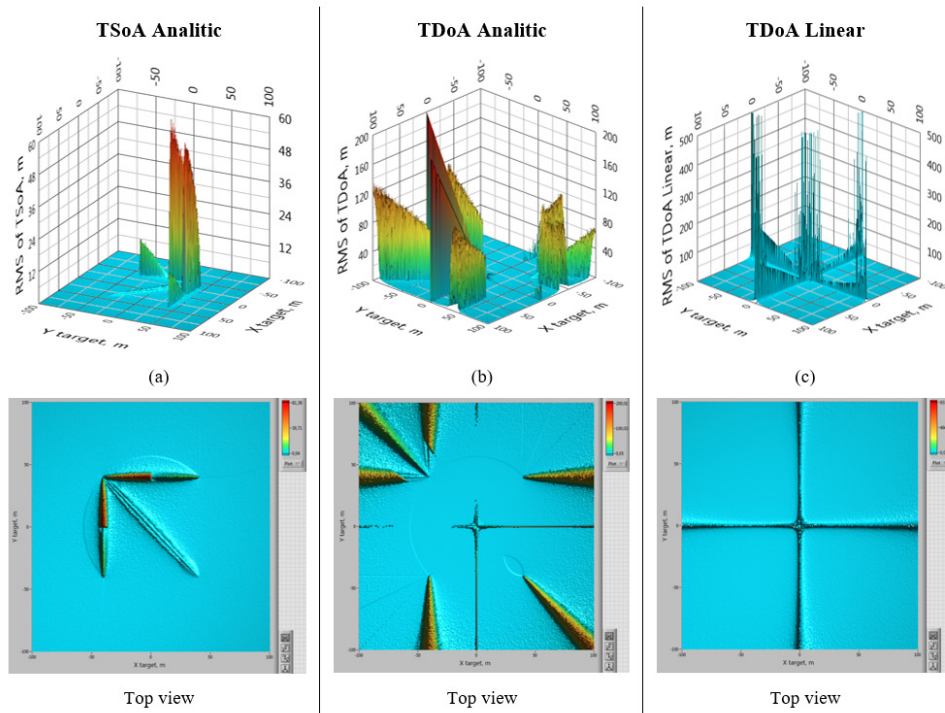


Fig. 2. Location of gross errors in determining the coordinates of an object on a plane for methods (a) TSoA Analytic, (b) TDoA Analytic, (c) TDoA Linear

Gross errors are common to all three methods under study. The errors in the TDoA Linear method are especially large. In addition, this method has significantly worse parameters of susceptibility to signal arrival time fluctuations, which was established in our previous studies [8, 12]. As can be seen from Fig. 2, the gross errors of all three methods have different positions on the plane. In the TSoA and TDoA methods, the positions of gross errors intersect only at the center of the BS location. Their position already suggests the idea of merging these two methods in order to eliminate gross errors associated with zeroing the determinants of systems of equations.

The RMS minima for determining object coordinates are achieved at line intersection angles (ellipses or hyperbolas) close to  $90^\circ$ . Fig. 3 shows the positions of the lines (ellipses and hyperbolas) at the minimum RMS values of the TSoA and TDoA methods with a Gaussian noise arrival time deviation of 0.4 ns. It is clearly seen that the true value of the position of the object is determined by the intersection of three lines. There are a significant number of points of intersection of the two lines. The algorithm proposed by us in [12] allows us to choose exactly the point of intersection of three lines from all the points of intersection of the lines.

Gross errors in determining the location of an object occur when the determinants of systems of equations are set to zero. Gross errors of the TSoA method are illustrated by the example shown in Fig. 4 a. The eccentricity of the ellipse L is equal to one, and in the presence of noise, the common triple point of intersection of the ellipses is constantly thrown between two closely spaced arcs of the ellipse L.

In the TDoA method, the number of failed configurations is doubled compared to the TSoA method. The first unsuccessful configuration corresponds to the eccentricity value equal to infinity ( $\epsilon = \infty$ ), the second unsuccessful configuration corresponds to the eccentricity value equal to one ( $\epsilon = 1$ ). Examples of both such configurations are shown in Fig. 4, b, c. At  $\epsilon = \infty$ , both branches of the hyperbola merge into one straight line (Fig. 4, b) and the configuration is symmetrical about the horizontal axis. The TDoA method cannot determine the final intersection point: either this point is located at coordinates  $[0; -100]$  m, or at  $[0; +100]$ .



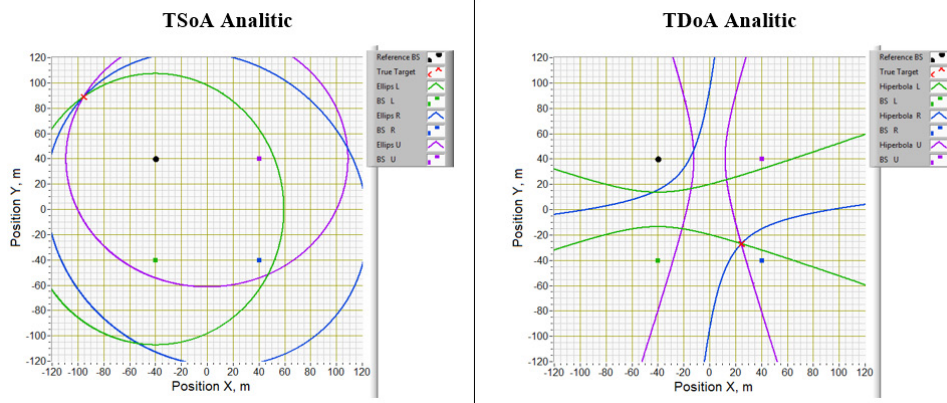


Fig. 3. Positions of ellipses and hyperbolas at minimum RMS values  
 (a) View of ellipses at minimum RMS TSoA 0.061 m, whereas TDoA method has RMS 45.8 m,  
 (b) View of hyperbolas at minimum RMS TDoA 0.058 m, whereas TSoA method has RMS 0.68 m

This type of error is the most significant, and can actually greatly harm the positioning system. It should be noted that the TSoA method copes well with this problematic configuration. For  $\varepsilon = 1$ , the branches of the hyperbola also merge into straight lines emerging from points with BS coordinates and diverging in different directions from the BS. The gross error is explained by rearranging the solution from one branch of the hyperbola to another. In this case, the errors are not as drastic as compared to the previous configuration, but they can also lead to unexpected consequences in a real system. The TSoA method works in this configuration as well. Thus, if the decision is correctly switched from the TDoA algorithm to the TSoA algorithm, depending on the configuration of the BS location and the object, blunders in many areas of the positioning system coverage can be eliminated. This is exactly what we offer in the combined TSoA/TDoA method.

The method proposed in [12] for hyperbolic equations can significantly reduce gross errors associated with the vanishing of determinants. The method consists in successive reassignment of each base station to the reference one. Thus, configurations are formed according to the number of BS in the system, in the case under consideration there will be four of them. All distances between the points of intersection of lines are recorded in a single 2D distance matrix, then three minimum distances between points in the distance matrix in all four configurations are determined and the point of intersection of three hyperbolas is determined from them. The method of reassigning each BS to the reference one made it possible to significantly reduce gross errors over the entire area of the positioning system operation. The TSoA method showed particularly good results. The root-mean-square deviation of the RMS maxima decreased by 60 times, leaving only one maximum in the center of the positioning system zone. The reassignment of the BS to the reference ones for the TDoA method made it possible to reduce the standard deviation of the RMS maxima by 2.5 times, to reduce the area of the positioning system service area, where gross errors occur. However, there are still zones with gross errors. That is, it turns out that the TDoA method is more accurate inside the BS perimeter, and the TSoA method is more accurate than the TDoA method outside the BS perimeter. So, the advantages of the TSoA method over the TDoA method include fewer gross errors and better accuracy outside the BS perimeter, and the advantage of TDoA over TSoA should include more accurate work inside the BS perimeter. The combined TSoA/TDoA method has the potential to combine the benefits of these two methods into one.

#### Simulation of the combined TSoA/TDoA method for estimating object coordinates with fluctuations in the measurement of arrival times

The combined TSoA/TDoA method assumes the choice of the best method for the accuracy of determining the coordinates and the absence of gross errors from TSoA or TDoA methods, depending on

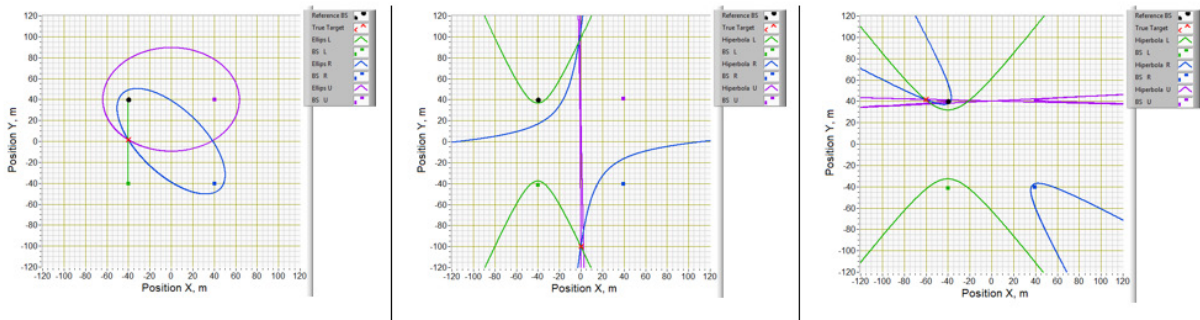


Fig. 4. Positions of ellipses and hyperbolas at maximum RMS values  
 (a) View of ellipses at maximum RMS TSoA 61.4 m, whereas TDoA method has RMS 0.09 m,  
 (b) View of hyperbolas at maximum RMS TDoA 200 m. The hyperbola  $U$  has an eccentricity  $\varepsilon = \infty$ ,  
 whereas TSoA method has RMS 0.064 m, (c) View of hyperbolas at maximum RMS TDoA 46 m.  
 The hyperbola  $U$  has an eccentricity  $\varepsilon = 1$ , whereas TSoA method has RMS 0.061 m

the location of the BS and the object. The main idea of the proposed method is to combine the distances between the intersection points for both methods into a single 2D matrix and search for the minima of the distances between the intersection points of lines (ellipses and hyperbolas) from this single matrix. Thus, the algorithm chooses the TSoA or TDoA method. To identify the correct (true) point of intersection of the three lines, Algorithm 1 is proposed, which is an implementation of the combined TSoA / TDoA method.

**Algorithm 1.** Identifying of the true solution

1. Changing the reference BS according to 4 configurations of the spatial arrangement of the BS. Each BS once becomes a reference.
2. Formation of a 2D matrix of coordinates of the points of intersection of lines: each of the 4 lines (each line corresponds to the configuration of the BS) contains 12 coordinates of the points of intersection (6 points of intersection of ellipses and 6 points of intersection of hyperbolas).
3. Calculation of distances between the points of intersection of lines (6 points of ellipses and 6 points of hyperbolas). Between 6 points of intersection of lines, 15 distances between points are calculated for ellipses and 15 distances between points for hyperbolas.
4. Formation of a 2D distance matrix: 4 lines (each line corresponds to the BS configuration) contain 30 distances between the intersection points of lines: 15 distances between the intersection points of ellipses and 15 distances between the intersection points of hyperbolas. The distance table is common for the TSoA and TDoA methods, thus combining the two methods TSoA and TDoA.
5. Selection of 9 consecutive minima from a 2D distance table. Formation of 1D matrices for the values of 9 minimum distances, 9 configuration indices and 9 indices in the distance table.
6. Separation of 9 minimum distances, 9 configuration indices and 9 indices in the distance table on the basis of ellipses or hyperbolas. If the index in the distance table is less than 15, then this is the intersection point of the ellipses, if the index in the distance table is greater than or equal to 15, then this is the intersection point of the hyperbolas.
7. Selecting the BS configuration. If there are points of intersection of ellipses, then the configuration with ellipses is selected. If there are several intersection points of the ellipses, then the BS configuration with the minimum value of the distance  $D$ .
8. Selection of an index in the table of distances in a certain (item 7) configuration of the BS, corresponding to the minimum distance between the points of intersection of the lines.
9. According to the identified configuration index (item 7) and the distance index (item 8) from the 2D matrix of coordinates of the points of intersection of the lines (item 2), we select the coordinates of the object.

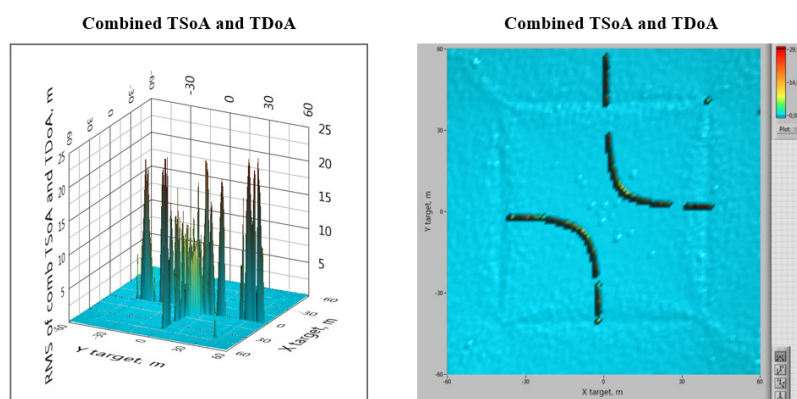


Fig. 5. The location of gross errors in determining the coordinates of the object on the plane of the combined method TSoA/TDoA (a) RMS of TSoA/TDoA, (b) Top view

The selected coordinates are closest to the true coordinates of the target. The remaining coordinates are either false, or determine the coordinates of the object with a larger error.

Fig. 5 shows the location of gross errors in determining the coordinates of an object on the plane of the combined TSoA/TDoA method, obtained using simulation. As before, the calculation of the root mean square (RMS) deviation was carried out for the number of computational experiments 100, the arrival time deviation was 0.4 ns.

The simulation results show that the combined TSoA/TDoA method makes it possible to reduce the RMS maxima by a factor of 4 compared to the TDoA method, and further reduce the area of the positioning system service area where gross errors occur. In areas where there are no gross errors, the RMS position determination coincides with the TDoA method, which, as indicated above, had advantages over the TSoA method. However, it should be noted that it was not possible to completely eliminate gross errors, although they significantly decreased.

Fig. 6 shows the dependences of the standard deviation of the estimate of the object's coordinates on the standard deviation of the Gaussian white noise of the times of arrival of radio signals in the BS for the matrix linearization algorithm and the proposed analytical combined TSoA/TDoA algorithm. Dependencies are calculated for object coordinates  $[x; y] = [39; -7]$  and  $BS_C$  coordinates  $[x_C; y_C] = [-40; 40]$ ,  $BS_L$   $[x_L; y_L] = [-40; -40]$ ,  $BS_R$   $[x_R; y_R] = [40; -40]$ ,  $BS_U$   $[x_U; y_U] = [40; 40]$  meters. This location of the object and the BS is a rather complicated configuration for determining the coordinates, however, the combined method allows you to determine the coordinates of the object with high accuracy.

It follows from the simulation results that the proposed combined TSoA/TDoA method provides an 8 times higher accuracy in determining the object's coordinates compared to the hyperbolic equation linearization method. The combined TSoA/TDoA method works with high accuracy ( $\sim 1$  m) with BS desynchronization up to 8 ns, while the linearization method starts to give gross errors (failures) already at 4 ns BS desynchronization. The proposed algorithm significantly outperforms the widely used positioning algorithm based on the linearization of hyperbolic equations.

## Discussion

The combined TSoA/TDoA method based on the analytical solution of elliptic and hyperbolic equations, unlike many existing methods, allows you to obtain an accurate solution for determining the coordinates of an object based on the measurement of arrival times. The advantages of the combined method are the high accuracy of determining the coordinates of the object, a significant reduction in the zones in which gross errors occur due to the vanishing of the determinants of the systems of equations. The meth-

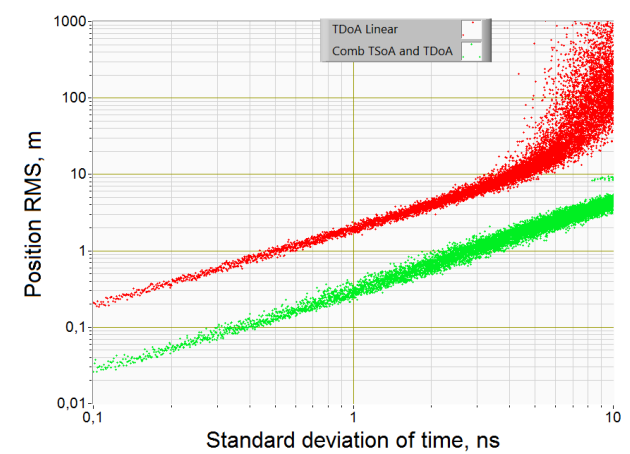


Fig. 6. Dependence of the RMS estimate of the determination of the object's coordinates on the plane versus the deviation of the Gaussian white noise of arrival times for the combined TSoA/TDoA and TDoA Linear methods

od allows you to automatically choose the best solution from elliptic and hyperbolic equations. A certain problem in the implementation and practical use of the combined method may be the limited capabilities of microprocessor technology for the implementation of calculations of expressions with radicals, which is necessary in the analytical exact method proposed by us. However, it should be noted that the computing element base is rapidly developing, the introduction of low-cost processors is expected, which allow calculating mathematical functions with radicals in real time. In many applications, such as “smart city” traffic control systems, all calculations can be performed on a computationally powerful server. In this example, restrictions on mathematical data processing are removed.

To accurately determine the moment of arrival of a radio signal from an object to base stations, various forms of radio signals are used. The wider the spectrum of the radio signal, the more precisely it is localized in time. Therefore, ultra-wideband (UWB) signals with a wide spectrum have advantages over signals with a shorter spectrum and are used in positioning systems. In our article, the question of the shape of the used radio signal is not the subject of research.

Time-of-arrival measurement errors occur for three main reasons: radio signal propagation attenuation, radio multipath, and time desynchronization at base stations. In this work, to assess the accuracy of determining the coordinates of an object, Gaussian white noise is used, which is added to the difference and the sum of the signal arrival times. Without diminishing the importance of studying the influence of multipath propagation and attenuation of a radio signal during propagation, we nevertheless believe that the approach we used to study noise immunity allows us to compare the TSoA and TDoA methods.

As a promising area of research, we consider the joint TSoA/TDoA method based on solving a system of equations by the intersection of a hyperbola with an ellipse. The joint TSoA/TDoA method will reduce the number of BSs in a multi-position system by one compared to the combined TSoA/TDoA method studied in this article.

In future work we intend to conduct a research on the effect of multipath propagation of a radio signal, take into account the attenuation of a radio signal during propagation, develop a mathematical model and investigate the joint TSoA/TDoA method, as well as extend the proposed algorithms to 3D space and consider the applicability of the proposed methods for determining the coordinates of a set of objects.

### Conclusions

A feature of this work is the construction of a positioning system based on the solution of exact analytical equations, which eliminates the need to use iterative procedures when calculating the coordinates of an

object. A comparative analysis of the advantages and disadvantages of the two main methods for determining the coordinates of an object, TSoA and TDoA, was carried out, and based on the analysis, a combined TSoA/TDoA method was proposed. As a result of the simulation, it was revealed that the combined TSoA/TDoA method has an accuracy of determining the coordinates of an object an order of magnitude higher than the frequently used method of linearizing hyperbolic equations. The proposed method will provide local positioning systems with the possibility of increasing the maximum detection and control range of objects with a low effective area scattering.

## REFERENCES

1. **Zekavat R., Buehrer R.M.** Handbook of position location: Theory, practice and advances. John Wiley & Sons, 2019.
2. **Kuptsov V.D., Ivanov S.I., Fedotov A.A., Badenko V.L.** Rain attenuation in millimeter wave, centimeter wave and visible light ranges, IOP Conference Series: Materials Science and Engineering. 2021, Vol. 1047, p. 12197.
3. **Díez-González J., Álvarez R., Sánchez-González L., Fernández-Robles L., Pérez H., Castejón-Limas M.** 3D TDoA Problem Solution with Four Receiving Nodes, Sensors. 2019, Vol. 19, p. 2892.
4. **Foy W.H.** Position-location solutions by Taylor-series estimation, IEEE Trans. Aerosp. Electron. Syst. 1976, Vol. 12, pp. 187–194.
5. **Chan Y.T., Ho K.C.** A simple and efficient estimator for hyperbolic location, IEEE Trans. Signal Process. 1994, Vol. 42, pp. 1905–1915.
6. **Ivanov S., Kuptsov V., Badenko V., Fedotov A.** RSS/TDOA-based source localization in microwave UWB sensors networks using two anchor nodes, Sensors. 2022, Vol. 22 (8), p. 3018.
7. **Novák D., Gregor L., Veselý J.** Capability of a Ground-Based Passive Surveillance System to Detect and Track Spaceborne SAR in LEO Orbits, Remote Sens. 2022, Vol. 14, p. 4586.
8. **Kuptsov V.D., Ivanov S.I., Fedotov A.A., Badenko V.L.** High-precision analytical TDoA positioning algorithm for eliminating the ambiguity of coordinates determination, IOP Conference Series: Materials Science and Engineering. 2020, Vol. 904, p. 012013.
9. **Vesely J., Van Doan S.** Analytical Method Solving System of Hyperbolic Equations, Proceedings of the 2015 25th International Conference Radioelektronika, Pardubice, Czech Republic, 21–22 April 2015, Pp. 343–348.
10. **Van Doan S., Vesely J.** The Effectivity Comparison of TDOA Analytical Solution Methods, Proceedings of the 2015 16<sup>th</sup> International Radar Symposium (IRS), Dresden, Germany, 24–26 June 2015, Pp. 800–805.
11. **Van Doan S., Vesely J., Janu P.** The Measurement of TDOA Short Baseline, Proceedings of the International Conference on Military Technologies (ICMT), Brno, Czech Republic, 19–21 May 2015, pp. 1–5.
12. **Kuptsov V., Badenko V., Ivanov S., Fedotov A.** Method for remote determination of object coordinates in space based on exact analytical solution of hyperbolic equations, *Sensors*. 2020, Vol. 20 (19), Pp. 5472–5491.
13. **Li S., Hua J., Zhong G., Lu W., Jiang B.** A TSoA based Localization Algorithm in Wireless Networks, Proceedings of the 2016 IEEE 11th Conference on Industrial Electronics and Applications (ICIEA), Hefei, China, 05-07 June 2016, Pp. 526–530.
14. **Xiong W., Bordoy J., Schindelbauer C., Gabbrielli A., Fischer G., Schott D.J., Hoeflinger F., Rupitsch S.J., So H.C.** Data-Selective Least Squares Methods for Elliptic Localization With NLOS Mitigation, IEEE Sensors Letters. 2021, Vol. 5 (7), Pp. 1–4.
15. **Amiri R., Behnia F., Sadr M.A.** Exact Solution for Elliptic Localization in Distributed MIMO Radar Systems, *IEEE Transactions on Vehicular Technology*. 2018, Vol. 67 (2), Pp. 1075–1086.
16. **Lay K.T., Chao W.K.** Mobile Positioning Based on TOA/TSoA/TDOA Measurements with NLOS Error Reduction, Proceedings of 2005 International Symposium on Intelligent Signal Processing and Communication Systems, Hong Kong, 13–16 December 2005, Pp. 545–548.

17. **Panwar K., Babu P.** Robust Multistatic Target Localization in the Presence of NLOS Errors and Outliers, IEEE Signal Processing Letters. 2022, Vol. 29, Pp. 2632–2636.

18. **Zheng X., Hua J., Zheng Z., Peng H., Meng L.** Wireless Localization based on the Time Sum of Arrival and Taylor Expansion. Proceedings of 19<sup>th</sup> IEEE International Conference on Networks (ICON), Singapore, 11–13 December 2013, Pp. 1–4.

19. **Al-Samahi S.S.A., Zhang Y., Ho K.C.** Elliptic and hyperbolic localizations using minimum measurement solutions, Signal Processing. 2020, Vol. 167, p. 107273.

#### INFORMATION ABOUT AUTHORS / СВЕДЕНИЯ ОБ АВТОРАХ

**Vladimir D. Kuptsov**

**Купцов Владимир Дмитриевич**

E-mail: kuptsov@spbstu.ru

<https://orcid.org/0000-0001-8594-9423>

**Sergei I. Ivanov**

**Иванов Сергей Иванович**

E-mail: ivanov\_si@spbstu.ru

<https://orcid.org/0000-0002-2882-0380>

*Submitted: 11.05.2023; Approved: 25.06.2023; Accepted: 06.07.2023.*

*Поступила: 11.05.2023; Одобрена: 25.06.2023; Принята: 06.07.2023.*

# Telecommunication Systems and Computer Networks

## Телекоммуникационные системы и компьютерные сети

Research article

DOI: <https://doi.org/10.18721/JCSTCS.16205>

UDC 681.518.3



### INFLUENCE OF TECHNOLOGICAL PROCESSES ON THE UNCERTAINTY OF SYSTEMS MEASURING LIQUEFIED NATURAL GAS ENERGY

*A.V. Safonov*<sup>1</sup> ✉

<sup>1</sup> LLC “Oil and Gas Systems”,  
Shchelkovo, Moscow region, Russian Federation

✉ [safavs@yandex.ru](mailto:safavs@yandex.ru)

**Abstract.** The article shows a new measuring technology and a statistical approach to control the measured values and parameters of technological processes that reduce the uncertainty of systems measuring the amount of liquefied natural gas energy (LNG). An increase in the consumption of liquefied natural gas requires the use of measuring technologies that take into account changes in physical and chemical properties, process parameters, and other factors affecting the uncertainty of measuring systems at subzero temperatures of working fluids. A measuring technology is presented that takes into account the influence of technological processes and changes in the properties of LNG. The application of a statistical approach to the control of measured values makes it possible to reduce the influence of technology and changes in physico-chemical properties on the uncertainty of the of systems measuring mass, volume, density and energy of LNG. The developed system of metrological support increases the accuracy of measurement systems of LNG energy by 1.5–2 times. The solution is relevant for information and measurement systems for determining the amount of energy of liquefied hydrogen.

**Keywords:** measurement system, uncertainty, energy, stratification, reliability, statistical, liquefied natural gas

**Citation:** Safonov A.V. Influence of technological processes on the uncertainty of systems measuring liquefied natural gas energy. *Computing, Telecommunications and Control*, 2023, Vol. 16, No. 2, Pp. 55–70. DOI: 10.18721/JCSTCS.16205

Научная статья

DOI: <https://doi.org/10.18721/JCSTCS.16205>

УДК 681.518.3



## ВЛИЯНИЕ ТЕХНОЛОГИЧЕСКИХ ПРОЦЕССОВ НА НЕОПРЕДЕЛЕННОСТЬ ИЗМЕРИТЕЛЬНЫХ СИСТЕМ КОЛИЧЕСТВА ЭНЕРГИИ СЖИЖЕННОГО ПРИРОДНОГО ГАЗА

А.В. Сафонов<sup>1</sup> ✉<sup>1</sup> ООО «Системы Нефть и Газ»,  
г. Щелково, Российская Федерация✉ [safavs@yandex.ru](mailto:safavs@yandex.ru)

**Аннотация.** В статье показана новая измерительная технология и статистический подход контроля измеряемых величин и параметров технологических процессов, которые позволяют уменьшить неопределенность измерительных систем количества энергии сжиженного природного газа. Увеличение потребления сжиженного природного газа требует применения измерительных технологий, которые учитывают изменение физико-химических свойств, параметров технологического процесса, и других факторов, влияющих на неопределенность измерительных систем при отрицательных температурах рабочих жидкостей. Представлена измерительная технология, учитывающая влияние технологических процессов и изменение свойств СПГ. Применение статистического подхода при контроле измеряемых величин позволяет уменьшить влияние технологии и изменения физико-химических свойств рабочих углеводородных жидкостей на неопределенность ИИС массы, объема, плотности и энергии СПГ. Разработанная система метрологического обеспечения в 1,5–2 раза повышает точность измерительных систем энергии сжиженного природного газа. Решение актуально для информационно-измерительных систем определения количества энергии сжиженного водорода.

**Ключевые слова:** измерительная система, неопределенность, энергия, стратификация, достоверность, статистический, сжиженный природный газ

**Для цитирования:** Safonov A.V. Influence of technological processes on the uncertainty of systems measuring liquefied natural gas energy // Computing, Telecommunications and Control. 2023. Т. 16, № 2. С. 55–70. DOI: 10.18721/JCSTCS.16205

### Introduction

Reception-transmission of liquefied natural gas (LNG) during transportation by sea vessels, reception and shipment to storage tanks are made on the basis of the amount of energy equivalent to the transferred volume of LNG. Measurements of the actual values of the volume of transferred LNG are currently carried out by a static method using level measurement systems when LNG is poured into a storage tank or tanker tanks using calibration and correction tables of tank capacity. The component composition and physico-chemical properties of LNG are determined in the laboratory from a sample selected by a special sampling device according to a given technological regulation [1, 5]. The values of density and calorific value are calculated based on the results of determining the component composition in laboratory conditions by gas chromatographic method [5, 13]. The methods for determining the density and calorific value when performing commodity transport operations (CTO) are described in the international standards GIIGNL [1–6, 8]. The accounting unit used in the calculations between the Seller and the Buyer is the amount of energy transferred: the equivalent of volume (mass) of the transferred LNG. LNG energy is defined in MJ or British thermal units MMBtu,  $1 \text{ MMBtu} = 1.055 \cdot 10^9 \text{ J}$  [5, 11].

The accuracy of measuring the level and the volume of LNG in the tank is determined by the uncertainty of the liquid–gas interface associated with the boiling point of LNG, which characterizes the



equilibrium state of any liquefied gas at boiling point. The uncertainty of level measurements depends on the uncertainty of tank calibration, on the technical condition, volume and type of tanks, sea waves, the type of system used and the thoroughness of measurements, the processes of “evaporation” and “boiling”, changes in the component composition of LNG [12]. The uncertainty of the tank calibration depends on the chosen calibration method and the discreteness in the construction of the calibration table [5, 11, 18, 19, 23–25].

When determining the actual volume in the tank, it is necessary to take into account the physico-chemical properties of a particular grade of LNG, for which the coefficients of volumetric expansion and compressibility differ. Additional influencing factors in determining the volume of LNG in the tank are the technical condition, dimensions, type of tank and thermal insulation, the magnitude of the coefficients of linear and volumetric expansion of materials and structural elements of tanks. During the voyage, it is important for the preservation of physicochemical properties to maintain the pressure in the tanker tanks greater than the pressure of LNG in shore tanks, this is necessary to limit evaporation during transportation, storage and unloading [11].

The daily volume of LNG evaporation in a tanker depends on the size of the tanks, the ratio of the liquid phase surface in the tanks to the loading volume, climatic and marine conditions (water temperature, air, sea condition, etc.) and thermodynamic characteristics of the loaded LNG (supercooling depth, etc.). Numerical values of evaporation vary from 0.18% to 0.25% of the total volume of LNG in existing tankers, and up to 0.10% for LNG tankers of new designs equipped with a new thermal insulation system [11, 28].

The static method of volume measurements is not applicable in the joint use of LNG storage terminals, when LNG belonging to several owners is pumped through the cargo fleet, loading ramps and supply pipelines: in this case, it is impossible to reconcile volumes with tankers by sellers [28]. In such cases, a dynamic method of measuring mass or volume by flow converters is used. The static methods employed today, with the use of level measurement systems in the tanker, make it possible to determine the volume of LNG with an uncertainty of 0.7–0.9% [28]. Factors affecting the accuracy of volume measurements in tanks using level systems are due to the heterogeneity/uncertainty of the measured liquid, the formation of a gas phase in the field of level measurements, which differs for different grades of LNG. These factors increase the uncertainty of determining the volume by  $\geq 1\%$  [11, 28]. Methods used in information and measurement systems (IMS) and sampling systems, methods for determining density, component composition and calorific value [16]. Volume measurements using level systems do not always allow determining the volume and amount of LNG energy with the required accuracy stated by the current regulatory and technical documents (RTDs), which is a natural change in the physico-chemical properties of LNG [11, 16, 26, 27].

The problem of determining the amount of LNG energy and transferring units of quantities from standards to measuring systems at subzero temperatures is caused by the difficulty in ensuring the homogeneous state of LNG during sampling and measurements. The increase in LNG consumption requires the use of advanced information and measurement systems to determine the amount of energy of liquefied natural gas (IMSLNG), including using dynamic systems with flow converters, appropriate measurement technologies that take into account changes in physical and chemical properties, process parameters, and other factors affecting the accuracy of determining the amount of energy. The developed IMSLNG should take into account these changes, and the applied measurement technologies of testing and control should ensure reliable measurements [11].

#### **Analysis of technological processes affecting the uncertainty of density and calorific value**

Determination of the density and the highest calorific value of the transmitted LNG is based on the determination of the component composition by gas chromatographic analysis. The method allows us to determine the volume fraction of the highest calorific value, and mass units are used for commercial operations, therefore it is necessary to measure the density of LNG [1–6, 8, 11, 15]. The contribution of the

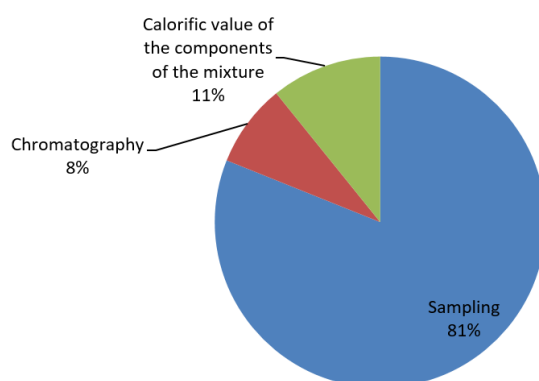


Fig. 1. Uncertainty budget of the highest calorific value

highest calorific value is up to 30% in the total uncertainty of the amount of transferred LNG energy. In the uncertainty of the highest calorific value, the greatest contribution is associated with sampling technology and can reach 81% (Fig. 1).

Density is the main input value in the equations for determining the mass and the highest calorific value of LNG. The contribution from the uncertainty of density is at least 40% in the uncertainty budget of the amount of transferred LNG energy.

GIIGNL standards allow two methods for determining LNG density [4, 5].

The first, a direct measurement method, using a density converter or a density channel of a mass flow converter installed in a tank or measuring pipeline. The second, indirect, currently used, consists in determining the density by component composition using gas chromatographic method. The main disadvantage of the first method is the lack of primary and working density standards that allow us to determine and confirm the actual density values in working conditions. When calibrating density converters and density channels of mass flow converters, liquids are currently used as a working medium, which differ significantly in their properties from the physico-chemical properties of LNG.

In the absolute majority of cases, water or petroleum products with a density and viscosity that differ from the properties of LNG are used for calibration, when conversion coefficients are used to bring them to negative temperatures. Recalculation of calibration results performed at positive temperatures of 20–25 °C to the operating conditions of LNG with a temperature of minus 162.5 °C and a pressure of 0.5–1.0 MPa introduces additional uncertainty, the value of which can reach 1.0 kg/m<sup>3</sup> or more. Therefore, direct density measurement methods currently have limited application and are used only for technological control [12]. The disadvantages of the second, indirect, measurement method include significant contributions from the sum of uncertainties determined by the sampling location, the type of sampling system selected, the sampling and storage method, the thoroughness with which the operator took the sample, the type of analyzer and the measurement method [8, 9, 11, 19, 20].

The main problem of LNG density measurements for direct and indirect methods is the difficulty of ensuring a homogeneous state of the liquid flow in the area of the converter and sampling system. In fact, the flow is inhomogeneous, consisting of a liquid and a gas phase, in which the number and ratio of phases vary. Moreover, in some cases, measurements become impossible, or the measurement results exceed the permissible limits of uncertainty, and this is due to the technological process, instability of the composition and properties of LNG [8, 9, 13, 16, 29].

The actual values of uncertainties in the results of LNG density measurements by density converters or density channels of mass converters caused by the above conditions are at least 3–5 kg/m<sup>3</sup> [11]. In laboratory conditions, the Kleinram and Wagner hydrostatic method or the Klosek-McKinley pycnometric method can be used. These methods are currently not used in commercial operations due to the length of

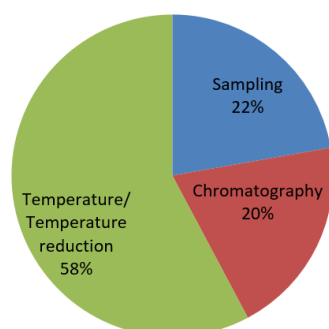


Fig. 2. Uncertainty budget of density measurements

the measurement process and the high cost of unique equipment, but are used only for research in laboratory conditions [5, 8, 9].

The density measured in the laboratory from the selected sample will always differs from the density of LNG in the measuring pipeline or in the tank. The problem of density measurements at the site of operation remains unresolved [20]. A similar situation was with measurements of the density of commercial oil during commercial operations, when in the mid-eighties of the last century, the urgent task was to find the reasons for exceeding the error in the mass of oil at CTO. The reason for exceeding the permissible uncertainty in mass was the measurement of oil density by hydrometers in the laboratory, when light fractions evaporated, and the hydrometer measured oil with a different density. Moreover, with an increase in the time interval between sampling and measurements, the density of oil also changed more. The reason for the excess of uncertainty in the mass of oil was eliminated after special reference density measuring instruments that receive a unit of magnitude from state standards appeared in Russia. Density standards are designed to monitor metrological characteristics and verify density converters at the place of operation [8, 9, 11].

The second group of indirect methods, which are the main ones at present, includes various methods for determining the density by the component composition of LNG [11], for example: the Watson method, the Elfacuten method, the Miller graphical method, the Heese method, the Klosek-McKinley method. A promising method of spectroscopy proposed by C.V. Raman is based on molecular level studies, a method that is less dependent on changes in pressure and flow velocity in the sampling system line and with better repeatability of measurement results. However, the method has limited application due to the duration of measurements, high cost and qualification of personnel [5, 11].

In accordance with the requirements of the GIIGNL standard [5], the method of determining density by component composition and temperature makes the greatest contribution to the uncertainty of determining density. Uncertainty of component composition determination by gas chromatography is 0.09% according to GIIGNL [4, 5, 13]. The values of contributions to the total standard uncertainty of calorific value measured by indirect, gas chromatographic measurement method are presented in the diagrams in Fig. 1 and Fig. 2. The greatest contribution to the uncertainty budgets of density measurements and higher calorific value is made by sampling, temperature measurement and temperature reduction.

The analysis of density and calorific value uncertainties proves the necessity of using a direct method of LNG density measurements, the use of which eliminates the largest components associated with evaporation and temperature conversions increasing the accuracy of density and calorific value measurements. [11, 23–25].

The actual values of the uncertainty of determining the component composition are much higher, depend on factors not previously taken into account, and this is the uncertainty of sampling, which depends

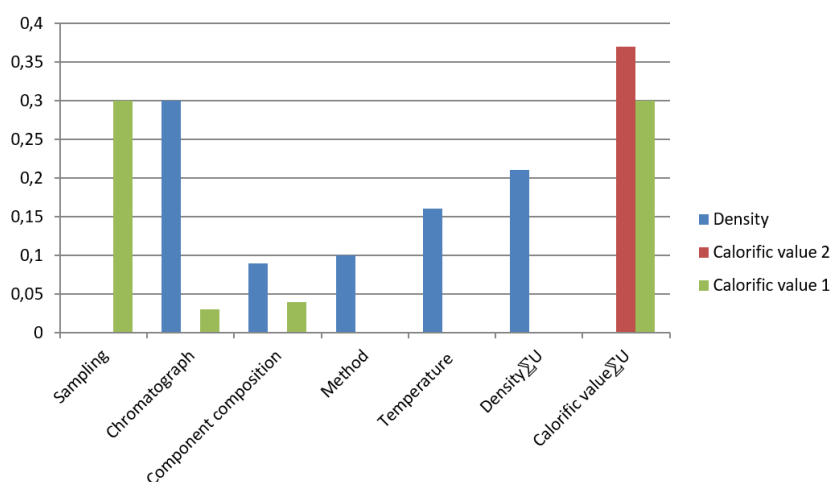


Fig. 3. Uncertainty budget of calorific value of IM system

on the phase state of the flow [10]. Density and calorific value in the total uncertainty of the amount of LNG energy are presented in Fig. 3.

Taking into account the real values of uncertainties, we obtain the LNG density determined by the GIIGNL methods [5], reduced by temperature and pressure to operating conditions, which gives results significantly different from the actual values of  $\geq 10 \text{ kg/m}^3$ .

#### Analysis of the influence of technological processes on the stratification of flows of multicomponent liquids

The main influencing factors on stratification and homogenization of a multicomponent LNG stream are velocity, pressure of the flow in the pipeline and pressure of saturated vapors [24]. The results of studies of the flow processes of mixtures of hydrocarbon liquids have shown that stratification of the LNG mixture flow occurs at speeds of less than 1.5–2 m/s and pressures of less than 0.4 MPa, the values of which may vary depending on the component composition of a particular LNG grade [11].

Complete mixing of the flow occurs at speeds of more than 2.5–3 m/s and pipeline pressure of at least 0.5–0.7 MPa as shown in Fig. 4.

When the flow velocity exceeds more than 5–6 m/s, the flow becomes stratified again, further increase in pressure fails to return the flow to a homogeneous state.

To reduce the total standard uncertainty of LNG energy, it is necessary to reduce the uncertainties associated with volume measurement and sampling. It is necessary to apply methods to increase the representativeness of sampling and to assess the reliability of sampling, density measurement and to develop equations of natural gas state taking into account the influencing factors [13, 16, 29].

#### Analysis of the impact of technological processes on the reliability of sampling

During the period of pumping a batch of LNG with the help of a control multipoint (tubular) probe, profile tests are carried out, during which the distribution of the estimated LNG quality indicators is determined, for example the value of the density or methane content selected along the pipeline section [13]. As a base value, the sampling results obtained from the control probe, the number of sampling points along the pipeline section ( $n+2$ ), compared with the working probe are taken [13]. When removing the profile from each point located along the diameter of the pipeline, each sample is taken into a separate container. All selected samples are analyzed, and based on the obtained measurement results, a graphical dependence of the distribution of the values of these values over the diameter of the pipeline is constructed. According to the obtained dependence, the averaged values of the value for the period corresponding to sampling for this flow profile are determined [13]:

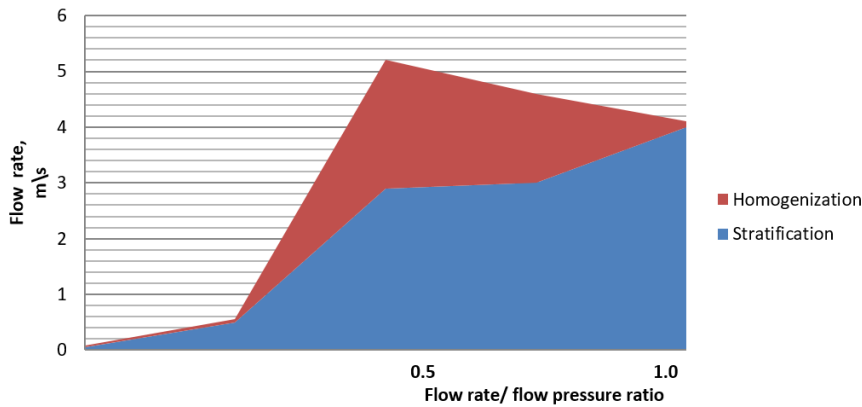


Fig. 4. Phase state of the LNG mixture flow depending on the velocity and pressure

$$W_{avg_j} = \frac{1}{D} \sum_{i=1}^n W_i \Delta X_i, \quad (1)$$

where  $D$  is pipeline internal diameter, mm;  $\Delta X_i$  is distance between sampling points, mm;  $W_i$  is quality indicator value of  $i^{\text{th}}$  point sample, %;  $n$  is number of sampling points [13].

During the period of LNG pumping, at least three profiles are removed at the operating flow rate. The value of the quality indicator is estimated for the period of the set time of sampling of the test sample during shipment/loading. The basic value of the quality indicator value for the period of sampling of the combined sample under study is calculated by the formula:

$$W_{bas} = \frac{1}{T} \sum_{j=1}^k W_{avg_j} \Delta t_j, \quad (2)$$

where  $\Delta t_j$  is time period for which  $j^{\text{th}}$  profile is defined, minutes;  $W_{avg_j}$  is average value of a quantity in  $j^{\text{th}}$  profile by equation (6), %;  $T$  is time of sampling of the combined sample under research, minutes [13].

The assessment of the reliability of sampling is considered satisfactory when the deviations of the average values of the estimated value according to the results of measurements of three flow profiles do not exceed 5% [13].

The results of studies on the deviation of the density and content of methane in the LNG mixture were carried out on a pipeline with a diameter of 250 mm at five cross-section points. Figure 5 shows density deviations of more than 5% (417–442 kg/m<sup>3</sup>) along the pipeline section of stratified flow and homogeneous LNG flow, when density deviations along the pipeline section do not exceed 2% (430–438 kg/m<sup>3</sup>). To create a homogeneous flow, the pressure in the pipeline after the sampling point was increased by 24% [13].

Figure 6 shows deviations of methane content of more than 7% (88–95%) along the pipeline section for stratified flow and homogeneous LNG flow, when density deviations along the pipeline section do not exceed 4.5% (92–96%).

Estimation of sampling uncertainty. The research results have shown that sampling depends on the phase state of the working media flow, which makes the greatest contribution to the uncertainty budget of the measured values: component composition, density and calorific value – the main indicators that require verification during LNG reception and transmission operations. With the experimental evaluation method, a measurement procedure is performed to directly assess the uncertainty of the measurement result. With the theoretical evaluation method, each source of uncertainty is quantitatively assessed separately and in combination in the budget in accordance with the methodology adopted for this purpose

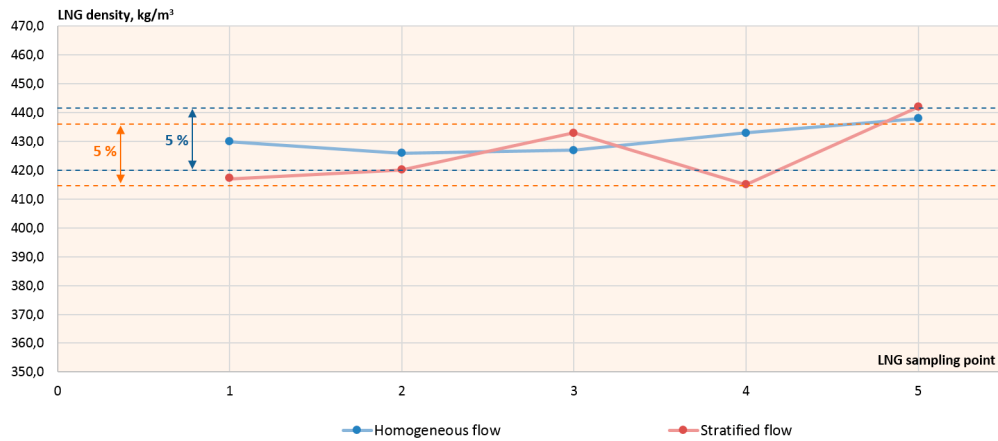


Fig. 5. Sampling reliability estimate in density determination

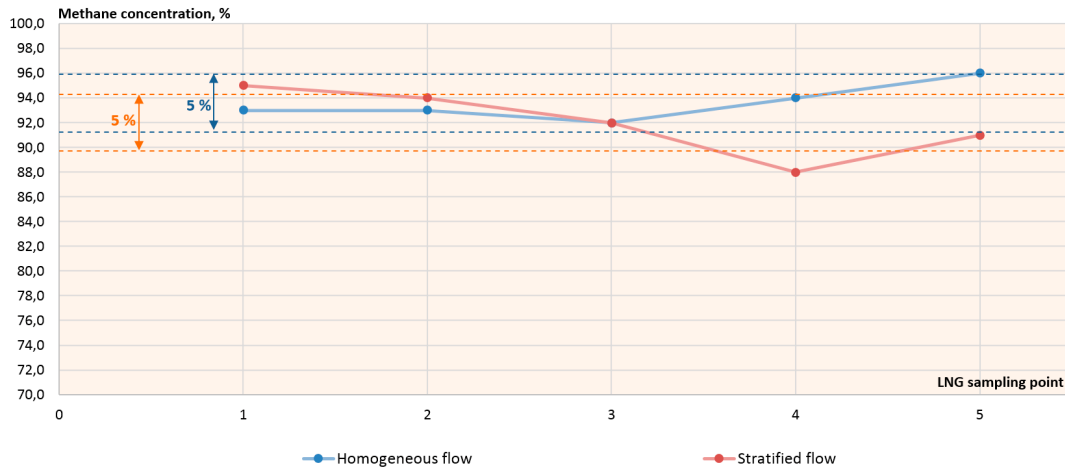


Fig. 6. Sampling reliability estimate in methane content determination

for assessing the reliability of sampling [16]. The dispersed nature of the LNG mixture leads to a dispersion of the measurement results of the samples taken, which is caused by the different composition of the samples actually taken causing an additional contribution to the total uncertainty [16]. The experimental approach is widely used in practice, for example, the “double sampling method”. The implementation of the method requires less time and costs, which is especially important for one-time studies of various target objects. The “double sampling method” usually involves the work of one sampling operator and one sampling scheme; the same plan can be used with different operators to take into account the subjective contribution to uncertainty. The random effects model of a single sampling object can be described by the following formula:

$$X = X_{true} + \varepsilon_{sample} + \varepsilon_{analysis}, \tag{3}$$

where  $X_{true}$  is actual value of the measured variable;  $\varepsilon_{sample}$  is uncertainty component due to with drawal procedure;  $\varepsilon_{analysis}$  is uncertainty component due to selected analysis procedure.

For a single target object, when the sources of variance are independent, the variance of the measurement result  $\sigma^2$  can be represented by the equation:

$$\begin{aligned}
 u_c(V) = & \left[ u_c(V_{cal})^2 + u_c(V_{phase\ boundary})^2 + u_c(K_{temp})^2 + \right. \\
 & \left. + u_c(K_{cal\ op\ temp})^2 + u_c(V_{cool})^2 + u_c(V_{heat})^2 \right]^{1/2}, \quad (4) \\
 \sigma_{meas}^2 = & \sigma_{sample}^2 + \sigma_{analysis}^2,
 \end{aligned}$$

when approximating the variance by statistical methods, we obtain:

$$\mathbf{u}_{meas}^2 = \mathbf{u}_{sample}^2 + \mathbf{u}_{analysis}^2, \quad (5)$$

To improve reliability, it is suggested to consider sampling uncertainty  $\mathbf{u}_{sample}$  with the following components not included before:  $\mathbf{u}_{flow}$  as uncertainty due to heterogeneity of LNG multi-component flow and  $\mathbf{u}_{sample\ type}$  as uncertainty due to probe type:

$$\mathbf{u}_{sample}^2 = \mathbf{u}_{flow}^2 + \mathbf{u}_{sample\ type}^2, \quad (6)$$

where  $\mathbf{u}_{flow}$  is uncertainty due to natural stratification and low density component distribution in the upper section of pipeline and higher density components in the lower section. Currently, only the uncertainty of the analysis and evaporation of the selected sample during preparation is evaluated. The presence of a gas phase in the sampling zone must be monitored using the phase state indicator (PSI) of the flow. It is also permissible to control the flow at the sampling site using a pressure converter installed after the sampling probe to control the back pressure value recommended for specific technological conditions and the LNG grade [16]. In this case, the sampling uncertainty is determined taking into account the contribution of sampling variance not previously taken into account: the phase state of the flow and the type of sampling system [16]. Then the sampling uncertainty is calculated using a formula that takes into account the possible stratification of the multicomponent flow, the type of sampling probe used, the uncertainty of analysis/measurement in determining the component composition and the uncertainty associated with sample storage and sample preparation for measurements [28, 29]:

$$\mathbf{u}_{sampling} = \left( \mathbf{u}_{flow}^2 + \mathbf{u}_{sample\ time}^2 + \mathbf{u}_{analysis}^2 + \mathbf{u}_{sample\ prep.}^2 \right)^{1/2}, \quad (7)$$

#### Analysis of the impact of technological processes on the uncertainty of calculating the amount of LNG energy

To increase the efficiency and reduce the uncertainty of IMSLNG in determining the amount of LNG energy, it is recommended to apply an improved static method for determining volume using currently used level measurement systems, currently used and a new, dynamic method for measuring mass, volume and density using volume, mass and density converters, a direct method of static measurements. The formula for calculating the total amount of energy  $E$ , MJ, enclosed in the volume of transferred LNG at CTO is proposed by the GIIGNL standard [5].

$$E = V_{LNG} \cdot D_{LNG} \cdot GCV_{LNG} - E_{transf. gas} \pm E_{fuel gas}, \quad (8)$$

where  $V_{LNG}$  is volume, m<sup>3</sup>;  $D_{LNG}$  is density, kg/m<sup>3</sup>;  $GCV_{LNG}$  is gross calorific value, MJ/kg;  $E_{transf. gas}$  is energy of transferred gas (gaseous phase), MJ;  $E_{fuel gas}$  is energy of auxiliary gas per period of loading, MJ, positive when loading and negative when offloading [29].

To measure the actual values of the transferred LNG energy, four equations of state were developed for liquefied natural gas. The equations can be used for IMSLNG, in static method of measurement, which is

based on indirect measurements of liquefied natural gas volume with level measurement system according to current GIIGNL standard [5].

They can be applied to dynamic IMSLNG using indirect and direct methods of volume and mass measurements, volume and mass converters, and for a new method of direct static measurements of the mass of liquefied natural gas.

**Improvement of IMSLNG using an indirect method of static volume measurements using level measurement systems and laboratory analyzers of density and component composition.** To determine the amount of energy, the following formula is proposed, which takes into account the influencing factors of technological processes related to the determination of density, volume and calorific value, not previously taken into account [29].

$$E = V_{LNG} \cdot D_{LNG} \cdot GCV_{LNG} - E_{transf. gas} \pm E_{fuel gas} \pm D_{LNG} \cdot GCV_{LNG} \cdot u_c(V) \pm \pm V_{LNG} \cdot GCV_{LNG} \cdot u_c(D_{LNG}) \pm V_{LNG} \cdot D_{LNG} \cdot u_c(GCV_{LNG}), \quad (9)$$

where  $V_{LNG}$  is volume of loaded/offloaded LNG, m<sup>3</sup>;  $D_{LNG}$  is density of LNG mix, kg/m<sup>3</sup>;  $GCV_{LNG}$  is gross calorific value of LNG, MJ/kg. It is necessary to consider additional values such as standard measurement uncertainty of volume, density, and calorific value.

When assessing the uncertainty of determining the volume, Eq. (10), in addition to the GIIGNL standard [5], we need to take into account the uncertainties of technological processes affecting the result of measurements of the LNG level of the liquid-gas interface, temperature differences during calibration and operation of the tank, gradients of temperature changes of the tank material during loading and unloading.

$$u_c(V) = \left[ u_c(V_{cal})^2 + u_c(V_{phase boundary})^2 + u_c(K_{temp})^2 + u_c(K_{cal op temp})^2 + u_c(V_{cool})^2 + u_c(V_{heat})^2 \right]^{1/2}, \quad (10)$$

where  $u_c(V_{cal})$  is combined standard volume uncertainty, which depends on tank calibration curve, level measurement in liquid-gas interface boundary  $u_c(V_{phase boundary})$ , uncertainty of temperature measurement along tank height  $u_c(K_{temp})$ , uncertainty of temperature difference while tank calibration and service  $u_c(K_{cal op temp})$  taking into account temperature gradient during tank walls cooling/heating  $u_c(V_{cool})$  and  $u_c(V_{heat})$  while loading/offloading respectively (in m<sup>3</sup>).

When density uncertainty is estimated by gas chromatography and using Eq. (11), there are additionally included uncertainties due to chromatograph type and method of defining the composition, tank temperature difference while sampling and in laboratory  $u_c(K_{temp})$ , flow phase condition in sampling area, and calorific value [18].

$$u_c(D) = \left[ u_c(D_t)^2 + u_c(D_p)^2 + u_c(D_{sampling})^2 + u_c(D_{chrom})^2 + u_c(D_{composition})^2 + u_c(K_{temp})^2 + u_c(D_{phase})^2 + u_c(GCV_{sampling})^2 \right]^{1/2}, \quad (11)$$

where  $u_c(D)$  is combined standard uncertainty of density, depending on temperature  $u_c(D_t)$ , pressure  $u_c(D_p)$ , sampling and sample storage  $u_c(D_{sampling})$ , density measurement by composition  $u_c(D_{chrom})$ , composition measurement  $u_c(D_{comp})$ , and heterogeneity of LNG mix in sampling area  $u_c(D_{phase})$ , kg/m<sup>3</sup>. In case of measurement with density meter,  $u_c(D)$  is sum of uncertainty due to meter calibration  $u_c(D_{cal})$  and uncertainty due to LNG phase condition.



$$u_c(D) = \left[ u_c(D_{cal})^2 + u_c(D_{phase})^2 \right]^{1/2}, \quad (12)$$

Using the direct method of density measurement allows us to eliminate uncertainties due to sampling and sample storage, reducing by temperature and pressure, composition determination, and chromatograph type, which contribute up to 40% to the total uncertainty.

When calorific value uncertainty is estimated using Eq. (13), there are additionally included uncertainties due to determination of composition, density, flow phase condition, and tank temperature difference in sampling area and in laboratory  $u_c(K_{temp})$ .

$$u_c(GCV_{LNG}) = \left[ u_c(GCV_{LNG\ component})^2 + u_c(GCV_{sampling})^2 + u_c(D)^2 + u_c(GCV_{LNG\ phase})^2 + u_c(K_{temp})^2 \right]^{1/2}, \quad (13)$$

where  $u_c(GCV_{LNG})$  is combined standard uncertainty of gas calorific value, depending on gas composition  $u_c(GCV_{LNG\ component})$ , sampling and sample storage  $u_c(GCV_{LNG\ sampling})$ , heterogeneity of LNG mix in sampling area  $u_c(GCV_{LNG\ phase})$ , MJ/kg [18].

**Improvement of IMSLNG using an indirect method of dynamic measurements with and volume flow transducers and in-line density transducers.** In order to determine energy content, we propose the following formula which additionally includes the factors related with determination of density, volume, and calorific value not included before [14]:

$$E = V_{LNG} \cdot D_{LNG} \cdot GCV_{LNG} - E_{transf. gas} \pm E_{fuel gas} \pm D_{LNG} \cdot GCV_{LNG} \cdot u'_c(V) \pm \pm V_{LNG} \cdot GCV_{LNG} \cdot u_c(D_{LNG}) \pm V_{LNG} \cdot D_{LNG} \cdot u_c(GCV_{LNG}), \quad (14)$$

where  $u'_c(V)$  is combined standard uncertainty of volume measurement, depending on volume flow meter calibration uncertainty  $u_c(V_{cal m})$ , presence of gaseous phase in liquid  $u_c(V_{phase})$ , operating liquid temperature difference during calibration and loading/offloading  $u_c(V_{temp})$ , m<sup>3</sup>.

When using Eq. (15) to estimate volume uncertainty, there are additionally included uncertainties due to flow phase condition and meter temperature difference during calibration and operation  $u_c(K_{temp})$ .

$$u_c(V) = \left[ u_c(V_{cal m})^2 + u_c(V_{phase})^2 + u_c(V_{temp})^2 \right]^{1/2}, \quad (15)$$

$$u_c(D) = \left[ u_c(D_t)^2 + u_c(D_p)^2 + u_c(D_{sampling})^2 + u_c(D_{chrome})^2 + u_c(D_{composition})^2 + u_c(K_{temp})^2 + u_c(D_{phase})^2 + u_c(CGV_{sampling})^2 \right]^{1/2}, \quad (16)$$

where  $u_c(D)$  is combined standard uncertainty of density, depending on temperature  $u_c(D_t)$ , pressure  $u_c(D_p)$  in liquid and gas phases, sampling and sample storage  $u_c(D_{sampling})$ , density measurement by composition  $u_c(D_{chromat})$ , composition measurement  $u_c(D_{composition})$ , phase condition of LNG mix in sampling area  $u_c(D_{phase})$ , kg/m<sup>3</sup>.

$$u_c(GCV_{LNG}) = \left[ u_c(GCV_{LNG\ comp})^2 + u_c(GCV_{LNG\ sampling})^2 \right]^{1/2} \quad (17)$$

$$+ u_c \left( GCV_{LNG\ phase} \right)^2 + u_c (D)^2 + u_c \left( K_{temp} \right)^2 \Big]^{1/2}, \quad (17)$$

where  $u_c(GCV_{LNG})$  is combined standard uncertainty of gas calorific value determination, depending on gas composition  $u_c(GCV_{LNG\ comp})$ , sampling and sample storage  $u_c(GCV_{LNG\ sampling})$ , heterogeneity of LNG mix in sampling area  $u_c(GCV_{LNG\ phase})$ , MJ/kg.

**Improvement of IMSLNG using a direct method of dynamic measurements with mass and mass flow measuring transducers.** To determine the amount of energy, the following formula is proposed, which takes into account factors related to the measurement of mass and calorific value. The amount of LNG energy is determined by a formula that takes into account [29]:

$$E = M_{LNG} \cdot GCV_{LNG} - E_{transf. gas} \pm E_{fuel gas} \pm GCV_{LNG} \cdot u_c(M) \pm M_{LNG} \cdot u_c(GCV_{LNG}), \quad (18)$$

$$u_c(M) = \left[ u_c(M_{cal m})^2 + u_c(M_{phase})^2 + u_c(M_{temp})^2 \right]^{1/2}, \quad (19)$$

where  $u_c(M)$  is combined standard uncertainty of mass measurement, depending on mass flow meter calibration uncertainty  $u_c(V_{cal m})$ , presence of gaseous phase in liquid  $u_c(M_{phase})$ , operating liquid temperature difference while calibration and loading/offloading  $u_c(M_{temp})$ , kg.

When using the Eq. (20) to estimate calorific value uncertainty, there are additionally included uncertainties due to effect of sampling and sample storage, LNG flow phase condition, and temperature difference in laboratory and in field  $u_c(K_{temp})$ ,

$$u_c(GCV_{LNG}) = \left[ u_c(GCV_{LNG\ comp})^2 + u_c(GCV_{LNG\ sampling})^2 + u_c(GCV_{LNG\ phase})^2 + u_c(D)^2 + u_c(K_{temp})^2 \right]^{1/2}, \quad (20)$$

where  $u_c(GCV_{LNG})$  is combined standard uncertainty of gas calorific value measurement, depending on gas composition  $u_c(GCV_{LNG\ comp})$ , sampling and sample storage  $u_c(GCV_{LNG\ sampling})$ , phase condition of LNG mix in sampling area  $u_c(GCV_{LNG\ phase})$ , MJ/kg [29].

**Improvement of IMSLNG using the developed direct method of static measurements of LNG mass [29]** in a tank with the use of weight measuring systems. The amount of energy is determined by the formula:

$$E = M'_{LNG} (\Delta\phi_{LNG}) \cdot K_{mass} \cdot GCV_{LNG} - E_{transf. gas} \pm E_{fuel gas} \pm M_{LNG} (\Delta\phi_{LNG}) \cdot u_c(GCV_{LNG}) \pm GCV_{LNG} \cdot u_c(M_{LNG}), \quad (21)$$

where  $M'_{LNG}$  is LNG mass measured in tank, kg;  $\Delta\phi_{LNG}$  is correction coefficient, taking into account the acceleration of gravity and deviation of the geographical area of service from the calibration site for load cells, nondimensional quantity;  $u_c(M_{LNG})$  is weight measuring system calibration uncertainty, kg.

$$u_c(GCV_{LNG}) = \left[ u_c(GCV_{LNG\ comp})^2 + u_c(GCV_{LNG\ sampling})^2 + u_c(GCV_{LNG\ phase})^2 + u_c(D)^2 \right]^{1/2}, \quad (22)$$

where  $u_c(GCV_{LNG})$  is combined standard uncertainty of gas calorific value determination, depending on gas composition  $u_c(GCV_{LNG\ comp})$ , sampling and sample storage  $u_c(GCV_{LNG\ sampling})$ , phase condition of LNG mix in sampling area  $u_c(GCV_{LNG\ phase})$ , MJ/kg.

Correction coefficient  $K_{mass}$  for effect of buoyancy in the air when measuring LNG mass in tank by gravimetric method:

$$K_{mass} = 1 - \frac{D_{air}}{D_{LNG}}, \quad (23)$$

where  $D_{air}$  is ambient air density, kg/m<sup>3</sup>;  $D_{LNG}$  is liquefied natural gas density, liquid, kg/m<sup>3</sup>.

#### Analysis of the control system/diagnostics of technological processes and the impact on the IMS of the amount of LNG energy

The continuous monitoring system, based on the results of the evaluation of the measured value and the parameters of the technological process, develops solutions that allow performing two measurement tasks.

**The first measuring task of the control system.** Collection, processing and analysis of measuring information coming from level, temperature, pressure, gas chromatographs converters and systems, and if available, from mass, volume and density flow converters. Output of information about technological parameters: “normal state” and “change of technological process parameters”, requiring operator intervention. In case of a violation of the phase state of LNG (the presence of gas), which affects the uncertainty of measurements of mass, volume, level, density and component composition, recommendations are issued for changing the parameters of the technological process or for applying correction coefficients to determine the actual amount of energy transmitted by LNG. IMSLNG measurement results are monitored during loading, unloading, transportation and storage. The list of controlled parameters is determined by the technological regulations and measurement methodology.

**The second measuring task of the control system.** Monitoring of IMSLNG characteristics, measuring transducers and systems of level, temperature, pressure and gas chromatographs, dynamic density, volume and density converters. Collection and analysis of values of technological process parameters. The frequency of monitoring of IMSLNG characteristics is specified in the technological regulations and measurement methodology. The application of a statistical approach to the assessment of measured values and parameters of technological processes, using the improved method of control charts by W. Shuhart [17, 21, 29] allows us to ensure and maintain processes at a stable level to perform reliable measurements, Table 1.

Table 1

#### Determination of the limits of permissible deviations of IMSLNG (level, volume, density and calorific value)

Measured (estimated) value	Standard values of the measured value are not used		Standard values of the measured value are set by the measurement procedure	
	Estimated value	2–4σ control limits	Estimated value	2–4σ control limits
$p$	$\bar{p}$	$\bar{p} \pm 3\sqrt{\frac{\bar{p}(1-\bar{p})}{n}}$	$p_0$	$p_0 \pm 3\sqrt{\frac{p_0(1-p_0)}{n}}$
$np$	$n\bar{p}$	$n\bar{p} \pm 3\sqrt{n\bar{p}(1-\bar{p})}$	$np_0$	$np_0 \pm 3\sqrt{np_0(1-p_0)}$
$c$	$\bar{c}$	$\bar{c} \pm 3\sqrt{\bar{c}}$	$c_0$	$c_0 \pm 3\sqrt{c_0}$
$u$	$\bar{u}$	$\bar{u} \pm 3\sqrt{\frac{\bar{u}}{n}}$	$u_0$	$u_0 \pm 3\sqrt{\frac{u_0}{n}}$

Note:  $n$  is the volume of the subgroup;  $p$  is the proportion of nonconformities in the subgroup;  $np$  is the number of inconsistencies in the subgroup;  $c$  is the number of subgroup mismatches;  $u$  is the number of inconsistencies per unit in the subgroup;  $\sigma$  is the standard deviation of the process of the estimated value.

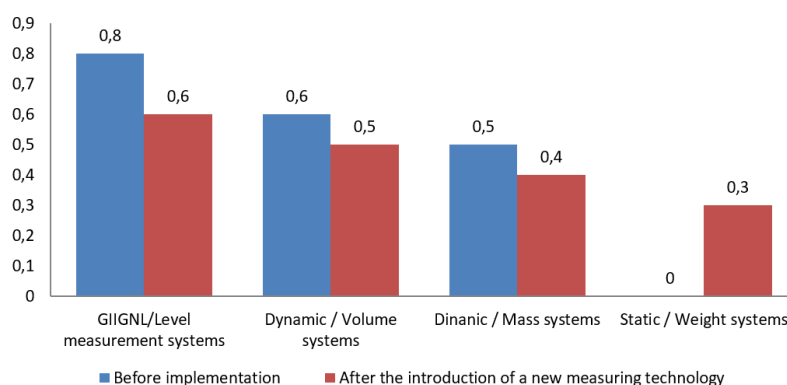


Fig. 7. Comparison of IMSLNG uncertainty budgets

The use of measurement technologies aimed at reducing the uncertainty of IMSLNG using the developed methods for assessing the reliability of sampling, taking into account changes in technological processes and monitoring / diagnostic systems do not involve large capital expenditures that can be attributed to maintenance and operation, or work carried out as part of technical re-equipment. Reducing the uncertainty of IMSLNG makes it possible to reduce maintenance and operation costs by 1.5–2 times and determine the amount of transferred LNG, excluding losses associated with changes in technological processes and physico-chemical properties. But the most accurate method, independent of the parameters of technological processes, in determining the amount of LNG energy, Figure 7, is the direct mass method using weight measuring systems [28].

IMS based on weight measurement systems allows you to determine the amount of energy with an expanded uncertainty of not more than 0.3%. In this case, four factors remain the main sources of uncertainty – a direct measurement of mass and density, a sampling system and an indirect gas chromatographic method for determining the calorific value [28].

### Conclusion

The inclusion of factors influencing the determination of the amount of LNG energy into the uncertainty budget does not increase the uncertainty budget, but allows to reduce uncertainty by eliminating and reducing the influencing factors due to the process technology. Therefore this provides the expansion of the functionality of the IMS and conditions for determining the actual values of the component composition, density, calorific value, volume and mass of LNG. Based on the equations of state of LNG technological processes, a mathematical model was developed for calculating the amount of transferred energy, which makes it possible to reduce uncertainties by ensuring control of the phase state of the flow and reliable sampling. It allows selecting the parameters of technological processes to evaluate the results of determining the volume, mass, component composition, density, calorific value, taking into account their contribution to the budget of uncertainties in the amount of LNG energy [29].

The developed methods and new measuring technology, the use of a statistical approach in the control of measured quantities and parameters of technological processes reduce the influence of technology and physical and chemical properties on the uncertainty of the IMS of mass, volume, density and energy of LNG [14]. This solution develops the system of metrological support of IMS using static and dynamic methods, reduces operating costs and financial risks in the course of receiving and transferring LNG goods and transport operations in the Russian Federation and export operations. The metrological support system makes it possible to increase the accuracy of the IMS of LNG energy by 1.5–2 times. The solution is relevant for IMS to determine the amount of energy of liquefied hydrogen.

## REFERENCES

1. ISO 8943:2007 Refrigerated light hydrocarbon fluids-Sampling of liquefied natural gas-Continuous and intermittent methods.
2. ISO 6578:2017 Refrigerated hydrocarbon liquids – Static measurement – Calculation procedure.
3. ISO 20519:2017 Ships and marine technology – Specific for bunkering of liquefied natural gas fueled vessels.
4. ISO 21903:2020 Refrigerated hydrocarbon fluids – Dynamic measurement – Requirements and guidelines for the calibration and installation of flowmeters used for liquefied natural gas (LNG) and other refrigerated hydrocarbon fluids.
5. LNG Custody Transfer Handbook. 6th Edition. (GIIGNL), 2021. URL: <http://www.giignl.org/>
6. NBS – National Bureau of Standards: LNG Measurement – A User’s Manual for Custody Transfer, 1985.
7. The experience of the “Caldon” company’s specialists, CPAS: conference of US oil companies, 2011.
8. **Gurevich M.S., Safonov A.V., Safonova M.A.** Metrology of measurements of quantity and quality indicators of LNG, International Conference “Metrology for LNG”, NMI “VSL”, Delft, Niderlandy, 2013.
9. **Safonova M.A.** Participation of the IMS company in the international project of creating a calibration station on liquefied natural gas, 1st International Congress “LNG Congress Russia 2014: An innovative way of development of the Russian gas industry”, Chamber of Commerce and Industry of Russia, Russian Gas Society and the Ministry of Energy of the Russian Federation: Moscow, March 13–14, 2014.
10. Eurochem / EUROLAB / CITAC / Nord test / MAC Manual: Measurement uncertainty associated with sampling: a guide to methods and approaches, edited by M. Ramsey and S. Ellison; trans. 1st ed. 2007, Kiev: Yurka Lyubchenko, 2015.
11. **Safonov A.V., Sladovskiy A.G., Domostroyev A.V., Churayeva M.A.** Improvement of liquefied natural gas density measurements, *Avtomatizatsiya, telemekhanizatsiya i svyaz v neftyanoy promyshlennosti [Automation and Informatization of the fuel and energy complex]*, 2020, No. 9, pp. 8–12.
12. **Safonov A.V., Ipolitov B.A., Popov K.V.** Dinamicheskiye izmereniya massy i obyema szhizhennogo prirodnogo gaza [Dynamic measurements of the mass and volume of liquefied natural gas], *Glavnyy metrolog*, 2021, No. 2 (119), pp. 24–33.
13. **Safonov A.V.** Assessment of the reliability of liquefied natural gas sampling, *Avtomatizatsiya, telemekhanizatsiya i svyaz v neftyanoy promyshlennosti [Automation and Informatization of the fuel and energy complex]*, 2021, No. 4, pp. 16–22.
14. **Safonov A.V.** Local verification schemes for measuring instruments of the quantity and quality of liquefied natural gas, *Avtomatizatsiya, telemekhanizatsiya i svyaz v neftyanoy promyshlennosti [Automation and Informatization of the fuel and energy complex]*, 2021, No. 6, pp. 38–44.
15. **Churayeva M.A., Smitz Ye., Safonov A.V.** LNG Calibration Station, 9th International Metrological Conference “Topical issues of metrological support for measuring the flow and quantity of liquids and gases”: VNIIR – branch of FSUE “VNIIM named after D.I. Mendeleev”, Kazan, 2021.
16. **Safonov A.V.** Estimation of uncertainty when sampling liquefied natural gas, *Avtomatizatsiya, telemekhanizatsiya i svyaz v neftyanoy promyshlennosti [Automation and Informatization of the fuel and energy complex]*, 2021, No. 8, pp. 5–10.
17. **Shuhart U.E.** Economic quality control of the manufactured product, K. Van Nustrand. New York, 1931.
18. **Bernandelli G.** Emerson in the LNG market chain. Daniel Systems LNG Metrology Solution, European Flow Measurement Workshop. Noordwijk, 2017.
19. **Miano M., et al.** Calculation models for prediction of Liquefied Natural Gas (LNG) ageing during ship transportation, European Gas Research Group. Project “MOLAS”. 2010.
20. Contractual Guidelines – Quantity and Quality, Society for Gas as a Marine Fuel, 2022.

21. Gy P. Chemometrics and intelligent laboratory systems, *Elsevier*. Spain. 2004. No. 74, pp. 61–70.
22. Govier G.V., Aziz K. The Flow of Complex Mixtures in Pipes, N.Y.: Van Nostrand Reinhold, 1972.
23. LNG and gas quality and measurement manual for LNG carriers calling at terminal. Offshore LNG Toscana S.p.A. LNG and Gas Quality and Measurement Manual, 06/06/2017
24. Liquefied Natural Gas Densities: Summary of Research Program at the National Bureau of Standards, U.S. Department of Commerce, National Bureau of Standards, Library of Congress Catalog Card Number: 83-600608. National Bureau of Standards Monograph (U.S.), Monogr. 241 p. (Oct. 1983)
25. Richter M., Kleinrahn R., Span R. Metrology for LNG, Delft: VSL, 2013.
26. Van Wijngaarden H., van der Grinten J.G.M. Evaluation of the Caldon scaling methodology to convert water calibrations of an ultrasonic meter, type LEFM, into an LNG meter curve, NMi Report No. C-SP/606627-HvW/Rap. 2006; Operational experience with ultrasonic meters for allocation measurement of LNG, H. Kurniawan, M. Scott, G. Brown et al. Houston, 2013.
27. Lucas P., Bükler O., Kenbar A., et al. World's first LNG research and calibration facility, FLOMEKO 2016 (Sydney, September 26–29, 2016). URL: <http://www.semanticscholar.org>.
28. Safonov A.V. Measurement of liquefied natural gas mass, *Avtomatizatsiya, telemekhanizatsiya i svyaz v neftyanoy promyshlennosti [Automation and Informatization of the fuel and energy complex]*, 2020, No. 10, pp. 9–14.
29. Safonov A.V. Improving the accuracy of information-measuring and control systems of the amount of energy based on the equations of state of liquefied natural gas, *Avtomatizatsiya i informatizatsiya TEK [Automation and Informatization of the fuel and energy complex]*, 2022, No. 7, pp. 34–39.

#### INFORMATION ABOUT AUTHOR / СВЕДЕНИЯ ОБ АВТОРЕ

Andrey V. Safonov  
Сафонов Андрей Васильевич  
E-mail: safavs@yandex.ru

*Submitted: 22.05.2023; Approved: 30.06.2023; Accepted: 06.07.2023.*

*Поступила: 22.05.2023; Одобрена: 30.06.2023; Принята: 06.07.2023.*